INFRASENSE, Inc.

Non-Destructive Measurement of Pavement Layer Thickness

Final Report

Caltrans No. 65A0074

Submitted to the

California Department of Transportation
Sacramento, CA 95819

by

Infrasense, Inc.
14 Kensington Road
Arlington, MA 02476

April 25, 2003

Technical Report Documentation Page

1. Report No.	2. Government Accession No.	3. Recipient's Catalogue No.
FHWA/CA/OR-2003/03 ~~XXXXXXXXXXXXXXXX~~ FHWA/CA/TL-		

4. Title and subtitle	5. Report Date
NON-DESTRUCTIVE MEASUREMENT OF PAVEMENT LAYER THICKNESS	April 25, 2003
	6. Performing Organization code
7. Authors: Kenneth R. Maser	8. Performing Organization Report No.
9. Performing Organization Name and Address Infrasense, Inc. 14 Kensington Road Arlington, MA 02476	10. Work Unit Number
	11. Contract or Grant No. 65A0074
12 Sponsoring Agency Name and Address California Department of Transportation Sacramento, CA 95819	13. Type of Report and Period Covered Final: Jan 1, 2001 – Dec. 31, 2002
	14. Sponsoring Agency Code

15. Supplementary Notes

16. Abstract

The overall objective of the reported work has been to rapidly determine the average pavement thickness on a newly constructed pavement section to within 0.1 inch of the true value, without extensive reliance on cores. The project has been divided into two tasks—one for asphalt pavement and one for concrete pavement. The asphalt task has focused on two adaptations of ground penetrating radar (GPR), one involving the use of an air-launch horn antenna, and one using dual ground-coupled antennas in a common midpoint (CMP) measurement mode. The concrete task has included the CMP method and conventional Impact-Echo methods. The work has involved theoretical analyses, laboratory testing on small slabs and simulated pavement materials, testing at full scale pavement test facilities, and testing on 11 newly constructed pavement sections in California. The California test sites included full depth asphalt, asphalt overlays, and full depth concrete pavements. The thickness data collected with the tested devices has been correlated with thickness results obtained from over 170 cores taken at points in the test areas. For the asphalt pavements, both GPR methods have been shown to be capable of measuring the average section thickness to within 0.1 inches of the average core value. The CMP method, however, appears to be limited to asphalt thickness greater than 3 inches. For the concrete pavements, the two impact-echo methods tested were shown to be able to measure the average section thickness to within 0.16 and 0.24 inches of average core value. All of the methods required the use of a single calibration core per site to achieve the reported accuracy.

17. Key Words	18. Distribution Statement
Pavement Thickness, Quality Assurance, Pay Factors, Ground Penetrating Radar, Impact-Echo	No restrictions. This document is available to the public through the National Technical Information Service, Springfield, VA 22161

19. Security Classif. (of this report)	20. Security Classif. (of this page)	21. No. of Pages	22. Page
		104	0

Table of Contents

PAGE

Figures:

PAGE

PAGE

Tables:

Disclosure Statement

Subcontractors for this work were:

Geophysical Survey Systems, Inc. (GSSI)
Radar Solutions International
Worcester Polytechnic Institute
Drexel University
University of Illinois
Wiss, Janney, and Elstner
España Geotechnical Consulting

Disclaimer Statement

"The contents of this report reflect the views of the author who is responsible for the facts and the accuracy of the data presented herein. The contents do not necessarily reflect the official views or policies of the STATE OF CALIFORNIA or the FEDERAL HIGHWAY ADMINISTRATION. This report does not constitute a standard, specification, or regulation."

Acknowledgements

The author would like to acknowledge: Ms. Laura McGrath of Infrasense for her assistance with all aspects of the data analysis; Dr. Paul Foxworthy of Infrasense for his assistance in arranging access to sites, conducting field tests, and obtaining core data; Ms. Doria Kutrubes and Ms. Adriana Heinz of Radar Solutions International (RSI) for their assistance with the collection of the GPR data; Dr. Roger Roberts of GSSI for conducting the laboratory GPR studies and developing the CMP processing algorithm; Professor John Popovics of the University of Illinois for support with the analysis and implementation of mechanical wave methods; Mr. Alex Gibson of the University of Illinois for his assistance in collection and analysis of Impact-echo data; Professor Rajib Mallick of Worcester Polytechnic Institute for his assistance with the design of the asphalt test pit; Mr. Alfredo Rodriguez of Caltrans for his assistance in conducting the field tests; and Dr. T. Joseph Holland for providing assistance and guidance as the Caltrans Project Manager. The author would also like to acknowledge the Caltrans resident engineers who assisted in providing access to and information about the California pavement test sites that were included in this study, including Martin Clark (US50), Brent Bullard (US180), Henry Wells (US99), Gerry Santiago (I-505), Frank Latham (SR14), Jose Ventocella (SR30), and Michael Chou (SR30). Fijnally, the author would like to acknowledge Geophysical Survey Systems, Inc., Worcester Polytechnic Institute, the FAA National Airport Pavement Test Center, The FHWA Turner Fairbanks Research Center, the National Center for Asphalt Technology (NCAT) at Auburn, University and the New Hampshire Department of Transportation for providing test facilities; and Olson Instruments, Inc. for providing test equipment.

Executive Summary

The objective of this project was to evaluate and demonstrate non-destructive test methods to determine the thickness of new pavement to within 2.5 mm (0.1 inch). Various methods were evaluated and tested in the laboratory and in the field. A series of final evaluations were carried out on test pavements in California. For asphalt pavement, two methods based on ground penetrating radar (GPR) technology met the objectives of this project. The horn antenna GPR method collects data continuously and handles the full range of expected thickness values. The CMP GPR method is a point measurement method, and can evaluate thickness greater than 80 mm. For PCC pavement, the impact-echo (IE) method was found to be the most effective available thickness measurement technology. However, the accuracy obtained with the impact-echo method was 50 mm (0.2 inches) and fell short of the project objective.

Deficiencies in the thickness of newly constructed pavements and overlays reduce the life of the pavement and increase costs to the agency. The ability to accurately quantify thickness deficiencies and the associated increase in life cycle cost is the basis for the implementation of pay factors. Cores determine local pavement thickness accurately, but they are time consuming, they damage the pavement, and they represent a very limited sample of the actual pavement. The objective of the reported work has been to test and recommend thickness measurement methods that are quick, non-destructive, reliable, and repeatable, and which can accurately represent the thickness of a newly constructed pavement section.

An analysis of the accuracy requirements for pay factor determination has been carried out. The analysis shows that to meet pay factor requirements, the thickness measurement method should be capable of determining the mean pavement thickness to within 2.5 mm (0.1 inch). The analysis also shows that it is necessary to obtain a large number of sample points to accurately characterize the mean pavement thickness. For example, a pavement with a 5 mm (0.2 inch) thickness standard deviation would require 70 cores to meet the 2.5 mm (0.1 inch) accuracy requirement. Alternative non-destructive methods, although less accurate than cores, can meet the accuracy requirement by providing many more data samples.

The project has been divided into two areas – asphalt pavement and concrete pavement. A preliminary evaluation of available methods led to the recommendation of three ground penetrating radar (GPR) methods for asphalt pavement and one of the GPR methods and two mechanical wave methods for concrete. These methods were evaluated with theoretical analysis and subsequently with a series of laboratory tests. In the laboratory these methods were applied to thickness evaluation using both simulated and actual slabs of pavement material. The results of the laboratory testing indicated that two of the GPR methods –the horn antenna method and the common midpoint (CMP) method have the potential to achieve the accuracy objectives of this project for asphalt pavement. The laboratory tests and analyses also indicated that the CMP method, along with the impact-echo (IE) and multi-receiver (MRT) mechanical wave methods had similar potential for concrete pavement. The CMP method, however, showed some limitations with early age concrete due to the high conductivity associated with the free water.

The selected methods were further investigated on full-scale test pavements, selected due to the availability of core thickness data for correlation. Thickness measurements with the various test methods were made on these pavements, and the results were correlated with core data. Based on the data from I-93, the FAATC and the FHWA ALF sites, it appeared that the horn antenna

method was capable of producing accurate asphalt thickness data on full-scale pavement thickness sections over a thickness range from 51 to 205 mm (2 to 8 inches). The CMP method produced similar results, but tended to overestimate the thickness and was limited to the evaluation of thickness greater than 76 mm (3 inches). Data from the NCAT site suggest that the type of surface material might influence the accuracy of the horn antenna thickness calculation. These data suggest that both methods would benefit by implementing some type of site-specific calibration. For concrete thickness, the CMP method applied to a two-year old concrete pavement provided accurate data for average thickness, although with somewhat more scatter than was obtained for asphalt. CMP thickness measurements on a continuously reinforced concrete pavement (CRCP) were less successful than on un-reinforced concrete pavement due to the influence of the reinforcement. Data collection methods to reduce the influence of the reinforcing were recommended. Impact-Echo method appeared to be capable of providing accurate concrete thickness measurements if some type of bias correction could be applied. Once again, this finding suggests some site-specific calibration to eliminate the bias. The results for the other mechanical wave method, the multi-receiver technique, were inconsistent. Given the developmental status of this method and the need to implement and test a new type of mechanical wave impact source, further study of this technique would be required before it could be evaluated under this project. Since such study was beyond the scope of this project, further evaluation of this technique was discontinued.

Final testing was carried out on 11 selected pavement sections in California, 6 asphalt sections and 5 concrete sections. Test sections were 305 meters (1000 feet) in length. Some were still closed to traffic due to ongoing construction, while others were already open to traffic. The asphalt sites were selected to represent three main conditions: (a) thick and thin asphalt on aggregate base; (b) asphalt on concrete; and (c) thick and thin asphalt overlays. The concrete sites were selected to represent variations in concrete thickness and age. Age was selected as a variable because of its influence on GPR penetration and on the mechanical wave velocity.

Each site was evaluated for thickness using the test methods recommended in this study. The asphalt sites were tested with the horn antenna and CMP methods. The concrete pavements were evaluated with two different impact-echo devices, along with the CMP method. After this evaluation, cores were taken for comparison with the test data. Twenty cores were taken at each asphalt site and ten at each concrete site. The thickness values determined from the various test methods were compared to the core values. The comparison showed generally good correlation, but also the need for a calibration at each site. One core location per site was selected for calibration. A method was developed to determine the optimum core location from the test data. Analysis of the calibrated thickness data showed that, for the asphalt pavements, both the horn antenna and CMP methods determined the average section thickness to within 2.5 mm (0.1 inches) of the average core value. The CMP method, however, appeared to be limited to measuring asphalt thickness greater than 89 mm (3.5 inches). For the concrete pavements, the two impact-echo devices tested were shown to be able to measure the average section thickness to within 4 and 6 mm (0.16 and 0.24 inches) of average core value, respectively. The CMP method did not perform as well, and is not recommended for future concrete thickness quality assurance.

This study has provided the specification of two GPR methods capable of measuring the thickness of new asphalt thickness with accuracy suitable for use with pay factors. Not only do the recommended methods provide adequate accuracy when compared to cores, but they are able to generate the number of thickness data points required to accurately characterize the pavement

thickness. This study has also provided a specification for impact-echo as a method for determining concrete pavement thickness. The accuracy obtained with impact echo did not reach the initial goal of 25 mm (0.10 inches). However, the method may be of interest for other applications.

It is recommended that the specified methods be evaluated on pavement sections whose size is more typical of construction project sections. The size of the section may determine whether or not a single calibration core, or multiple calibration cores are required. The relationship between the size of the section, the test data, and the number of calibration cores needs to be established.

1. Introduction

Pavement layer thickness is an important factor in determining the quality of newly constructed pavements and overlays, since deficiencies in thickness reduce the life of the pavement. For asphalt, the relationships between thickness deficiency and pavement life have been quantified using a performance model *(1)*. These relationships show, for example, that a 13 mm (0.5 inch) thickness deficiency on a nominally 91 mm (3.6 inch) thick pavement can lead to a 40 % reduction in pavement life. This reduction in pavement life has significant economic implications.

Current California practice for concrete paving involves determination of thickness by cores, approximately 3 per 305 m (1000 feet), and there are penalties for deficiencies in thickness. For asphalt, payment is made by the ton, which addresses the average thickness but not the variability. The concept of "pay factors", already implemented for other quality measures (such as density), provides a mechanism for transferring the cost of construction deficiencies to the contractor.

In order to implement pavement thickness as a measure of quality assurance and as a basis for pay factors, it is necessary to have an accurate and reliable method for making the thickness measurement. Cores are accurate, but they are time consuming, they damage the pavement, and they represent a very small sample of the actual pavement. Therefore, it is desirable to have a thickness measuring method which is quick, non-destructive, and which can generate an accurate and representative population of pavement thickness data points.

For asphalt pavement, ground-penetrating radar (GPR) is by far the most established technology for measuring pavement thickness. Evaluation studies have been carried out by over ten state highway agencies, by SHRP, MnROAD, and by the FHWA, all of which have documented the accuracy of GPR asphalt thickness vs. core samples *(2)(3)*. These studies have shown that for newly constructed pavements, the deviation between GPR and core results range from 2% -5% of the total thickness. Studies have also shown, that with proper equipment and data processing, GPR can accurately determine thickness for overlays as thin as 25 mm (1 inch) *(4)*. GPR can be collected continuously at various speeds, and thus allowing for the availability of a large number of thickness data points to be collected economically. Finally, GPR has also been effectively used to determine variations in asphalt density *(5)*. Such additional information would enhance the overall quality assurance program. Most of these GPR layer thickness studies have been carried out with "air-coupled horn" antennas, since these can be implemented at driving speed without lane closures. However, for the purposes of quality assurance, lower data collection speeds permit consideration of "ground-coupled" antennas as well. This alternative introduces some interesting and potentially attractive options that will be explored during this program.

For concrete pavement, the situation is different. The GPR wave attenuates more rapidly in concrete, especially new concrete, than it does in asphalt *(6)*. This is due to the free moisture and conductive salts that are present in the concrete mix. Also, the dielectric contrast between concrete and base is much smaller than it is between asphalt and base. These two factors in combination often lead to a diminished, sometimes absent, reflection at the base of the concrete. Therefore, air-coupled GPR is not a feasible technology for thickness measurement on new concrete. Ground-coupled GPR, on the other hand, provides more energy input into the pavement, and can overcome some of the penetration limitations of the horn antenna.
Mechanical wave techniques, on the other hand, work much more effectively than GPR in concrete. Concrete pavements are typically thick enough to fall within the measurement range of

mechanical wave measurements. Mechanical waves travel well in concrete, and there is usually a strong mechanical contrast between the concrete and the base material. Data collection is considerably slower than with GPR, but certainly faster and less expensive than coring.

Based on the background described above, the objectives of this project have been to:

1. Develop, evaluate and test advanced air-coupled and ground-coupled GPR methods for obtaining accurate asphalt pavement layer thickness data;
2. Develop, evaluate, and test ground-coupled GPR and mechanical wave methods for obtaining accurate concrete pavement thickness data;
3. Specify the use of these methods in the context of a quality assurance program.

In order to meet these objectives, Infrasense, Inc. has conducted a comprehensive research and evaluation program. The program combined theoretical study, laboratory testing, field testing on constructed test pavements, and field evaluations on selected California pavement sites. The following sections of this report describe these efforts in detail. The report discusses the accuracy requirements in Section 2, the methods that were evaluated in Section 3, theoretical analyses of the proposed methods in Section 4, laboratory studies in Section 5, preliminary field tests in Section 6, and tests on Caltrans pavements in Section 7. An equipment and method specification is presented in Section 8.

2. Accuracy Requirements For Pavement Thickness Quality Assurance

In order to use a non-destructive evaluation (NDE) technique for quality assurance (QA) and pay factors, it is necessary for the technique to provide a level of accuracy which is appropriate for the application. Accuracy is defined as the difference between the "true" pavement thickness and the "measured" pavement thickness. For pay factors, the accuracy in measurement of pavement thickness has to be sufficient to quantify the loss of pavement life. The loss of pavement life vs. thickness has been translated into pay factors for asphalt pavement by Deacon et. al *(1)*, and can be shown graphically as in Figure 1. The figure plots pay factor on the vertical axis vs. deviation of average pavement thickness. The deviation is the difference between the actual average pavement thickness and the average pavement thickness specified.

Note that the analysis was done for thickness increments of 5 mm (0.2 inch). In order to use this analysis, thickness measurements need to be accurate enough to ensure that the correct 5 mm (0.2 inch) interval (and the associated pay factor) is selected. Ideally, one would have perfectly accurate measurements. However, real measurement systems have errors. Even cores, which are taken as the standard measurement, introduce significant errors simply because they represent such a limited sample. Therefore, there will always be a possibility that the pavement thickness characterization will not fit the true range according to Figure 1. For this project, the accuracy objective has been specified as ± 2.5 mm (0.1 inch), which is interpreted to mean that the true mean thickness is equally likely to occur somewhere in a range of ± 2.5 mm (0.1 inch) around the measured mean thickness. Based on the 5 mm (0.2 inch) decision ranges of Figure 1, an accuracy of ± 2.5 mm (0.1 inch) indicates that the thickness range will be accurately classified at least 75% of the time.

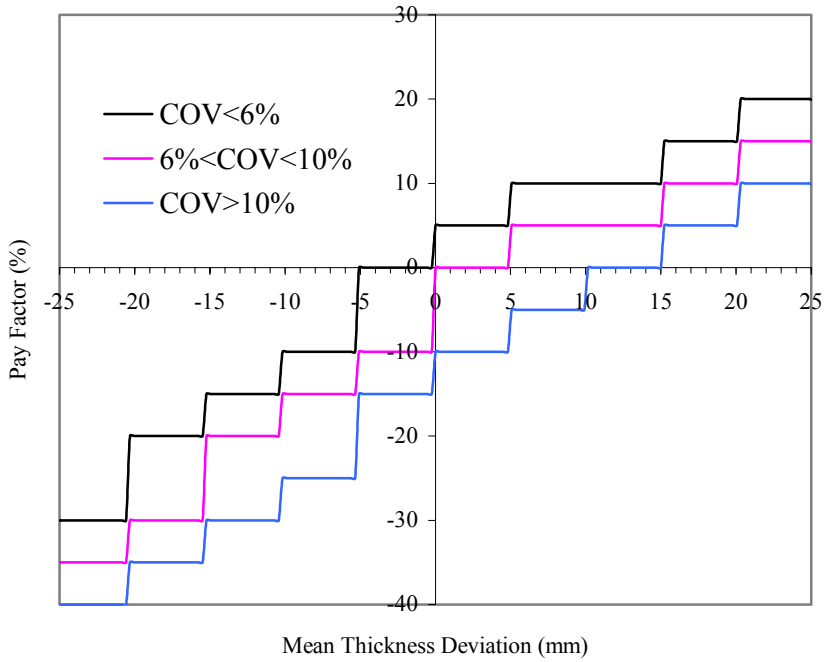

Figure 1 – Pay Factors vs. Mean Thickness Deviation (from Deacon, et. al.)

Figure 1 also indicates that the variability around the mean, as measured by the coefficient of variation (COV), also affects the pavement life and the associated pay factor. The coefficient of variation is defined as the standard deviation divided by the mean. Therefore, it would be desirable for the proposed NDE to accurately characterize both the mean thickness and the standard deviation.

In order to assess accuracy of an NDE method, one has to consider two sources of error: sampling error and measurement error. *Sampling error* represents the fact that there are an infinite number of pavement thickness values, and that we are only sampling a small number of these values to represent the entire pavement. Sampling error is large when we take a small number of samples (like coring) and when the pavement thickness itself is highly variable. Sampling error is reduced by taking more samples. Sampling error is therefore characterized by the standard deviation of the pavement thickness and the number of thickness measurements.

Measurement error is the difference between the measured thickness at a given location and the "true" thickness at that location. Measurement error is characterized by the variability of the measured thickness around the true thickness, and can be represented by a standard deviation. A recent study on PCC pavements in Indiana showed that the typical standard deviation of thickness measurements cores was 2.5 mm (0.10 inches) (*10*). Since cores are the most direct method for thickness determination, it is expected that the non-destructive methods considered under this program will have higher measurement errors.

A statistical analysis has been carried out to investigate the relationship between the measurement error, the variability of the pavement section, and the number of measurement points. A sample result of this analysis is shown in Figure 2. The figure shows the number of sample points required to achieve an accuracy of 2.5 mm (0.1 inch) with 90% confidence. The number of sample points is presented as a function of the standard deviation of the pavement thickness. Each of the four curves represents a measurement technology with different measurement errors, as characterized by a standard deviation.

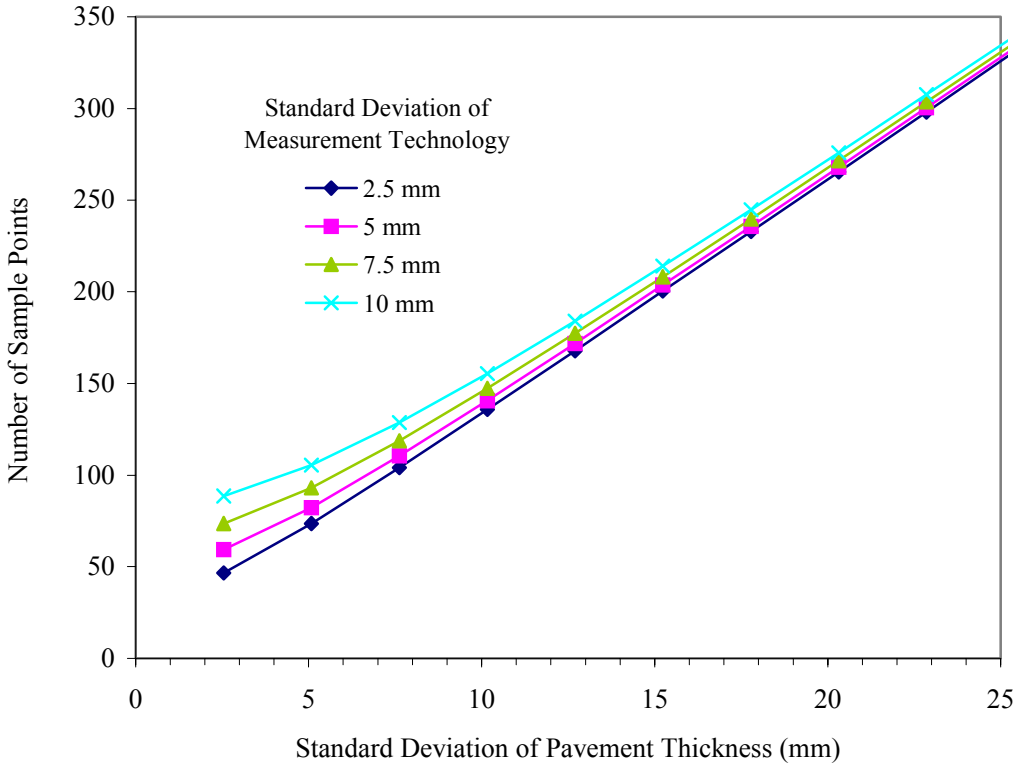

Figure 2 – Number of Samples Required to Achieve Accuracy of 2.5 mm (0.1 inch) with 90% Confidence

The curves show that the number of samples is primarily dependent on the variability of the pavement and less dependent on the standard deviation of the measurement. It also shows that for accurate measurements such as cores, the number of cores required to achieve an overall accuracy of 2.5 mm (0.1 inch) far exceeds the number of cores generally taken for pavement thickness QA.

For example, assuming that the standard deviation for core measurements is 2.5 mm (0.1 inch), a pavement with standard deviation of 5 mm (0.2 inches) requires 70 cores. For the same pavement, an NDE measurement technology with a standard deviation of 6 mm (0.25 inches) would require 100 samples.

It is clear from this analysis that the ability of non-destructive measurement methods to obtain a large number of data samples creates the potential for much more accurate pavement thickness characterization than can normally be expected from cores.

The following section will describe the non-destructive measurement methods that were considered and evaluated under this program.

3. Description of the Non-Destructive Test (NDT) Methods Evaluated Under This Project

The test methods evaluated under this project fall into two categories:

1. Electromagnetic Wave Methods (Ground Penetrating Radar)
2. Mechanical Wave Methods (Impact-Echo and others)

The following paragraphs will describe the fundamental aspects of the methods considered under this study.

3.1 Ground Penetrating Radar Methods

Ground Penetrating Radar (GPR) operates using short electromagnetic pulses radiated by an antenna which transmits these pulses and receives reflected returns from the pavement layers. Analysis of these reflected return signals yields information on the pavement layer thickness and electromagnetic material properties. Pavement thickness is calculated from the arrival time of the GPR reflection from the bottom of the pavement and the velocity of travel. The determination of the arrival time is made directly from the GPR signal. The velocity calculation requires some other process, as discussed in the specific methods below. The velocity is related to a material property called the *dielectric constant*. Typical values for velocity and dielectric constant for pavement materials are shown in Table 1.

There are two basic types of GPR systems used for pavement evaluation—the non-contact horn antenna systems and the contact ground-coupled systems. The following paragraphs discuss methods for implementing these systems for pavement thickness quality assurance.

Table 1 – GPR Velocities and Dielectric Constants for Pavement Materials

velocity				
metric		english	dielectric	note
m/ns	cm/ns	in/ns	constant	
0.100	10.0	3.94	9.00	typical for pcc
0.105	10.5	4.13	8.16	
0.110	11.0	4.33	7.44	
0.115	11.5	4.53	6.81	
0.120	12.0	4.72	6.25	
0.125	12.5	4.92	5.76	
0.130	13.0	5.12	5.33	typical for ac
0.135	13.5	5.31	4.94	
0.140	14.0	5.51	4.59	
0.145	14.5	5.71	4.28	
0.150	15.0	5.90	4.00	
0.155	15.5	6.10	3.75	

3.1.1 Horn Antenna GPR

Implementation of the *horn antenna method* is shown in Figure 3. The figure shows the geometry of the antenna and the GPR ray paths. The reflected pulses are received by the antenna and recorded as a waveform as shown. As the equipment travels along the pavement, it generates a sequence of waveforms, also shown in the figure. The layer boundary between the asphalt and base is clearly visible in this sequence of waveforms. These waveforms are digitized and interpreted by computing the amplitude and arrival times from each main reflection. For the *horn antenna method*, the pavement thickness can be computed from these amplitudes and arrival times according to the following equations *(2)*:

$$\text{Thickness (cm)} = \text{velocity} * \text{time}/2 \qquad (1)$$

$$\text{Velocity (cm/ns)} = (15)/\sqrt{\varepsilon_a} \qquad (2)$$

$$\varepsilon_a = [(A_{pl} + A)/(A_{pl} - A)]^2$$

where velocity is calculated from ε_a ,the dielectric constant of the asphalt; t is the time delay between the reflections from the top and bottom of the asphalt, computed automatically from each waveform; A is the amplitude of the reflection from the top of the asphalt, computed from each waveform; and A_{pl} is the amplitude of the reflection from a metal plate, obtained during calibration. The constant, 150, is half the speed of light in air. The factor 2 converts the measured round-trip time to one-way time.

The above equations are based on the assumption that the transmitting and receiving antennas are in the same location, and that the GPR ray path is perpendicular to the pavement surface. These assumptions are not completely true, but the error introduced by this simplification has not had an adverse effect on accuracy for standard pavement thickness applications. The error introduced by these assumptions will be examined in Section 4.1 of this report.

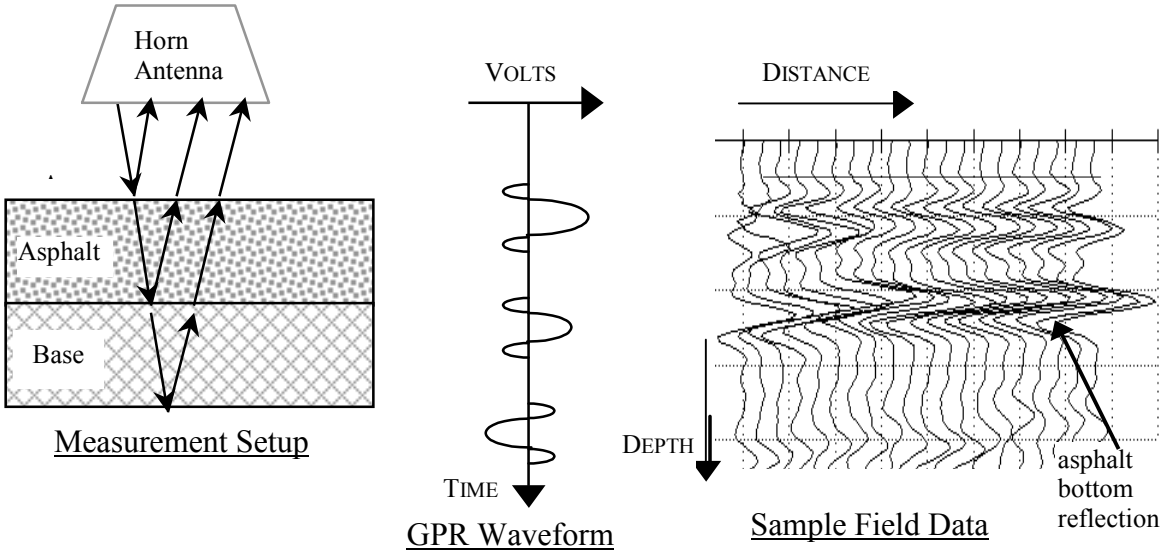

Figure 3 – Horn Antenna Method

3.1.2 Ground-Coupled GPR

Ground-coupled systems operate with the antenna directly in contact with the pavement. Because of this configuration, equations (1) and (2) can not be used, since the radar wave is launched directly into the pavement, and does not travel through air. Because of this configuration, the dielectric constant cannot be calculated directly from the data.

3.1.2.1 Calibrated Single Antenna Method

One approach to using a ground-coupled antenna is to replace Equation (2) with a calibration curve. The calibration would relate the direct coupling of the antenna to the dielectric constant and velocity of the surface material. The direct coupling is the transmission which goes directly from the transmitter to the receiver. This direct coupling is observed on the data before the detection of the reflected arrivals. Since the direct coupling involves transmission through the pavement material, it is reasonable to assume that a correlation could be established between the direct coupling and the dielectric constant and velocity in the pavement material. The establishment of this calibration curve will be discussed in further detail in Section 5 of this report.

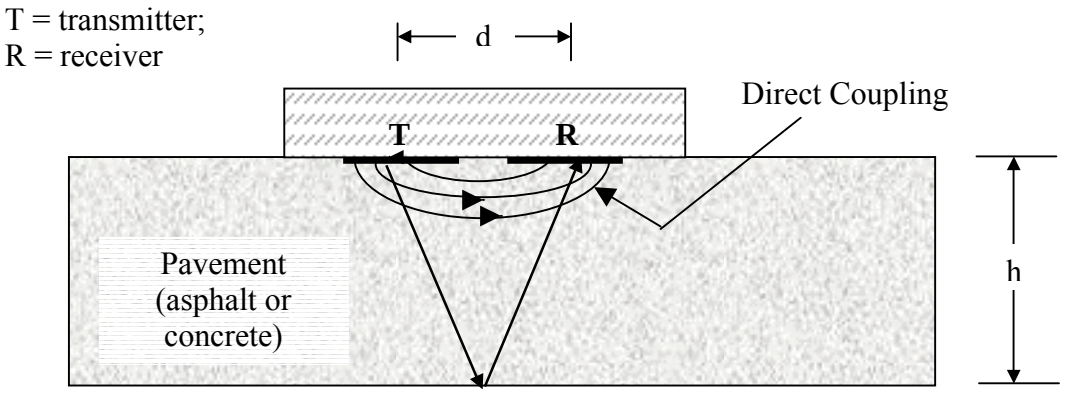

Figure 4 – Ground-coupled GPR Antenna Showing Direct Coupling

Given travel path equal to *V*t*, where *V* is the GPR velocity and *t* is the travel time, the thickness is calculated from the geometry as:

$$h = 0.5[\ (Vt)^2 - d^2\ ]^{1/2} \qquad (3)$$

3.1.2.2 Dual Antenna Common Midpoint (CMP) Method

An alternative method involves using two ground-coupled antennas. This method, called the *common mid-point method* (CMP), is shown in Figure 5. The CMP method uses two ground-coupled antennas, one of which acts as a transmitter and the other as a receiver. The two antennas are initially adjacent to each other, and are then moved at equal distances from the initial

midpoint. The implementation mechanism is such that a GPR scan is collected for each unit of movement (e.g., every 2 mm (0.08 inch)).

The reflected arrival from the bottom of the pavement takes on a hyperbolic pattern, whose Equation is *(7)*:

$$t_{tot}(i) = \frac{2}{V_2}\sqrt{x(i)^2 + d^2} \qquad (4)$$

where i = scan number

n = total number of scans

d = thickness of the pavement layer

V_2 = GPR velocity in pavement layer

x (i) = antenna distance from common midpoint at scan i

$t_{tot}(i)$ = arrival time of GPR pulse for spacing *x (i)*

By fitting the observe data with this equation, both the pavement layer velocity and layer thickness can be determined.

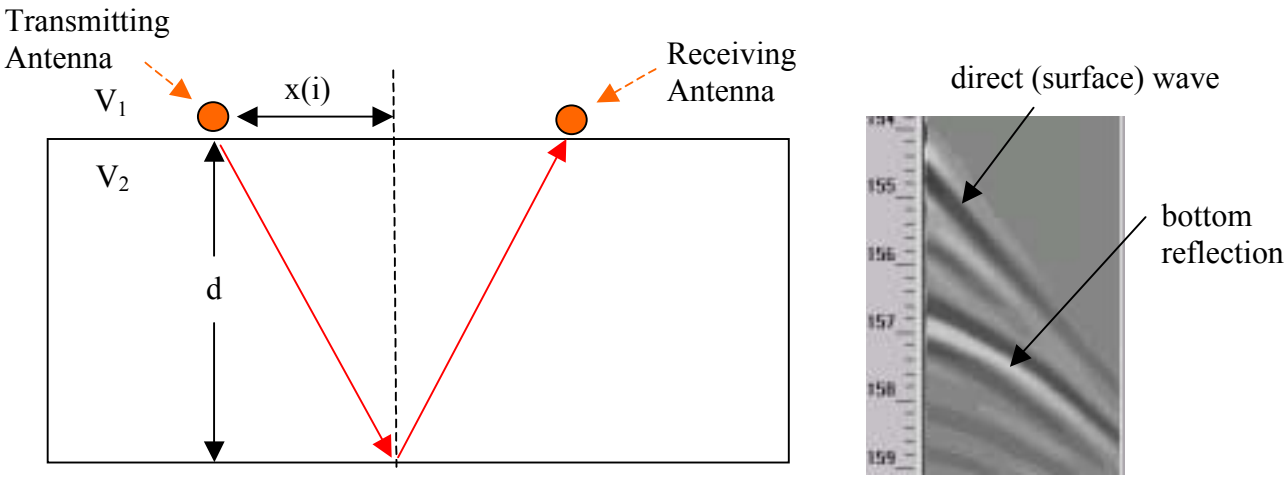

Figure 5 – Ground-Coupled Common Midpoint (CMP) Method

3.2 Mechanical Wave Methods for Concrete Thickness Evaluation

Mechanical wave methods are very similar in concept to electromagnetic wave methods. With mechanical wave methods, a pulse of mechanical energy is transmitted into the pavement, and a transducer receives the reflected waves from the pavement layers. Analysis of these reflected return signals yields information on the pavement layer thickness and mechanical material properties.

3.2.1 Impact-Echo

Impact-echo (IE) is a standardized mechanical wave technique for measuring the thickness of concrete pavement *(6). S*everal different sources of commercial equipment are available. A source and receiver are co-located on the pavement surface. The arrangement is shown schematically in Figure 6. The impactor can be a hand-held hammer, a small steel bearing, or a mechanically actuated impact device. The impact generates a pressure wave (p-wave) which travels down through the pavement and is reflected back from the bottom of the pavement. The reflection occurs due to the difference in mechanical wave velocity and density between the pavement and the base. This difference does not always occur, such as when the concrete pavement is placed over a lean concrete base with very similar mechanical properties. With lean concrete base, however, there is often a lack of bonding between the concrete pavement and the base. The lack of bonding produces a mechanical discontinuity sufficient to provide the reflection from the bottom of the pavement.

Much like in GPR, the wave travels twice the thickness of the pavement before returning to the surface, and the relationship between the thickness, the wave velocity, and the travel time is:

$$\text{Thickness (mm)} = V_p \, (t /2) \qquad (5)$$

where V_p is the p-wave velocity in the concrete and t is the round trip travel time. As shown in Figure 6a, the wave reflects repeatedly back from the surface into the pavement and back from the pavement bottom, producing the repetitive reflection pattern shown. Rather than measure the travel time directly as in GPR, it has been shown that measurement of the frequency spectrum of the reflected signal is much more effective. The reflected signal frequency characteristics are shown in Figure 6b. The frequency peak, f, or "thickness resonance" represents the repetition of reflected arrivals, or arrivals per second. The inverse of f is then the travel time. Therefore, Equation (3) becomes:

$$\text{Thickness (mm)} = V_p /2f$$

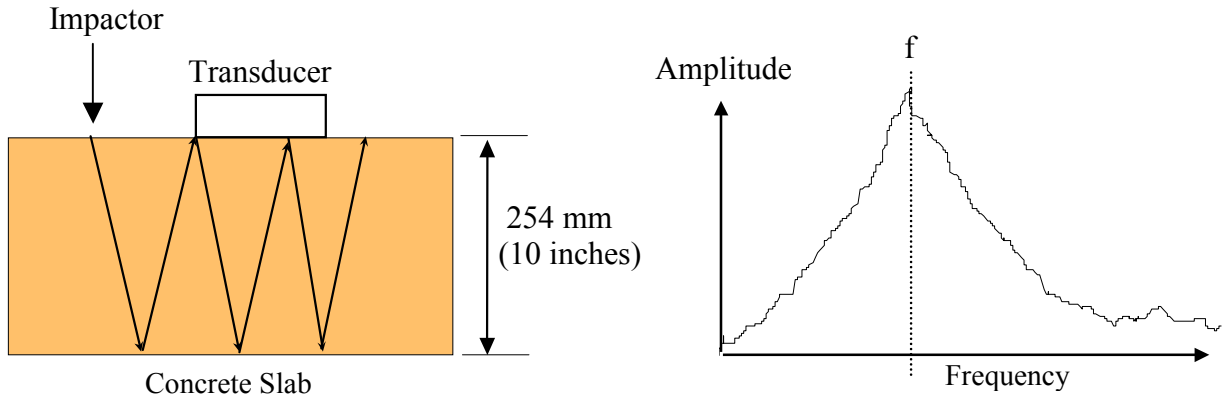

(a) Implementation and Wave Paths (b) Resulting Frequency Spectrum

Figure 6 – Impact-Echo Method

The ASTM specification for this method (*8*) shows Equation (5) to be:

$$\text{thickness (mm)} = 0.96\ V_p / 2f \qquad (6)$$

where the 0.96 factor represents the "plate effect" on the p-wave propagation velocity.

The p-wave velocity, required for the above calculation, needs to be determined independently. The ASTM specification offers a method by which the p-wave velocity is measured along the exposed surface of the material. This method uses two transducers placed on the surface of the material. An impactor strikes the concrete near the first transducer, and the p-wave arrives at the first and then at the second transducer. The time difference between p-wave arrivals is measured, and the time difference and transducer distance yields the velocity V_p. In practice, the velocity measurement is more difficult to make and to interpret than the impact-echo method.

The ASTM specification indicates that there is a 1%-2% error in thickness calculation introduced by the resolution limitations in measuring the thickness resonance. A second accuracy issue related to the impact-echo method is that the p-wave velocity measured at the surface does not necessarily represent the velocity through the depth. In fact up to 6% difference in V can be expected between surface and interior concrete *(7)*. Investigation of the influence of this procedure on the accuracy of impact-echo thickness measurements was one of the objectives of this work.

An alternative method for calculating the p-wave velocity is to use calibration cores. Using a core with known thickness, Equation (4) can be used to calculate V. However, since V_p may change from location to location, it is not clear how effective a single calibration core may be, nor is it clear how many calibration cores will be needed. This issue was also considered as part of this program.

A number of concrete pavement thickness accuracy studies have been carried out over the past several years. A summary of the results of these studies is shown in Table 2.

Table 2 – Summary of Previous Impact Echo Concrete Pavement Thickness Studies

Location/ Reference	Subsite	Core (mm)		Impact Echo (mm)		Difference of mean (mm)
		Mean	St Dev	Mean	St Dev	
Indiana (*10*)	n.a.	361	9	364	15	-4
Nebraska*	n.a.	256	4	253	4	3
Virginia (*11*)	Route 460	242	9	242	9	0
	Route 64	208	6	209	8	-1
Arizona (*12*)	200-LCB	205		203		2
	200-ASPB	209		212		-3
	200-DGAB-1	197		195		2
	200-DGAB-2	212		209		3
	300-LCB	294		291		3
	300-ASPB	294		300		-6
	300-DGAB-1	288		279		9
	300-DGAB-2	287		279		8

* FHWA study

The differences shown between the impact-echo and core data in Table 2 are generally small, and suggest that impact-echo could be sufficiently accurate to meet the accuracy requirements of this program. However, discussions with experienced practitioners have indicated that the small differences shown in Table 2 are not typical of field practice. As indicated earlier, the accuracy of impact-echo depends on the base material type, the contact conditions, and the concrete surface conditions. Consequently, it was felt that an independent assessment of impact-echo was necessary to evaluate its application for concrete pavement quality assurance.

3.2.2 Multi-Receiver Technique

In order to overcome the limitations of impact-echo described above, a second mechanical wave method was considered. This method, called the multi-receiver technique (MRT), uses reflected wave arrivals picked up by multiple receivers at different distances from the impact source. Figure 7 shows the instrumentation layout for the MRT.

The MRT makes use of simple time-domain p-wave reflection measurement that directly determines the pavement thickness without the need for external calibrations or concrete property assumptions. The MRT technique relies on detection and identification of the first p-wave reflection from the pavement-base interface. A schematic of the measurement configuration is presented in Figure 7. Working in the time domain, attention is generally focused on p-waves, since they have the highest propagation velocity. A mechanical wave source (impactor) acting at a point sends wave energy in hemi-spherical wavefronts in all directions within the pavement. The complete wave field is comprised of p-waves, S-waves (also called shear or transverse waves) and the Rayleigh surface wave. Thus the resulting wave phenomenon can be very complicated. Sensors that monitor the surface motion of the pavement are mounted on the surface. In this configuration, the first event recorded by the sensor at distance x1 from the impact location is the direct p-wave arrival along the surface (dashed line path in Figure 7), at time td1:

$$td1 = \frac{x1}{Vp} \tag{7}$$

From the geometric configuration, a p-wave reflected from an interface at depth h (solid line paths in Figure 7), will arrive at the same position at time tp1:

$$tp1 = \frac{\sqrt{x1^2 + (2 \cdot h)^2}}{Vp} \tag{8}$$

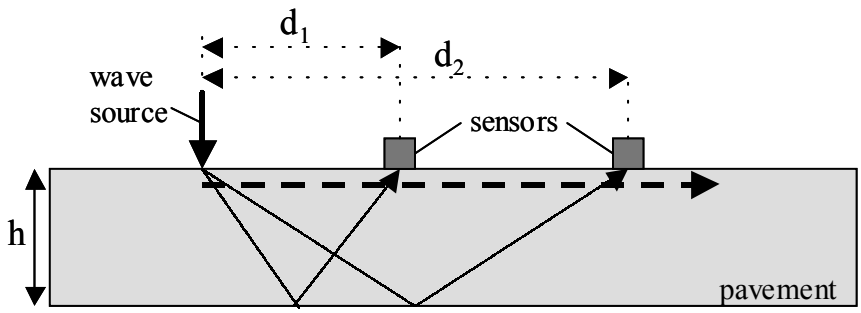

Figure 7 – Geometry of the Multi-Receiver Technique

Using the reflected p-wave arrival times for at least two positions, it is theoretically possible to calculate the thickness by solving for the two unknowns h and V_p:

$$h = \sqrt{\frac{x2^2 tp1^2 - x1^2 tp2^2}{4tp2^2 - 4tp1^2}}$$

and (9)

$$V_p = \sqrt{\frac{x2^2 - x1^2}{tp2^2 - tp1^2}}$$

Further, it is possible to make use of more than two sensors in this approach. The relationship between arrival time and distance is linear in the case of the direct arrival. In the case of the reflected p-waves, the relationship between the squares of time and distance is also linear. Therefore when squared reflected p-wave arrival time (tpi) 2 is plotted against squared sensor distance (xi) 2 for several (i) transducer locations, it becomes possible to fit the data to a straight line of the form:

$$y = a \cdot x + b \quad \text{where} \quad a = \frac{1}{Vp^2} \quad \text{and} \quad b = \frac{4 \cdot h^2}{Vp^2} \qquad (10)$$

Obtaining the slope (a) and y-intercept (b) of this line from a linear regression of data from multiple sensors, thickness can be determined using the following equation:

$$h = \sqrt{\frac{b}{4 \cdot a}} \qquad (11)$$

The multi-receiver approach has the benefit of naturally minimizing the effects of noise or inaccuracy that may be found in an individual signal.

3.3 Summary of NDE Methods

The methods described in this section are summarized below.

METHOD	TECHNOLOGY	APPLICATION	MEASUREMENT TYPE	MEASUREMENT RATE	PRIOR EXPERIENCE
Horn Antenna	Non-Contact GPR (electromagnetic)	asphalt	continuous	up to 9 m/sec (30 feet/sec)	extensive
Calibrated Single Antenna	Ground-Coupled GPR (electromagnetic)	asphalt or concrete	continuous	up to 1.5 m/sec (5 feet/sec)	none documented
Dual Antenna CMP	Ground-Coupled GPR (electromagnetic)	asphalt or concrete	point	estimated 2 min./point	limited for pavement
Impact-Echo	Mechanical Wave	concrete	point	estimated 30 sec./point	extensive
Multi-Receiver	Mechanical Wave	concrete	point	estimated 5 min./point	none documented

The summary table distinguishes the methods which are continuous vs. those which are "point". The continuous methods can collected data while the equipment is moved continuously along the pavement. The "point" methods must be set up to make a measurement at a particular point. An estimated rate of data collection has been indicated. Note that some of the methods are well established, while others are relatively new for this application.

4. Theoretical Evaluations

Theoretical studies were conducted in order to support the evaluation of the techniques described in Section 3. These studies provided an analytical framework for the horn antenna and CMP methods that were subsequently tested and evaluated in the field. In addition, the theoretical studies: (a) showed that the presence of tines in concrete pavement should not affect the implementation of the impact-echo method, and (b) confirmed the feasibility of the multi-receiver method and provided information on how it should be implemented.

4.1 Horn Antenna GPR

The horn antenna thickness equation (Equation (1) in Section 3) assumes that the GPR transmitter and receiver are in the identical location, and that the radar ray path is perpendicular to the pavement surface. These assumptions are standard for most GPR pavement thickness applications using the horn antenna. Due to the high degree of accuracy required for the QA application, these assumptions were reconsidered based on the true geometry of the transmitting and receiving horn antennas.

Figure 8 shows the type of horn antenna used for this project. The housing for the particular unit shown in this picture reveals the separate transmit and receive antennas. Figure 9 shows the geometry of the various ray paths associated with this antenna, including the direct coupling, the surface reflection, and the refracted transmission into and out of the pavement. This geometry is far more complex than the simple normal incidence model typically used. Alongside the model is a GPR scan showing the return pulses representing the key elements of the model. The first subscripts, d, p, and b refer to the direct coupling, the surface reflection, and the bottom reflection separately. The second subscripts, p and n, refer to the positive and negative part of the pulse, respectively.

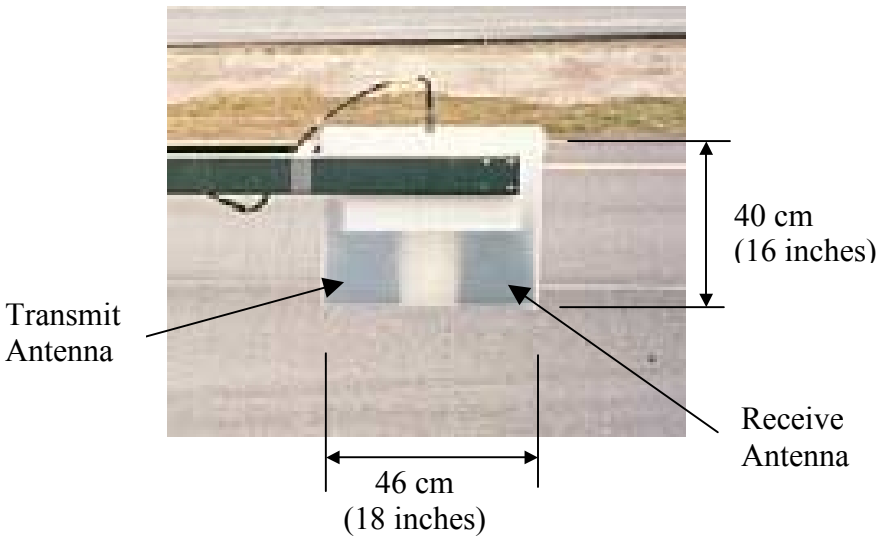

Figure 8 – Horn Antenna Geometry

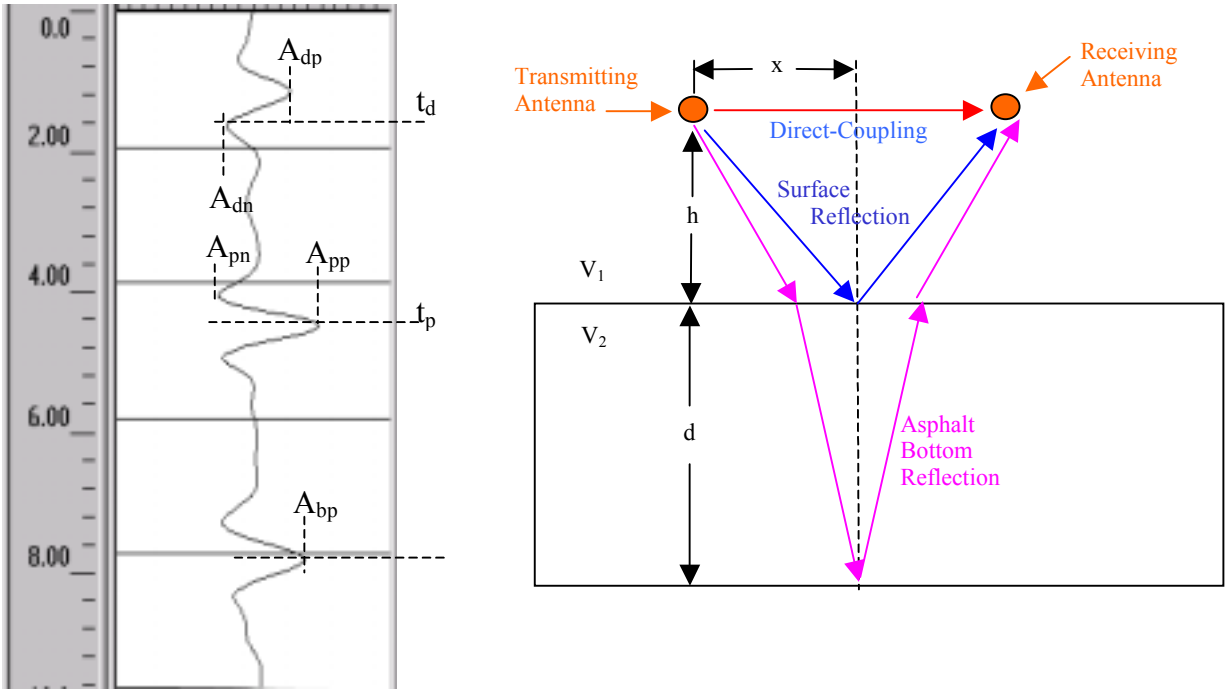

(a) Scan Showing Key Pulses (b) Geometry Showing the Two Antennas and Ray Paths

Figure 9 – Horn Antenna Model

The formulation of the thickness calculation based on the GPR scan and the geometry shown above is presented in Appendix A. The key differences between this formulation and the simplified one presented in Section 3 are:

1. Change in the asphalt GPR velocity calculation due to the angled ray path incident on the pavement surface;
2. Change in the travel time in the asphalt due to the angle of incidence and the refraction.

Two numerical studies were carried out using the Appendix A formulation to assess the magnitude of these differences.

The first study looked at the geometry effect on the pavement velocity calculation. The calculations of Appendix A were carried out for different antenna heights and different assumed asphalt dielectric properties. The results of the calculation are shown in Figure 10. The figure plots the percent difference between the geometric calculation of the pavement velocity and the one obtained using the simplified Equation (1). The results in the figure shows that the correctly calculated pavement GPR velocity ranges from 3.5% to 7.5% higher than what would normally be assumed. This difference depends on the antenna height and the pavement properties. The pavement property parameter used for this analysis is the reflection coefficient, ρ, which is allowed to range from 0.35 to 0.50. This is the typical range observed from field data. For the typical antenna operating height of 457 mm (18 inches), the difference ranges from 5% to 6%. What this means is that, using Equation (1) for thickness, the velocity should be 5% to 6% higher

than what is calculated in Equation (2). The increased velocity yields a proportionate increase in the calculated thickness.

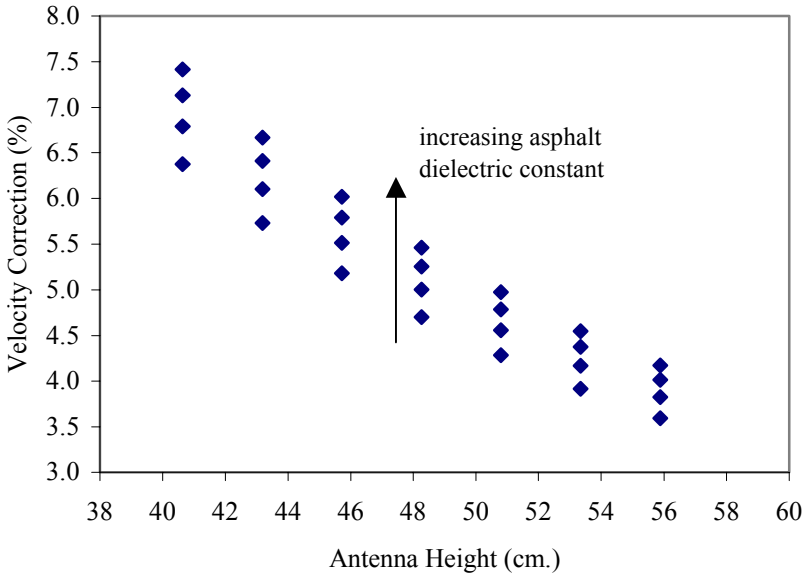

Figure 10 – Pavement GPR Velocity Correction
(using Figure 9 Geometry and Appendix A Equations)

The second study looked at the geometry effect on the calculation of the travel time in the asphalt. The actual travel time is longer than the perpendicular two-way travel time assumed in Eq. 1 due to the separation of the antennas and the refraction at the air-asphalt boundary. Therefore, equations (1) and (2) will overestimate the asphalt thickness. The degree of overestimation can be calculated using the equations of Appendix A. The result of such a calculation is shown in Figure 11.

In Figure 11, the percent difference between the perpendicular round trip and the refracted round trip time is presented as a function of the asphalt thickness. This difference also depends on the antenna height, which has been taken as 483 mm (19 inches) for this plot. One can see that the difference ranges from 1.3% to 1.9% over a range of thicknesses from 51 to 305 mm (2 to 12 inches).

Since this error results in an overestimation of asphalt thickness using Equation (1), it is opposite to the error associated with the computation of the GPR velocity. Therefore, the net error is in the range of 3% to 5%, or, in absolute terms, from 5 to 7.6 mm (0.2 to 0.3 inches) for a 155 mm (6 inch) thick pavement.

It is conceivable that one could incorporate these correction calculations into the data analysis software. The first correction is relatively simple, and could be incorporated into the standard antenna calibration procedure. The second correction, however, involves complex iterative calculations that would be cumbersome to implement. The alternative is to incorporate this correction as factor using the values established in Figure 11.

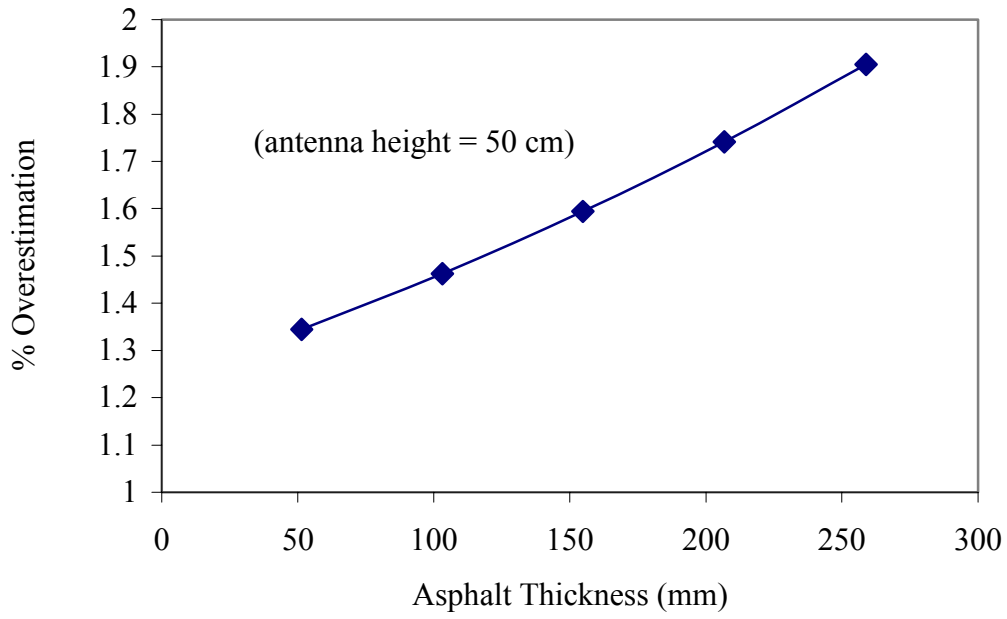

Figure 11 – Overestimation of Asphalt Thickness Due to Ray Path Geometry in Asphalt

4.2 Impact-Echo and Multi-Receiver Theoretical Calculations

In order to obtain a better understanding of the issues associated with the impact-echo and multi-receiver methods, a finite element model was formulated. This work was carried out by Professor John Popovics at Drexel University. The model was structured in such a way that results for both the IE and MRT methods could be simulated with the same basic model.

The Finite Element Simulation was carried out using the ABAQUS program. The 2- dimensional model was comprised of two layers, a 250 mm (10 inch) thick upper layer corresponding to the concrete pavement, and a 300 mm (12 inch) layer corresponding to the base. Four node bi-linear plane strain elements (CPE4 in ABAQUS Library) are used. All elements were of equal dimensions: 5 by 5 mm (0.2 x 0.2 inch) squares. The material definitions are summarized in Table 3.

Corresponding nodes on the surface between the two layers were tied in order to prevent relative displacements. Nodes corresponding to the lower surface of the base layer were restrained in the vertical direction. Also, energy absorbing boundaries were provided at the vertical sides so as to prevent reflection of stress waves. The impact was simulated as a half-sine pulse of 40 micro-second duration. The dynamic response of the structure was obtained in the time domain through direct integration using a 0.5 microsecond time-step. The load was applied to a single node located on the top surface at 0.5 m from one side (at point A). Vertical (out-of-plane) components of displacement and acceleration were recorded at points A and B using a time sampling frequency of 2 MHz.

Table 3 – Material Definitions for Finite Element Model

Material	Material Parameters			Wave Velocity	
	Density [kg/m**3]	E [MPa]	Poisson's Ratio	Compression [m/sec]	Surface [m/sec]
Concrete	2400	34560	0.2	4000	2225
Stiff Base (CTB)	2200	7330	0.25	2000	1059
Compliant Base (agg)	1920	200	0.3	347.5	188

Figure 12 shows the finite element mesh used for this modeling. Note that the 5 mm (0.2 inch) grid was chosen to be small enough to represent the depth of a tine. The influence of tined surfaces was one of the studies carried out with this model.

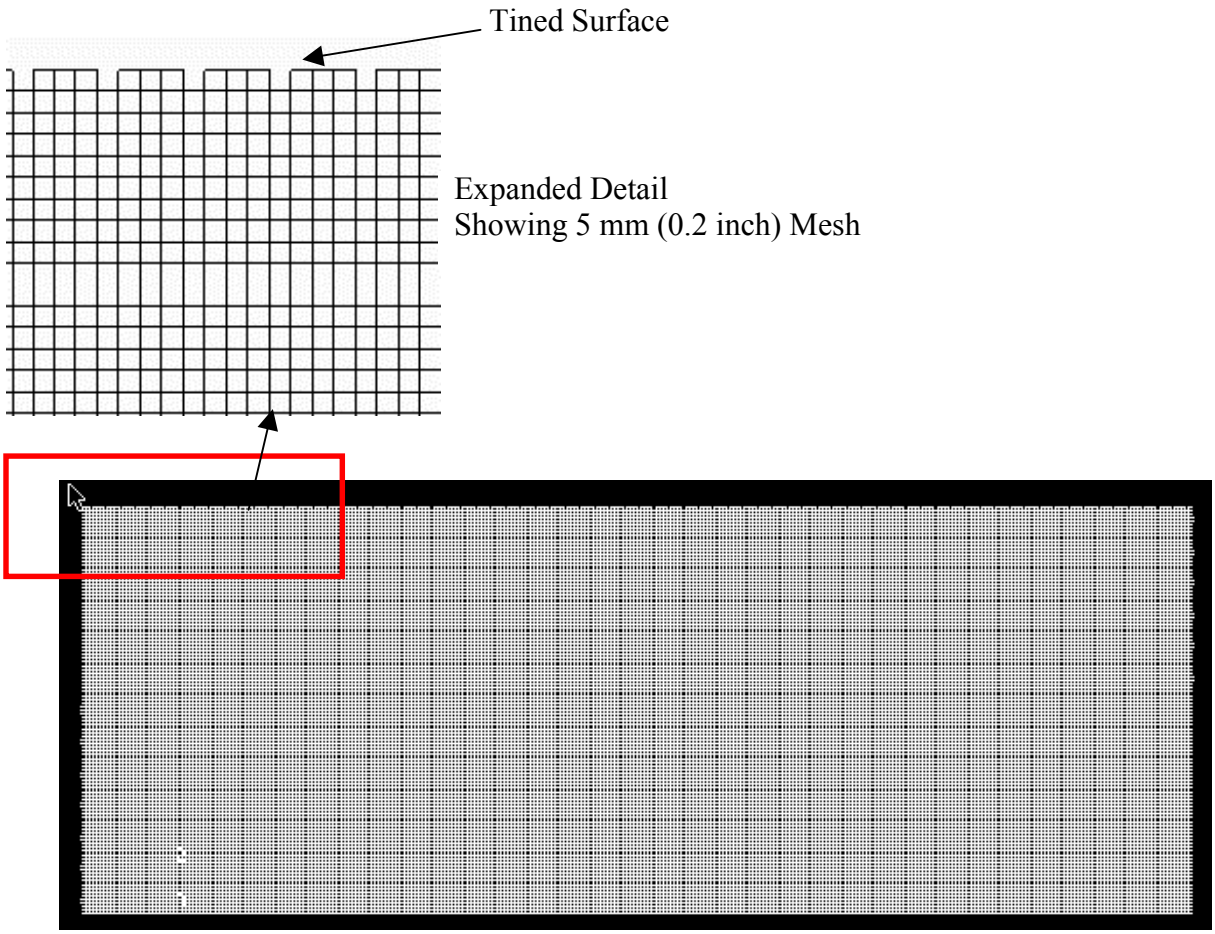

Figure 12 – Finite Element Mesh Representing Concrete Slab

4.2.1 Impact-Echo Modeling and the Effects of Tines

The finite element model was used to evaluate the influence of tines on the impact-echo measurement. The Caltrans concrete finishing specification, 40-1.10, specifies that "Spring steel tines of the final texturing device shall be rectangular in cross-section, 2.4 to 3.2 mm (0.09-1.25 inch) wide, on 19 mm (0.75 inch) centers, and of sufficient length, thickness and resilience to form grooves approximately 5 mm (0.2 inch) deep in the fresh concrete surface". Previous impact echo concrete thickness studies did not specifically mention tines, and there was some concern that the presence of tines would have some unexpected influence on the impact-echo method.

In order to model the effect of tines, two finite element models were used, one which had a smooth surface, and one which had a tined surface (as shown in the insert of Figure 12). The tine dimension in the "tine" model has been idealized, based on the element width, as 5 mm wide by 5 mm (0.2 x 0.2 inch) deep, with a centerline spacing of 17.5 mm (0.69 inch). These dimensions come fairly close to the specification. The model study considered three pavement thicknesses: 200, 250, and 300 mm (8, 10, 12 inches).

A typical result is shown in Figure 13. The red line in each plot represents a measurement point 5 mm (0.2 inch) from impact, and the blue line represents a measurement point 45 mm (1.8 inch) from the impact.

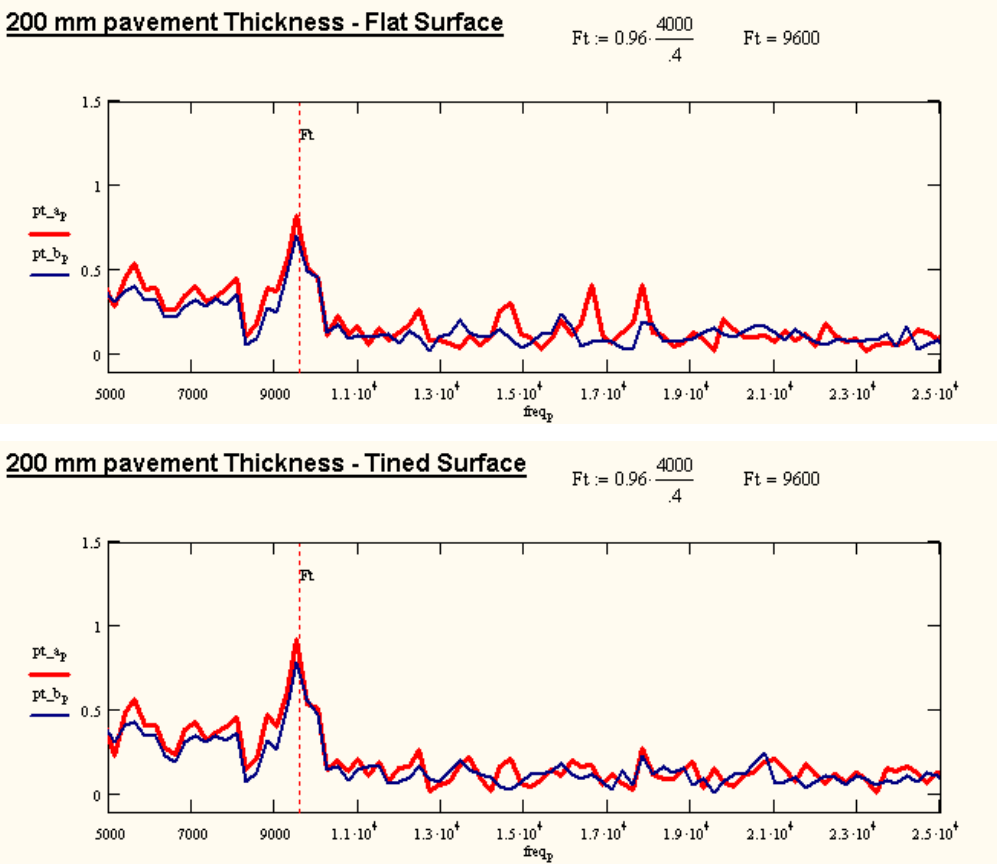

Figure 13 – Finite Element Model Results: Tines vs. Smooth Surface

The plotted data shows that the thickness resonance is not affected by the presence of tines. The vertical dashed lines in each plot represents the thickness resonance calculated from the ASTM specification formula. The plots show that this calculation agrees very closely with the output of the finite element model. Similar results regarding the influence of tines were obtained for the 250 and 300 mm (8, 12 inch) pavement models.

4.2.2 Modeling the Multi-Receiver Technique

The finite element model was used to simulate the multi-receiver technique. Through this simulation, it was possible to determine if the measurement was feasible, and how best to implement the measurement.

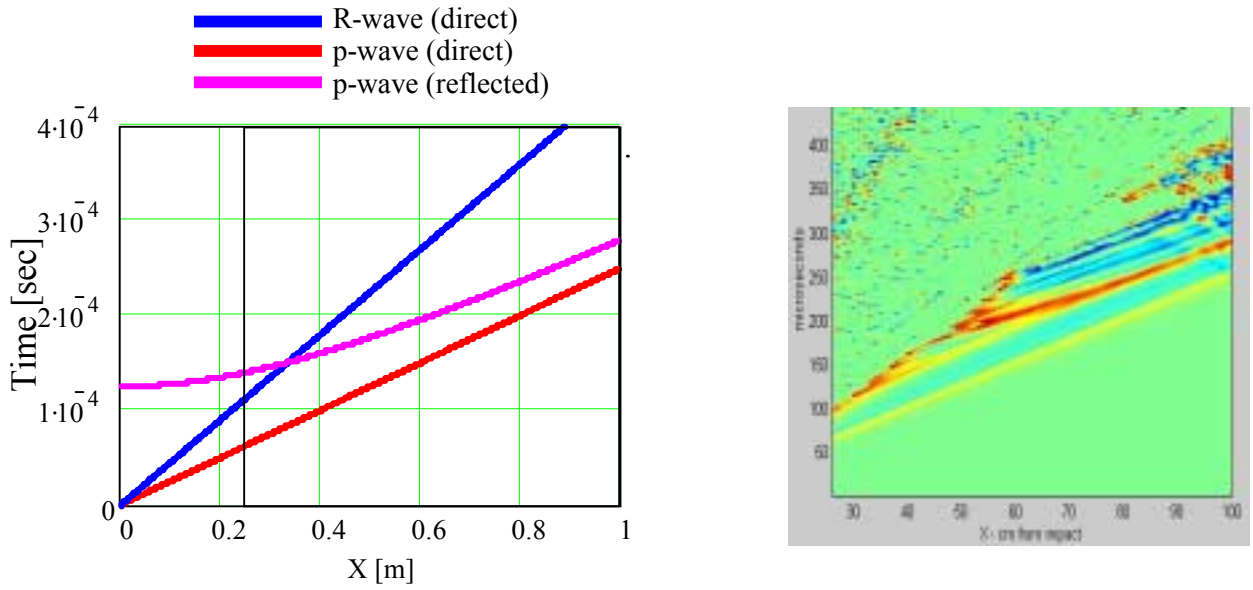

(a) Theoretical Arrival Times (b) Arrival Time From FEM

Figure 14 – Wave Arrival Times: Theory vs. Finite Element Model

Figure 14a shows the theoretical arrival times of the direct p-wave, the direct Rayleigh wave, and the reflected p-wave from the bottom of the concrete. Since the Rayleigh wave is of much higher amplitude, detection of the reflected p-wave has to occur at a distance greater than 0.35 meters (14 inches), after which the reflective wave will arrive sooner, and thus can be detected. Figure 14b shows the result of the finite element analysis, with the Rayleigh wave removed so that the lower amplitude signals can be visible. The represents the out-of-plane acceleration, and the colors represent the amplitude of this acceleration. The figure shows the direct p-wave arrival and the reflected p-wave arrival.

This numerical analysis demonstrated that it is possible to isolate the reflected p-wave pulse in the out-of-plane acceleration response, assuming an ultra-short duration (40 microsecond or less) impact source, more readily than from the in-plane acceleration or the displacement responses. The assumption that reflected arrivals are isolated for source-receiver spacing greater than two

times the pavement thickness, due to the arrival of the high amplitude Rayleigh surface wave, was also confirmed by the analysis. Within that spacing region, and assuming ultra-short impact, the first and second positive peaks of the out-of-plane acceleration signal were found to correspond to the expected arrivals of direct and reflected p-waves, respectively. Using the synthetic data produced by the FEM simulation, it was possible to isolate the reflected p-wave in the signal and compute the pavement thickness to within an accuracy of ± 1 mm.

4.3 Summary of Theoretical Studies

The theoretical studies described in this section have concluded the following:

1. Horn Antenna Method: Precise calculations of pavement thickness using the horn antenna must consider the complex ray path and refraction geometry. However, for a fixed antenna operating height the influence of this geometry can most likely be incorporated as a single calibration factor.

2. Impact-Echo Method: A simulation model has shown that the presence of tines on the pavement surface does not have any significant adverse impact on the impact-echo method.

3. Multi-receiver Method: Simulations models have confirmed the feasibility of this method. The models have shown that the p-wave reflection from the bottom of the pavement can be detected and distinguished from the direct p-wave arrivals. This separation occurs if a short (< 40 μsec) impact source is used, and if the arrival measurements are made at the appropriate distance from the source. The measurement is best made using out-of-plane (vertical) acceleration transducers.

5. Experimental Evaluations

A series of experimental arrangements were set up in order to resolve feasibility and accuracy issues associated with the various methods considered under this project. These arrangements included:

1. *Concrete and Mortar Slabs: These were used to simulate asphalt concrete for preliminary evaluation of ground-coupled antenna methods;*
2. *Oil Emulsion Tank: This was used to simulate asphalt of various thickness and dielectric properties for evaluation of GPR horn antenna and CMP methods;*
3. *Asphalt Test Pit: This was used to evaluation GPR horn antenna and CMP methods using real asphalt materials;*
4. *Variable Thickness Concrete Wall: This was used to evaluate impact-echo and CMP methods for concrete thickness.*

The laboratory tests confirmed the ability of the horn antenna and CMP GPR methods to accurately determine asphalt thickness, and the ability of the impact-echo method to accurately determine concrete thickness. The tests showed that the CMP GPR method was limited to asphalt thickness greater than 75 mm, and that it had difficulty with penetration of with young concrete. The tests also led to the elimination of the calibrated single antenna GPR method from further consideration.

5.1 Evaluation of Calibrated Single Antenna GPR Method

One possible GPR method, described in Section 3.2.1, used a single ground-coupled antenna for asphalt (and concrete) thickness evaluation in conjunction with a calibration curve. The calibration curve could relate the antenna direct coupling in the pavement material to the dielectric constant (and velocity) in the pavement material. In order to develop this calibration, a series of laboratory tests were conducted on available mortar slabs. Although they were made of cement mortar, the lack of large aggregate and the dry laboratory conditions gave them dielectric properties more similar to AC than to PCC.

A collection of Portland cement concrete blocks and discs, available at GSSI in New Hampshire, was used for this evaluation. Figure 15 shows all of the concrete blocks initially used in the investigation. The blocks have dielectric constants ranging from 4 to 9, a range which represents values typically found in asphalt (see Table 1). Figure 15 shows the arrangement of blocks evaluated during this study. The study was carried out using two different Model 5100 1.5 GHz antenna units. Data collection was carried out on 4 blocks and 2 discs. The dimensions of the selected blocks and discs were:

BLOCKS						DISCS			
LENGTH		WIDTH		THICKNESS		DIAMETER		THICKNESS	
M	FT	M	FT	MM	IN	M	FT	MM	IN
0.61	2	0.61	2	152	6	0.61	2	203	8
0.61	2	0.61	2	102	4	0.61	2	152	6
0.61	2	0.61	2	165	6.5				
0.61	2	0.61	2	43	1.7				

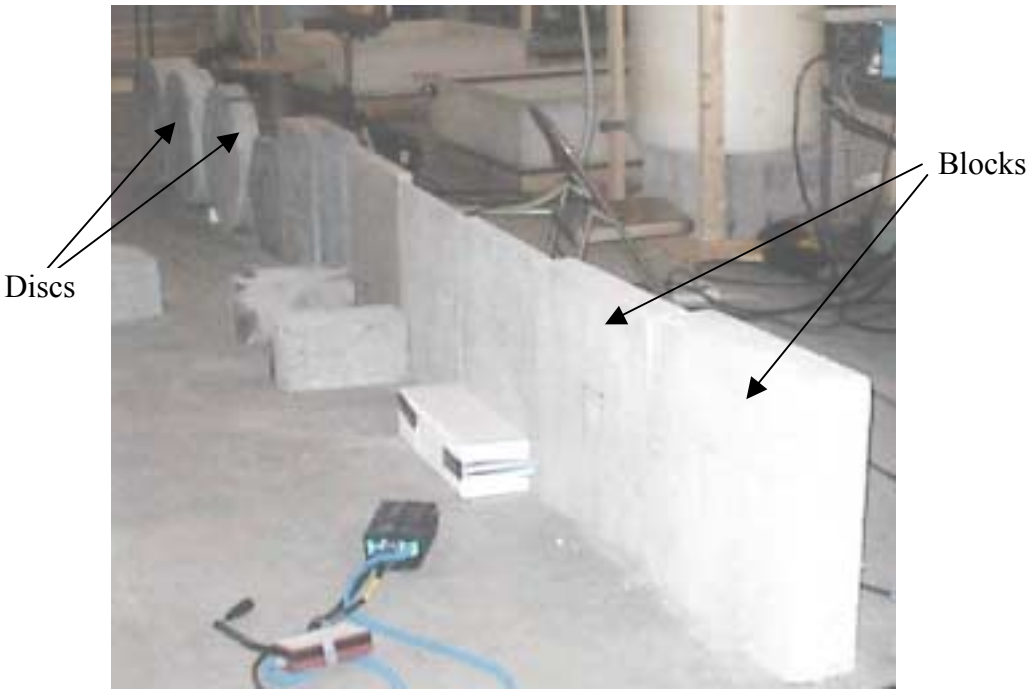

Figure 15 – Concrete Blocks and Discs Used in this Study

Data were subsequently collected with the antennas in direct contact with the surface of the blocks to generate a calibration curve used in calculating propagation velocities of unknown media. The true propagation velocities through the blocks were obtained using one-way travel time measurements and accurate measurements of the block thickness. The calculated velocities for the blocks versus the amplitude of the direct-coupling are shown in Figure 16.

There are four different datasets shown in Figure 16. The black circles are data from one of the antennas, denoted as Antenna #1 in the figure, collected on the unexposed side of the concrete blocks. The unexposed side is the side of the concrete block that was covered by plywood during the first 48 hours of curing. The blue circles are data obtained with Antenna #1 on the exposed side of the concrete blocks. Note the large differences in positive peak amplitude between the two datasets (black versus blue circles) from several blocks. This leads to the conclusion that the sides of the blocks cured differently, and inherently possess different near-surface propagation velocities. The direct-coupling measurement is only sensitive to the propagation velocity near the surface of the block. One significant assumption employed using the direct-coupling for velocity calculation is that the medium is homogeneous with respect to propagation velocity. This clearly is not the case for several of the concrete blocks, most notably the 610 mm by 205 mm (2 foot by 8 inches) circular disk and the 610 mm by 155 mm (2 foot by 6 inch) circular disk.

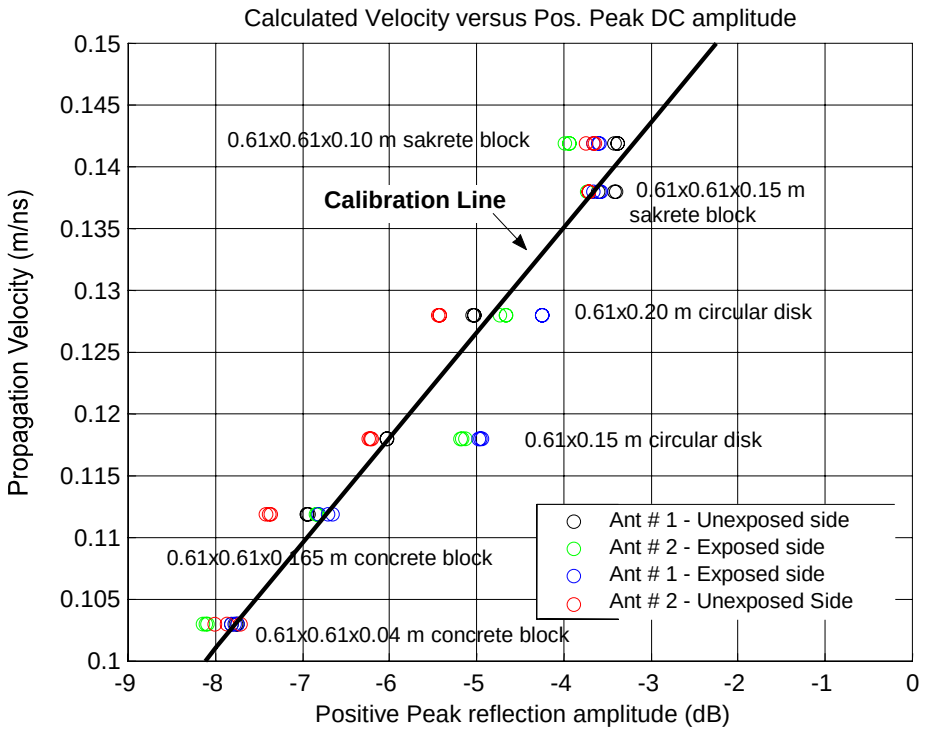

Figure 16 – Normalized Positive Direct-Coupling Peak vs. Propagation Velocity Obtained From a Series of Measurements on Velocity-Calibrated Concrete Blocks

The data in Figure 16 was used to define the calibration line shown, based on the best fit through the data points. This calibration line was then used for thickness evaluation of a second series of slabs as follows. Ground-coupled data was collected with the single model 5100 antenna on a set of Sakrete blocks ranging in thickness from 27 to 152 mm (1.06 to 5.98 inches). The data processing sequence for these data comprised:

1. Locating and recording the direct-coupling amplitude of each scan, and

2. Locating and recording the reflection arrival time from the concrete bottom relative to the arrival time of the direct-coupling.

The concrete propagation velocity for each scan was subsequently calculated using the calibration line of Figure 16, and the thickness was calculated using Equation (3). The data obtained from antenna #1 are shown in Figure 17.

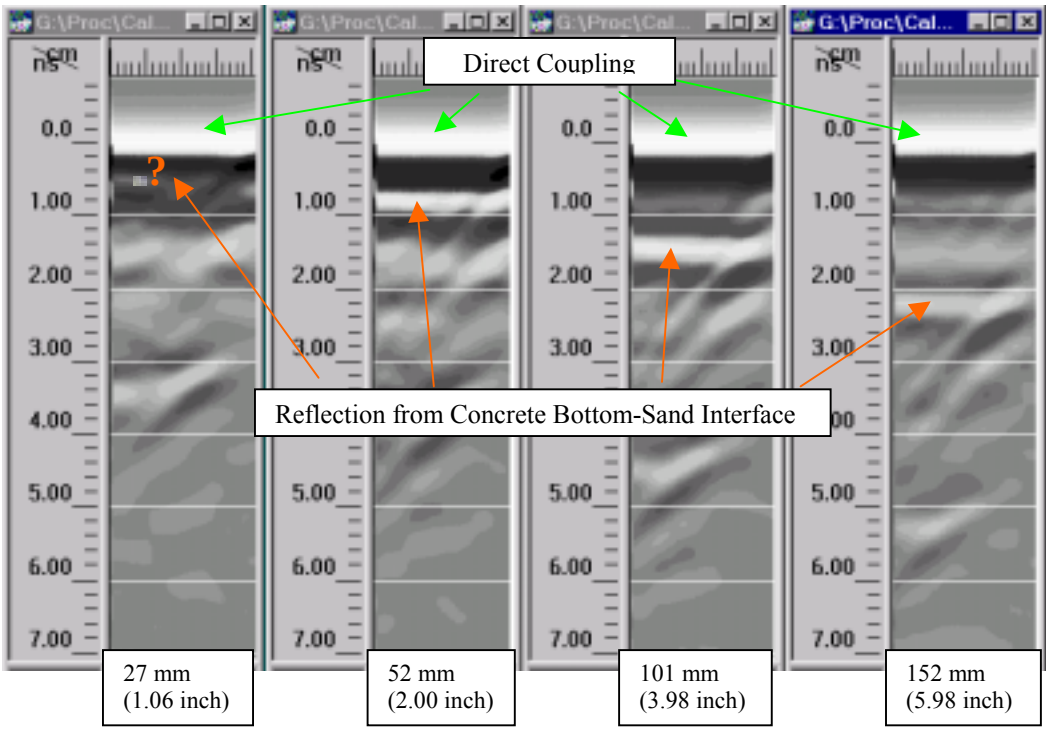

Figure 17 – Sample Data of Single Ground-Coupled Antenna on Sakrete Blocks

Table 4 presents the concrete thickness for the blocks obtained using a 25 scan average from the ground-coupled data.

Table 4 – Results for Single Ground-coupled Antenna

BLOCK THICKNESS (MM)	INTERFACE	CALC VEL (MM/NS)	CALCULATED THICKNESS (MM)	ERROR (MM)
27	MP*	179	NA**	
27	MP	195	NA	
27	Sand	141	NA	
27	Sand	140	NA	
51	MP	146	50	-1
51	MP	142	48	-3
51	Sand	147	51	0
51	Sand	145	50	-1
101	MP	146	101	0
101	MP	141	101	0
101	Sand	151	103	2
101	Sand	141	102	1
152	MP	145	160	8
152	MP	144	158	6
152	Sand	144	160	8
152	Sand	142	160	8

*MP = Metal Plate., **NA = Could not be determined

The table shows data collected with the block resting on a metal plate as well as on sand. The metal plate condition produced the strongest bottom reflection, and thus represents and ideal condition. Examination of the data provided in Table 4 reveals very good depth calculation results for the 51 and 102 mm (2.00 and 3.98 inch) concrete blocks. The calculated block thickness values obtained from data collected over the 152 mm (5.98 inch) concrete block deviate from the actual thickness by an average of 7.6 mm (0.3 inch). It is not clear why there is such a large discrepancy considering that the direct-coupling data from this block were used in the fitting of the velocity calibration line. No thickness calculations were possible from 27 mm (1.06 inch) thick concrete block data because the reflection from the concrete bottom could not be isolated from the direct coupling.

5.2 Oil Emulsion Tank Simulated Asphalt Testing of GPR Methods

The oil emulsion tank testing provided a controlled laboratory environment for evaluation of the GPR asphalt thickness methods representing a range of thickness values and simulated asphalt properties. The goals of the emulsion testing were to evaluate the accuracy of the different GPR methods and to see how that accuracy depended on the thickness and asphalt properties.

The emulsion testing was carried out at GSSI and is shown in Figure 18. The setup consisted of a large 570 liters (150 gallon) polypropylene storage vat connected via hoses and a gear pump to a

1.3 x 1.3 x 0.3 meter (47 x 47 x12 inch) polypropylene box used for data collection. The emulsion consists of a mixture of canola oil, distilled water and sodium lauryl sulfate. The sodium lauryl sulfate acts as the emulsifier. The radar propagation velocity in the emulsion is determined by the canola oil/water weight ratio of the emulsion.

The emulsion test was designed to approximate three different radar wave velocities simulating the range of propagation velocities typically observed in asphalt. Consequently, three different emulsions were mixed to obtain propagation velocities of approximately 15.3 cm/ns (5.9 inches/ns) (dielectric constant = 4), 13.7 cm/ns (5.4 inches/ns) (dielectric constant = 5.5), and 11.4 cm/ns (4.5 inches/ns) (dielectric constant = 7). Four different asphalt thicknesses (25, 76, 127, and 203 mm (1, 3, 5, 8 inches) were simulated by pumping the appropriate amount of emulsion out of the storage vat to cover a metal sheet placed at the bottom of the data collection box.

Data collection was initiated using the highest propagation velocity (lowest dielectric) emulsion. Subsequent reductions in velocity (and increases in the dielectric constant) are achieved by addition of water to the emulsion and remixing. Both horn antenna (GSSI Model 4108) and ground-coupled antenna (model 5100) data were collected for each of the four emulsion thicknesses. Model 4108 antenna data were obtained over the emulsion as shown in Figure 18. The antenna bottom was elevated approximately 51 cm (20 inches) above the emulsion surface for each measurement. Immediately following each horn antenna measurement over the emulsion, the horn antenna was moved over a metal sheet placed on the floor and data were collected for amplitude calibration purposes.

After collecting the horn antenna data a 3 mil polyethylene sheet was placed on top of the emulsion and the common-midpoint (CMP) setup containing the model 5100 antennas was placed on the emulsion as illustrated on Figure 19. Data were collected using the CMP setup placed on top of a 102 mm (4 inch) thick pad of Styrofoam for emulsion thicknesses of 25 and 76 mm (1 and 3 inches). CMP datasets were collected with the antennas in direct contact with the polyethylene sheet for emulsion thicknesses 76 mm (3 inch) and greater. The c-clamps shown in Figure 4 held the CMP setup so that it was effectively floating on the emulsion without displacing any emulsion underneath. Immediately after collecting the CMP data over the emulsion, a measurement was made with the CMP setup placed on a metal plate for calibration purposes. Tests using a single model 5100 antenna were also carried out using the polyethylene sheet.

Figure 18 – Data Collection Over the Emulsion Using the Model 4108 Horn Antenna

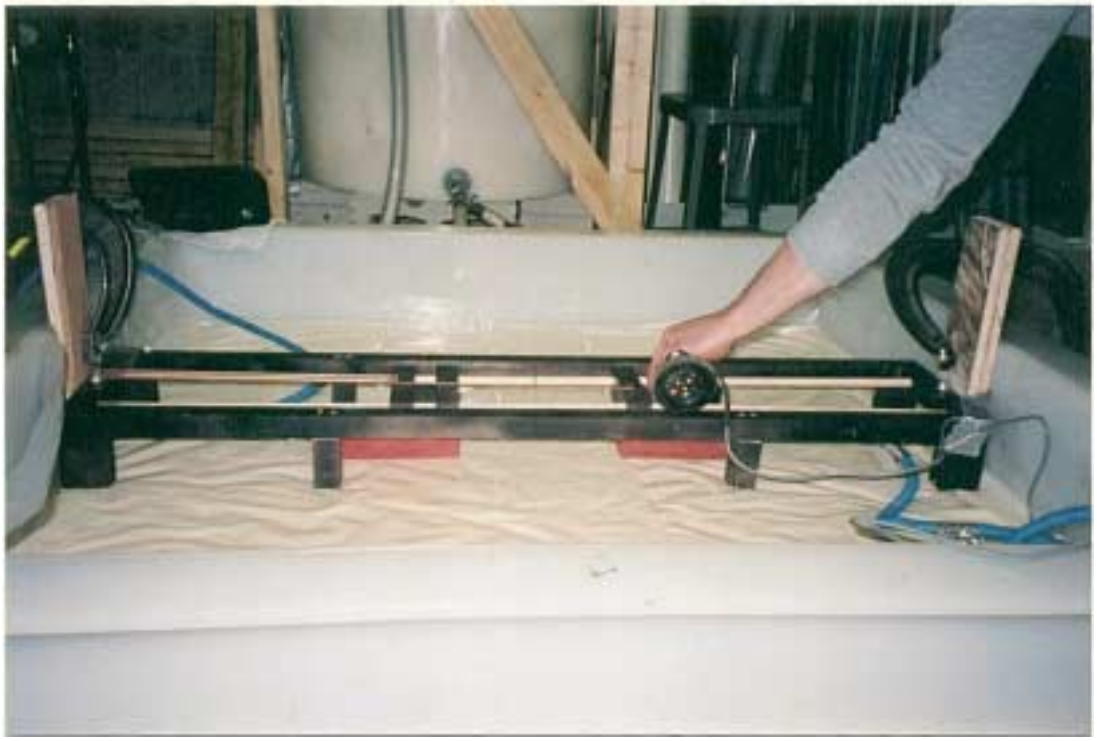

Figure 19 – CMP Setup in Emulsion Tank

Data analysis was carried out using the principles described in the previous sections. The details are described below.

5.2.1 Horn Antenna Data Analysis

The Model 4108 horn antenna data were collected with the antenna bottom positioned approximately 508 mm (20 inches) above the emulsion surface. Each measurement consisted of 128 scans using the following system (SIR-10H) control settings:

Scans/Sec	25
Samples/Scan	1024
Time Range (ns)	10
Filters	None
Transmit Mode	Standard

The data processing sequence applied to the horn antenna data required additional scans of data obtained using the same control settings. One set of scans was collected with the antenna placed at various heights above a large 1067 by 1181 mm (42 x 46.5 inches) metal sheet. This type of data is commonly referred to as metal plate calibration data. A second set of scans were obtained with the antenna bottom hoisted approximately 300 cm (10 feet) in the air and facing in the horizontal direction. These data are referred to as air-wave calibration data.

The processing steps applied to the horn antenna data are detailed below:

1. All Emulsion data were stacked. Basically, each 128 scan measurement was averaged to obtain 1 output scan.
2. The metal plate calibration data and air-wave calibration data were stacked.
3. All data were subjected to a low-pass Hamming FIR filter with a cutoff frequency of 3000 MHz.
4. All data were subjected to a high-pass Hamming FIR filter with a cutoff frequency of 500 MHz.
5. The location of the direct-coupling reflection was identified in all of the scans.
6. The air-wave calibration scan was subtracted from the metal plate calibration scans and the emulsion data scans.
7. The surface reflection was located in all of the metal plate calibration scans and emulsion scans.
8. The metal plate scan corresponding to the closest antenna height relative to the antenna height during data collection over the emulsion was found for each emulsion scan.
9. The radar propagation velocity inside the emulsion was calculated using the ratios of the metal plate and emulsion surface reflection amplitudes (normalized relative to the direct-coupling amplitudes of each scan), antenna height and the separation distance between the transmitting and receiving antennas. (See Appendix A)

10. The amplitude of the metal plate calibration scan was normalized to the amplitude of each emulsion scan and subsequently subtracted from each emulsion scan.
11. The reflection from the bottom of the emulsion was located.
12. The arrival time of the reflection from the bottom of the emulsion, the calculated radar propagation velocity, antenna height and transmit/receive antenna separation distance values were used to back-calculate the emulsion thickness. (see Appendix A.)

5.2.2 CMP Data Analysis

The CMP data collected over the emulsion were obtained using two model 5100 antennas mounted inside the CMP apparatus. The fixture was designed to provide quick and accurate CMP measurements. Data are collected by placing the antennas so that they are in contact, as shown in Figure 20a, and are slowly moved apart at the same rate from each other as shown in Figure 20b. The midpoint between the antennas remains fixed with respect to the medium.

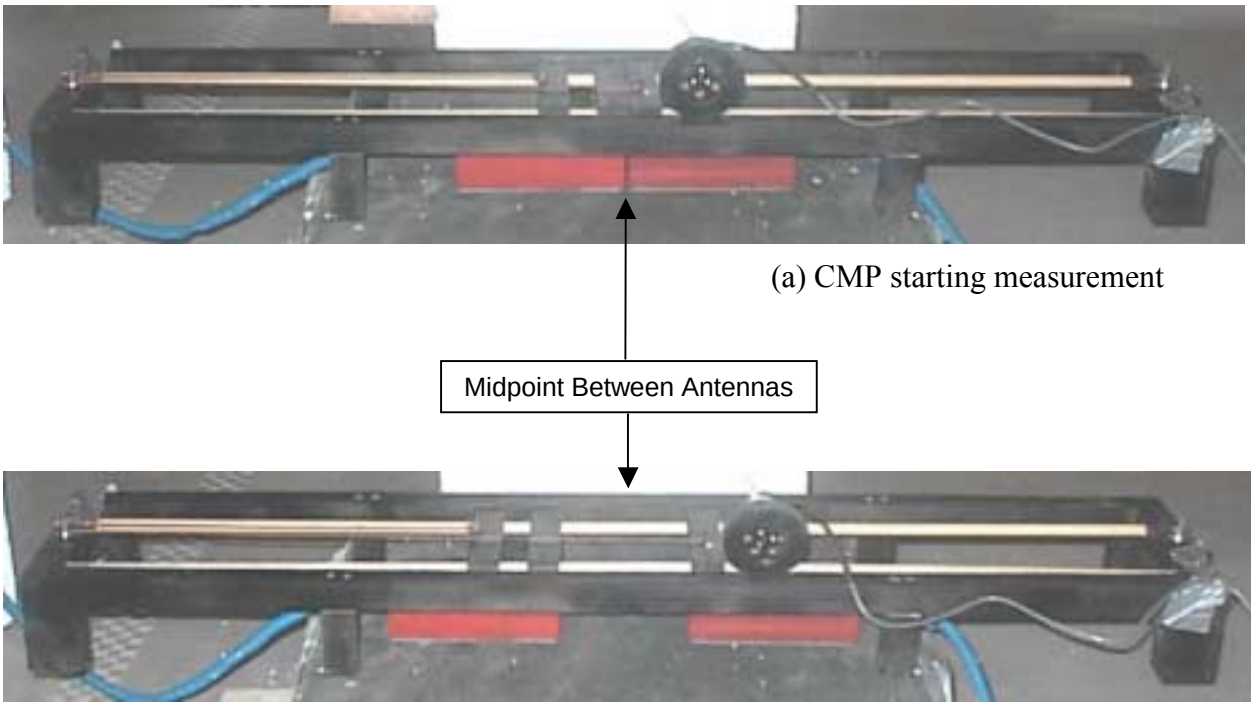

(a) CMP starting measurement

(b) CMP measurement in progress

Figure 20 – CMP Test Fixture Designed for Data Collection in the H-Plane Orientation.

The SIR-10H system settings used during data collection of the H-Plane CMP data are shown below.

Scans/Sec	30
Samples/Scan	512
Time Range (ns)	8-12
Filters	None
Transmit Mode	Standard

A 128 scan measurement with the two model 5100 antennas positioned 10 cm (4 inches) above a metal sheet was made immediately following each CMP measurement. This measurement was used as a time-zero reference point.

The data processing steps applied to the CMP data and the time-zero measurement are detailed below:

1. The 128 scans comprising the time-zero reference measurement were stacked to obtain one output scan.
2. The CMP data file was appended to the file containing the stacked time-zero scan.
3. Each resulting data file was subjected to a low-pass Hamming FIR filter with a cutoff frequency of 3000 MHz.
4. A routine was implemented to pick the reflection arrivals from the metal sheet in all of the scans.
5. The true time-zero was back-calculated from the reflection arrival of the metal sheet in the time-zero reference scan.
6. The true travel-times of all of the metal sheet reflections from the bottom of the emulsion are calculated using the time-difference between their respective arrival times and the true time-zero obtained in (5).
7. The separation distance between the transmitting and receiving antennas for each CMP scan is obtained using the initial separation distance and the separation distance increment between scans.
8. The time and distance values calculated in (6) and (7) are squared and put into a routine that calculates the least-squares-fit line through all of the data points.
9. The calculated propagation velocity through the emulsion is the square-root of the slope of the line and the calculated emulsion depth is the y-intercept of the line.

The first twenty-five scans are typically used in the calculation for layers with anticipated depths of less than 15 cm and the first 50 scans are used for deeper layers. Using a greater number of scans in the least-squares fitting routine had an adverse affect on the routine's performance. The processed data results are shown in Tables 2 and 3.

5.2.3 Analysis of Single Channel Ground-Coupled Data

At the same time the CMP data were collected, fixed-offset transmit-receive antenna data were also obtained. The fixed offset mode is the most common type of data collection implemented for general GPR applications. The following SIR-10H settings were used for collecting these data.

Scans/Sec	30
Samples/Scan	512
Time Range (ns)	8-12
Filters	None
Transmit Mode	Standard

Immediately following data collection a calibration measurement was made with the antennas radiating in air. This measurement served two purposes: (1) provide a reference amplitude for the velocity calculation, and (2) provide a time-zero used in the depth calculation. The data processing steps applied to the data are listed below.

1. The 128 scans comprising the calibration measurement were stacked to obtain one output scan.
2. The ground-coupled data file was appended to the file containing the stacked calibration scan.
3. Each resulting data file was subjected to a low-pass Hamming FIR filter with a cutoff frequency of 3000 MHz.
4. A routine was implemented to pick the direct-coupling arrival and the reflection arrivals from the metal sheet at the bottom of the emulsion in all of the scans.
5. The true travel-times of all of the metal sheet reflections from the bottom of the emulsion are calculated using the time-difference between their respective arrival times and the time corresponding to the peak of the direct-coupling arrival in the calibration scan.
6. The propagation velocity through the emulsion was calculated using the amplitude of the direct-coupling of each scan normalized relative to the direct-coupling amplitude of the calibration scan. This value was input into an equation describing normalized amplitude versus propagation velocity that was obtained from previous calibration measurements (see Figure 16). The output of the equation was the calculated propagation velocity.
7. The depth of the emulsion was calculated from a quadratic equation (Equation (3), Section 3.1.2.1) using the calculated propagation velocity (6), the emulsion bottom reflection time (5), and the known separation distance between the transmitting and receiving antennas.

5.2.4 Results of Emulsion Testing

The results of the data analysis of the three series of tests are summarized in Table 5. The table shows results for three different thicknesses and three different mix formulations, or a total of nine different simulated asphalt configurations. These nine configurations were evaluated with each of three antenna configurations.

Table 5 – Emulsion Test Results for the Three Antenna Configurations

EMULSION MIX	ACTUAL DEPTH (MM)	CALC. DEPTH (MM)	ERROR (MM)	CALCULATED VELOCITY (MM/NS)	CALCULATED DIELECTRIC
Horn Antenna (Model 4108) Results—					
1	74	72	-2	142	4.47
1	128	124	-4	140	4.59
1	200	179	21*	125	5.79
2	74	71	-3	131	5.27
2	122	119	-3	129	5.41
2	197	195	-2	126	5.68
3	74	68	-6	117	6.59
3	124	124	0	116	6.65
3	198	203	5	117	6.59
Dual Ground-Coupled Antenna (Model 5100) CMP Results—					
1	74	73	-1	157	3.63
1	128	123	-5	149	4.06
1	200	196	-4	138	4.7
2	74	78	4	145	4.3
2	122	112	-10	131	5.24
2	197	199	2	131	5.23
3	74	70	-4	132	5.13
3	124	123	-1	120	6.26
3	198	196	-2	113	7.12
Single Ground-Coupled Antenna (Model 5100) Results—					
1	74	62	-12	140	4.6
1	128	117	-11	144	4.34
1	200	195	-5	141	4.51
2	74	66	-8	134	4.99
2	122	119	-3	137	4.77
2	197	195	-2	133	5.07
3	74	62	-12	126	5.64
3	124	125	2	127	5.6
3	198	221	23	127	5.55

* problems in obtaining uniform emulsion mixing for this test

Table 6 summarizes the results of the tests listed in Table 5.

Table 6 – Summary of Emulsion Tank Test Results

METHOD	ERROR (MM)		
	AVERAGE	STDEV	AVERAGE ABS.
Horn Antenna*	-2	3	3
Ground-coupled CMP	-2	4	4
Ground-coupled Single Antenna	-3	11	9

The results can be summarized as follows:

1. Horn Antenna: The error for 7 of the 9 tests is within 4.5 mm (0.18 inch). One of the two with larger errors had a problem with the uniformity of the emulsion, a condition which is likely to produce an error with this method. This test data has been removed from the Table 6 results. There is a slight tendency to underestimate the thickness.
2. Ground-Coupled CMP: The error for 8 of the 9 tests is within 4.8 mm (0.19 inch). There is also a tendency to underestimate the thickness.
3. Single Ground-Coupled Antenna: The error is significantly larger for this method than for the other two methods. With the exception of one reading, all the errors appear to be negative, and could be reduced with some type of bias correction.

One other result not described above is that for the 25 mm (1 inch) emulsion layer thickness. None of the methods functioned properly in this condition, with different reasons for different methods. Note that the bottom condition for the emulsion "slab" was a metal plate. This condition served to maximize the refection from the bottom, and thus produce a "best case" condition. However, the metal plate causes problems for the horn antenna when it is so close to the emulsion surface. The reflection is so large that it is hard to locate the top of the emulsion in the data. This does not necessarily mean that the method cannot detect a 25 mm (1 inch) layer. On the contrary, studies have been carried out on pavement with thin overlays, and the results show that the horn antenna method is capable of detecting surface layer thickness down to 25 mm (1 inch) (*4*).

The ground-coupled methods did not work for the 25 mm (1 inch) thickness for different reasons. The CMP method requires a minimum thickness in order to separate the reflected GPR wave from the direct wave. Previous tests on concrete blocks indicated that this minimum thickness would be 76 mm (3 inch). The single antenna method requires a minimum thickness in order to separate the reflected GPR wave from the pavement bottom from the antenna direct coupling. Tests on the concrete blocks indicated that this minimum thickness needed to be 51 mm (2 inch).

5.3 Asphalt Test Pit

The emulsion tank provided some very clear information regarding the capability of the different GPR methods. The conditions, however, were idealized for simplicity. The tank bottom was a metal plate to maximize the bottom reflection, and the material was not actually asphalt. The objective of the test pit was to provide a means for testing the GPR asphalt thickness measurement methods under realistic asphalt conditions.

The test pit was prepared by Worcester Polytechnic Institute, MA under subcontract to Infrasense. The dimensions of the pit were 5 meters long by 1.2 meters wide by 533 mm deep (16 ft x 4 ft x 21 inches). Crushed stone aggregate was placed in the pit to four different heights (330, 381, 432, and 483 mm) (13, 15, 17, 19 inches). Asphalt was placed on top of the base, so that four slabs of different thickness (50, 100, 150 and 200 mm) (2, 4, 6, 8 inches) were available for testing. This arrangement was repeated a second time with a different asphalt mix. Figure 21 shows a cross section of the pit.

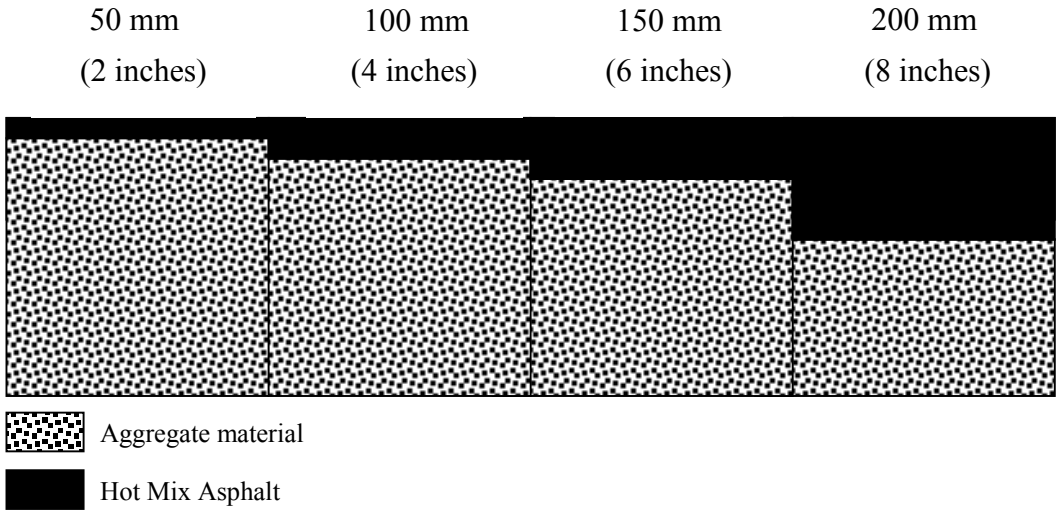

Figure 21 – Cross Section of Test Pit

Once constructed, the individual 1.2 m (4 foot) long pits were separated by piece of plywood. The pits were filled with a dense graded asphalt mix from Bardon Trimount's Wrentham plant. The mix meets the gradation and voids requirement of Type A mix used by Caltrans. The aggregate gradation is as follows:

SIEVE SIZE	PERCENT PASSING
19 mm	100
13 mm	95-100
10 mm	75-90
No. 4	55-61
No. 8	40-45
No. 30	20-25
No. 200	3-7

The difference between the two asphalt mixes was the aggregate source. For the first mix, the aggregate was a schist material from Ashland, while the second source used was predominantly feldspar from Wrentham. Since aggregate is the predominant constituent of the asphalt, it was felt that the different sources would yield differences in the GPR response.

The test pit during construction and after completion is shown in Figure 22.

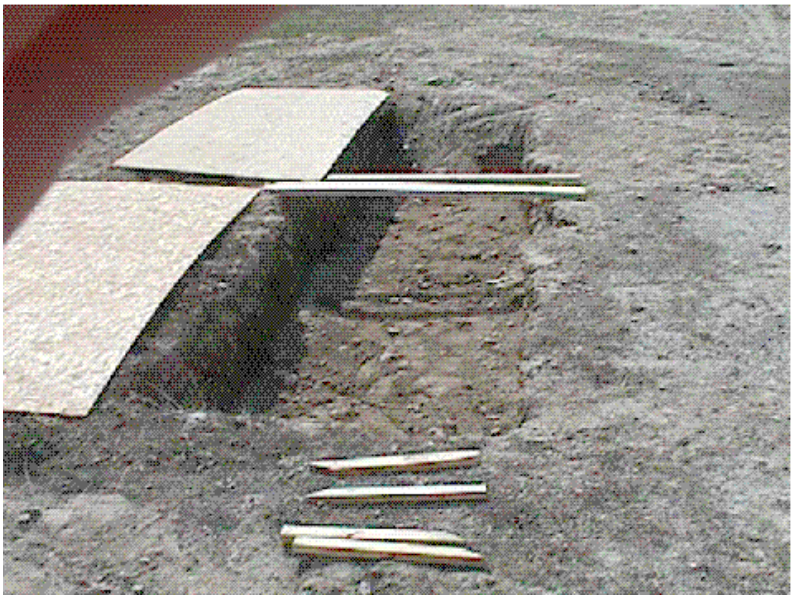

(a) Test Pit During Construction

(b) Asphalt Surface After Completion

Figure 22 – Asphalt Test Pit

Tests were carried out on the asphalt slabs of the test pit using the horn antenna and CMP methods, as shown in Figure 23.

(a) Using Horn Antenna

(b) Using Ground-Coupled Antennas with CMP Method

Figure 23 – Data Collection on Test Pit

A test grid was marked on the asphalt surface with grid lines spaced at 381 mm (15 inches). For the horn antenna tests, the antenna was mounted to the back of a vehicle using a modified bicycle rack, and traversed continuously along the three longitudinal grid lines (Figure 23a). Data was collected continuously at a rate of 30 scans per second. Manual markers were placed in the data when the centerline of the antenna crossed a transverse grid line. The CMP measurements were made at the grid intersection points, as shown in Figure 23b. The CMP mechanism shown in the figure is an upgraded version of the one that was used for the laboratory emulsion tests. The upgrade was designed to make the equipment more robust for field use.

After the tests were completed, a series of cores were taken. The cores were taken at the grid intersection points and in the center of grid cells. Five cores were taken for each thickness slab, or a total of 20 cores for each of the two asphalt mixes. Figure 24 shows the core layout.

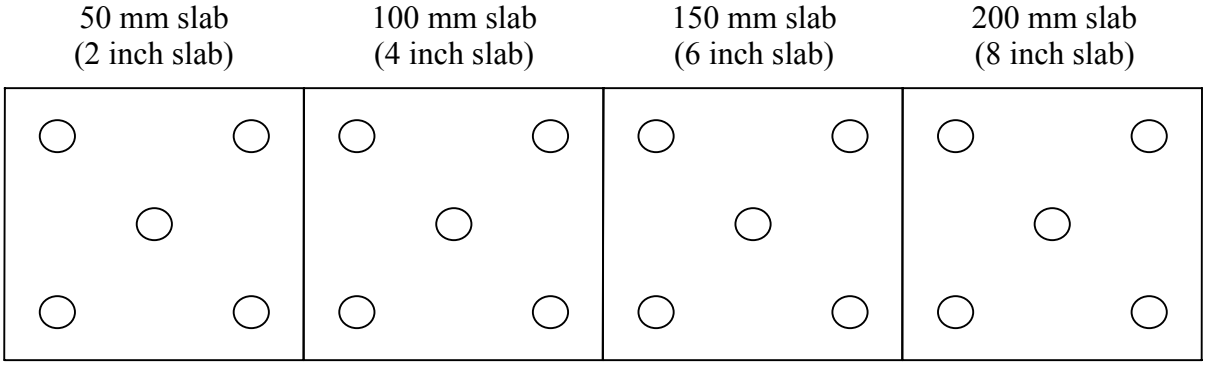

Figure 24 – Layout of Test Pit Cores

The data was analyzed for thickness, and cores from the test pit were compared with the thickness values calculated from the horn and CMP data. Table 7 summarizes the average of the five thickness values for each slab obtained for this comparison.

Table 7 – Average Thickness Values for Test Pit Slabs

	Test Slab	Core (mm)	GPR (mm)		Difference (mm)	
			CMP	Horn	CMP	Horn
Test Pit 1 (open graded base)	50	68	35	67	-32	-1
	100	105	109	82	3	-24
	150	140	139	116	0	-24
	200	191	210	182	19	-9
Test Pit 2 (uniform/dense graded base)	50	67	n.a.	72	n.a.	5
	100	120	130	119	9	-1
	150	163	173	172	10	9
	200	205	216	222	11	17

Table 7 data shows that the CMP method was not capable of detecting asphalt thickness in the neighborhood of 69 mm (2.7 inches). This finding is consistent with the earlier observation that the method was not able to detect thickness for asphalt less than 75 mm (3 inch) thick. Table 7 also shows that the horn antenna method was able to handle the entire thickness range. For the thickness range of 100 to 200 mm (4-8 inches), the difference between the core and both the horn and CMP values is larger than anticipated.

The larger differences between the core and GPR data encountered in Test Pit #1 were partially attributed to the lack of contrast with base material. Apparently the base had been formulated as an open graded material, considered ideal for drainage purposes, but unlike the uniformly graded material typically used for pavement bases. The effect on the GPR methods is that open graded materials have lower moisture content, and less dielectric contrast with the asphalt. Therefore, the asphalt bottom was not clear at a number of locations in Test Pit #1. Caltrans does employ open graded bases in some circumstances, and this condition may require some more detailed investigation for future use of this technology.

For Test Pit #2 the base material was replaced with a more typical uniformly graded base material, and the results were improved. However the discrepancies with the cores were still considered to be larger than desired.

One of the issues with the test pit is, that due to its relatively small size, the construction including the asphalt placement and compaction was carried out with hand equipment. As a result, the layer boundaries and structure appeared to be much less uniform that is normally seen on a constructed pavement. Figure 25 shows a sample of horn antenna data collected on the test pit. Note that there appear to be layer boundaries other than those associated with the asphalt bottom and the bottom of the base.

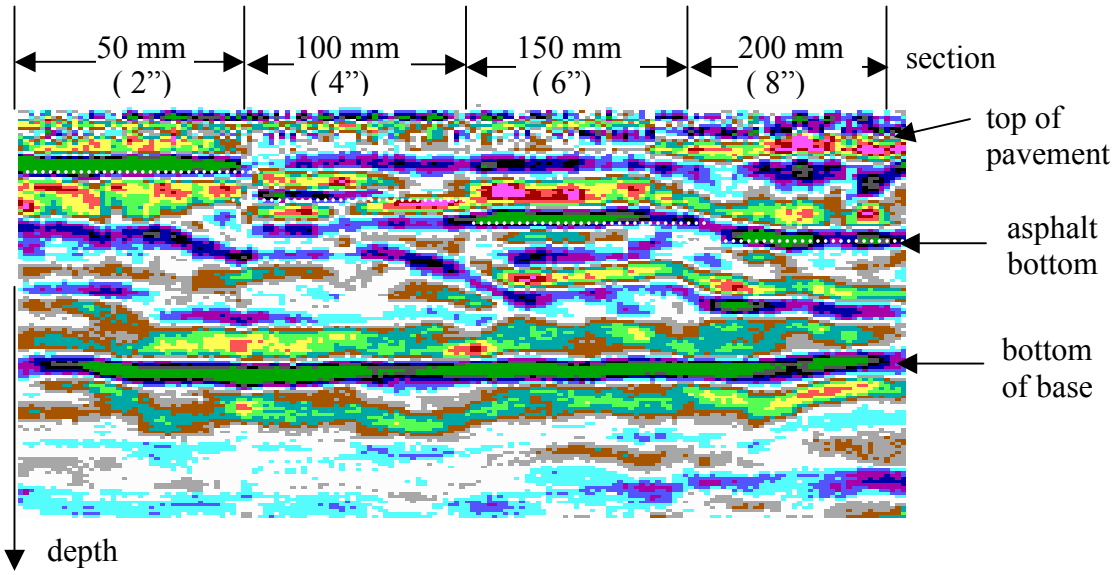

Figure 25 – Sample Horn Antenna GPR Data from Test Pit #2

It is anticipated that the hand equipment produced a much less uniform asphalt than would be produced by normal pavement machinery. This non-uniformity could explain the greater

discrepancies with the core data than would be encountered in full scale pavement. Subsequent testing for asphalt thickness was carried out on full-scale pavement sections.

5.4 Tests on Variable Thickness Concrete Test Slab

Laboratory testing of methods for determining concrete thickness was carried out using a specially constructed variable thickness concrete slab. The objective was to create a slab with thicknesses of 155, 205, 254 and 305 mm (6, 8, 10, 12 inches), and to test for thickness using impact-echo and CMP techniques. For convenience and access to the slab bottom, the slab was turned up on its side. The slab was un-reinforced concrete with outer dimensions of 1.3 x 2.5 meters (4 by 8 ft) and varying thickness. The concrete was vibrated and floated using a hand trowel. The block as it appeared just after pouring is shown in Figure 26.

(a) Pouring Concrete in Frame

(b) Variable Thickness Concrete Block Just After Pouring

Figure 26 – Variable Thickness Concrete Slabs

The concrete mixture contained glass fibers to provide increased tensile strength for handling. After curing, the block was lifted so that it was in the configuration of a variable thickness wall.

The block cured for 8 days with a polyurethane tarp on top. After 8 days, the block was placed on its side. During the process of lifting the block on its side, the block weight caused the forklift to slide and the block subsequently fell and broke in two places. Fortunately the fractures did not prevent data collection on the block. Figure 27 shows the slab in the vertical position during testing.

Figure 27 – Variable Thickness Concrete Slab During Testing

5.4.1 Impact-Echo Testing on Variable Thickness Concrete Slab

Impact-echo testing was carried out using two types of devices: one which measured both the thickness resonance and the surface p-wave velocity for the thickness calculation ("DOCTer"); and one which measures the thickness resonance only and used an assumed p-wave velocity ("CTG"). Twelve measurement points were defined on the slab, three in each thickness section, and three repeat measurements were made at each point. Figure 28 shows the layout of the test locations on the slab. The figure also shows the cracks which occurred during the movement of the slab. Each measurement point was centered laterally within the given thickness section.

Figure 28 – Slab Measurement Locations

Table 8 summarizes the results of these tests. For each of the 12 test locations, the table shows the actual thickness of the slab and then the results obtained with the impact-echo methods. The "DOCTer" equipment measures both the surface p-wave velocity, V_p, and the thickness resonance, F_t. The CTG equipment measures only the thickness resonance. The thickness calculation for the CTG equipment was obtained using the V_p value obtained from the DOCTer equipment.

The results show that on the average, both methods accurately characterize the thickness of the slab. There is some scatter, as indicated by the standard deviation of 12 mm (0.4 inches). Much of the scatter is related to the velocity measurement. It is reasonable to expect that, due to the quality control of the laboratory placement environment, the material is more homogeneous than the V_p values would lead us to believe. As an alternative, when the thickness values were calculated using the average V_p value for the entire slab (3831 m/s) rather than the local results, the scatter is reduced to a standard deviation of 6 mm (0.24 inches). This finding suggests that the mean of the V_p values would provide a more reliable basis for the thickness calculations.

The results from the slab testing show that impact echo is capable of producing accurate concrete thickness data. The laboratory arrangement is limiting, since the constant thickness sections are very small, and the boundaries produce extraneous signals which would not occur in a full scale pavement section. Also, one of the methods, the CTG, provided no direct means for determining the concrete p-wave velocity. That method would require some other means for determining the p-wave velocity, such as taking a core, using the known core thickness and the thickness resonance to calculate V_p, and then using that V_p value for the remaining measurements. The accuracy of this method for the slab test would depend upon which core was used for calibration. However, since the average velocity determined from the known thickness values equals the average velocity determined from the direct p-wave measurements, the "core calibration" procedure would, on average, produce results similar to those obtained with the direct p-wave measurements.

Table 8 – Summary of Impact Echo Tests on Variable Thickness Slab

Point	Thickness	DOCTer[1]			CTG[2]		Difference mm	
		Measured		Calculated	Measured	Calculated*		
		V_P	F_T	Thickness	F_T	Thickness		
	mm	m/s	Hz	mm	kHz	mm	DOCTer	Olson
1	305	3896	6104	306	5948	314	1	9
2	305	3703	6104	291	5948	299	-14	- 6
3	305	3947	5859	323	5948	319	18	14
4	254	4054	7568	257	7546	258	3	4
5	254	3846	7080	261	7014	263	7	9
6	254	3751	7324	246	7369	244	- 8	-10
7	205	3659	9033	194	9411	187	-11	-18
8	205	3845	8789	210	8878	208	5	3
9	205	4168	8789	228	8878	225	23	20
10	155	3847	12207	151	12607	146	- 4	- 9
11	155	3409	11719	140	11896	138	-15	-17
12	155	3845	12451	148	12429	148	- 7	- 7
	Mean	**3831**					**0**	**- 1**
	S. Dev	**194**					**12**	**12**

Notes: [1]Manufactured by Germann Instruments
[2]Manufactured by Olson Instruments
*Obtained using V_p values obtained from DOCTer

5.4.2 CMP Measurements on Variable Thickness Concrete Slab

The CMP method was also considered and evaluated as a method for the determination of concrete thickness. One of the key issues associated with the use of the CMP method is the limited penetration of GPR in new concrete. The free moisture in curing concrete increases its conductivity such that electromagnetic waves simply cannot penetrate. Once the free moisture is taken up in the curing process, the conductivity is reduced and waves can penetrate. Part of this task was to understand how long of a curing time is necessary before it is feasible to use GPR for pavement thickness measurements.

Data from the concrete blocks were obtained periodically as the blocks cured. The bottom 61 cm (24 inches) of the block was backed by 19 mm (0.75 inches) aggregate base material obtained from a local supplier following 26 days of curing. The estimated propagation velocity of the base back-calculated from the travel time in a 2-way measurement was 12 cm/ns (4.7 inches/ns). This meant that the propagation velocity in the concrete block was less than the base material and the reflection polarity from the concrete-base interface would be reversed relative to the reflection from a metal plate. In addition, a component of the reflection from the concrete bottom will contain energy that propagated along the concrete base interface, which is a potential source of error in the CMP depth calculation (see Section 3.0)

The reflection amplitude from the concrete-base interface was approximately 9 dB lower than the corresponding reflection with a metal plate placed in back of the concrete. This amplitude difference is significant because the concrete-base reflection is very close to the GPR equipment noise floor.

Visual analysis of the data revealed that the reflection from the concrete-base interface for the 155 mm (6 inches) thick concrete block was only above the noise floor in approximately the first 40 scans of the CMP. The reflection from the concrete-base interface in the 205 mm (8 inches) thick section of the block was not significantly above the noise floor up to 140 days of curing.

The 205 mm (8 inches) section of concrete block backed by a metal plate was above the noise floor of the radar system within 11 days of curing. CMP data processing from these data and data obtained previous on Virginia DOT and FAA pavement sites indicated that the most accurate thickness calculations were obtained from the portion of the CMP remaining after discarding the first 20 scans. The rational behind this finding has not yet been construed. Consequently, all CMP data with a positive polarity reflection that contains observable reflections from the concrete bottom out to 60 to 80 scans of the CMP measurement was processed without the contribution from the first 20 scans. Very weak positive polarity CMP data was processed out to only the first 40 scans with the contribution from the first 20 scans included.

All negative polarity data was processed only out to the first 40 scans. This is mainly due to the fact that the only negative polarity data in the database is from the 155 mm (6 inches) base-backed concrete block section at GSSI. Two easily calculated parameters, average reflection amplitude, and standard deviation from the least-squares fit line, provide a quantitative means for evaluating the confidence of the CMP thickness measurement.

Figure 29 shows the thickness error of the CMP calculation versus standard deviation of the least squares fit line using CMP data from the base-backed and metal-backed concrete. It is generally observed that there is a break in the CMP measurement accuracy at approximately 2.6mm. The thickness error increases greatly for higher standard deviations.

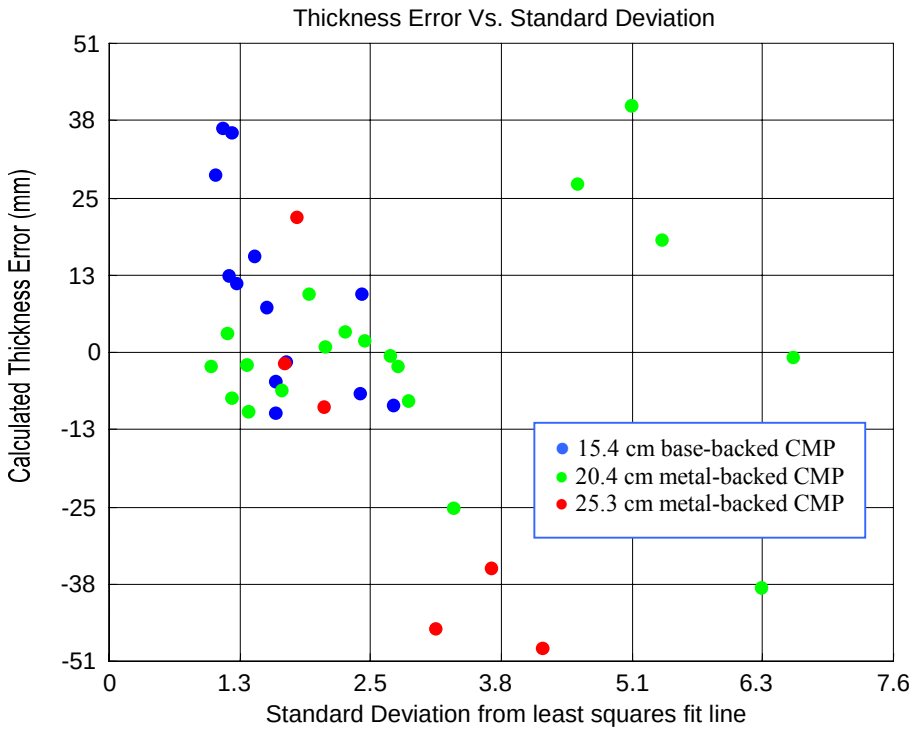

Figure 29 – Thickness Error Versus Standard Deviation Using Concrete Block Data Obtained as the Concrete Block Cured

6. Preliminary Evaluations on Full Scale Constructed Pavements

Candidate methods were tested on full-scale pavements and pavement test facilities. For asphalt thickness, the test results showed that both the horn antenna and CMP methods are capable of producing accurate asphalt thickness data on full-scale pavement thickness sections over a thickness range from 50 to 200 mm (2 to 8 inches). The results also show that due to surface material variations, some type of site-specific calibrations may be required with these methods to achieve the accuracy objectives of the project. For PCC pavement, the results showed that the impact-echo method is capable of providing accurate thickness measurements if adequately calibrated. The CMP method did not work as well, showing more scatter, and exhibiting limitations in the presence of reinforcement. Further consideration of the Multi-Receiver Technique was discontinued given the laboratory nature of the current state of the equipment, and the need to implement and test a new type of impact source.

6.1. Introduction

The laboratory tests described in Section 5 provided a great deal of insight into the capabilities of the various methods under consideration. Whereas the laboratory provided a great deal of flexibility in created different material types and thickness values, they were limited in their ability to reflect conditions as they occur in full scale constructed pavement. In order to bridge the gap between the laboratory tests and the final evaluations on Caltrans pavement, evaluations were carried out on a series of "test pavements". These pavements represented fully constructed pavement sites for which there was thickness ground truth, and/or which were constructed for research purposes and ground truth could be easily obtained.

Table 9 lists the sites where this testing was conducted, along with the testing dates and the site descriptions. One of these sites was a newly constructed pavement, for which core data was available. The other sites were research sites, which were well documented with cores.

Table 9 – Preliminary Test Sites

SITE	LOCATION	DESCRIPTION	TYPE	THICKNESS	DATE
I-93	Thornton, NH	In-service pavement rehab., total asphalt replacement	AC	115 mm mainline 50 mm shoulder	9/05/01
FAA Technical Center	Atlantic City, NJ	Pavement load testing research facility	AC PCC	127 and 254 mm 230 and 280 mm	6/8/01 and 10/18/01
FHWA ALF	McLean, VA	Pavement load testing research facility	AC	100 and 200 mm	10/19/01
NCAT	Auburn, AL	Pavement load testing research facility	AC	100 mm (all 52 sections)	10/22/01
VA-288	South of Richmond, Chesterfield County	New Pavement Construction	CRCP	254 mm	10/23/01

For the asphalt measurements, the horn antenna data collection was carried out using a portable "bike rack" arrangement mounted to a standard square receiver hitch at the back of a vehicle (Figure 30). An electronic distance wheel was mounted to the vehicle bumper to continuously record the position of the antenna during data collection. The CMP measurement setup, used both for asphalt and concrete, is shown in Figure 2b. The CMP test rig had the two antennas mounted to a mechanism which kept the antennas equidistant from the centerline, and electronically triggered data collection every two millimeters. The impact echo equipment used in these tests is discussed in Section 6.2 under Concrete Thickness Testing.

Figure 30 – Horn Antenna Equipment Setup

Figure 31 – CMP Equipment Setup

6.2 Asphalt Thickness Testing

6.2.1 I-93 in Thornton, NH

The asphalt pavement was completely removed and replaced on I-93 during the summer of 2001. The section tested had been repaved, and was about to be open to traffic. Two lanes were available for testing: the high speed lane, and the shoulder. The nominal asphalt thickness was 114 mm (4.5 inches) on the main line, and 51 mm (2 inches) on the shoulder. Both were supported by a granular base. The setup at the I-93 maintenance shed is shown in Figure 32. The pavement section is shown in Figure 32. Horn antenna data collection was carried out in short continuous strips as the vehicle drove down the lane. Data collection was initiated as the core location was approached, and a mark was placed in the data when the antenna passed alongside the core location. In this way, the data at the core location could be easily identified in the analysis. After the horn antenna data collection was completed, the core locations were revisited, and CMP measurements were made. CMP measurements were made in the longitudinal direction, with measurements carried out on each side of the core location, offset by approximately 150 mm (6 inches). Note that the data collection for both horn antenna and CMP measurements were offset from the core location. Previous experience with data collection directly over a previously cored location has shown that erroneous results are obtained due to the depth and composition of material used to fill the core holes (*Maser, SHRP Report*).

Figure 32 – I-93 Test Section, Northbound, South End, High Speed Lane

6.2.2 The FAA Technical Center (FAATC)

The FAA maintains a pavement test facility at its Technical Center in Atlantic City, NJ. The facility houses a 275 meter (900 ft.) long by 18 meter (60 ft.) wide test pavement. The pavement is laid out on a stationed grid. The pavement is composed of different types of pavement construction — some asphalt, and some concrete. Figure 33 shows an overall view of the test facility, along with the horn antennas data collection setup at the FAATC. Two asphalt sections were tested under this program — a 127 mm (5 inches) thick section (item 3-3) and a 254 mm (10 inches) thick section (item 3-2). Figure 34 shows the layout of these sections, with increasing station going from left to right. The 127 mm (5 inches) thick section was over a 276 mm (10 7/8 inches) thick base, while the 254 mm (10 inches) thick section was directly over subgrade.

The horn antenna tests at the FAATC were carried out in a series of longitudinal survey lines, starting at station 275 meters (900 feet) and going down station, each at a different offset from the centerline of the pavement. Each survey line was 46 meters (150 feet) long. The first 19 meters (62.5 feet) were in the 127 mm (5 inches) section, then there was a 7.6 meter (25 feet) transition section, and finally 19 meters (62.5 feet) in the 254 mm (10 inch) section. A sample of the raw data is shown in Figure 34.

Figure 33 – Horn Antenna Data Collection Setup at the FAATC

CMP testing was carried out at specific coordinate locations on the pavement grid. CMP data was collected at 9 locations on the grid. One location was adjacent to a previous core. Figure 35 shows sample CMP data collected on the two asphalt sections. The figure also shows data collected on a PCC section (to be discussed later). Subsequent to the testing, additional cores were taken and used for comparison with the horn antenna and CMP data. The asphalt core locations were selected based on the horn antenna data, which was used to generate a contour plot of asphalt thickness. This contour plot showed the thick and thin areas, and thus provided a means for selected core locations representing a range of thickness values. A sample contour plot with selected core locations is shown in Figure 36.

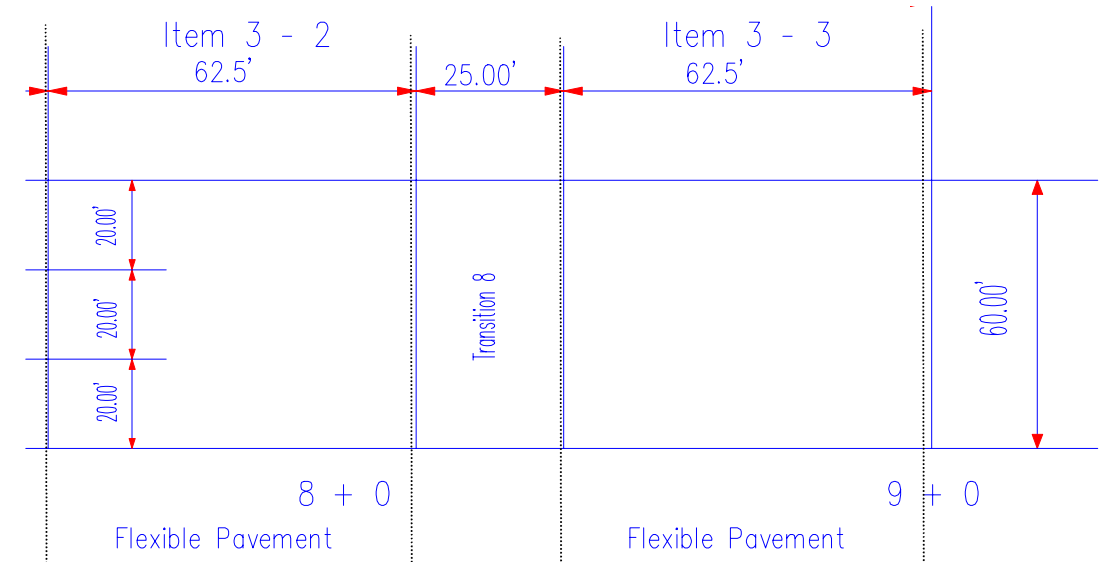

(a) Top View

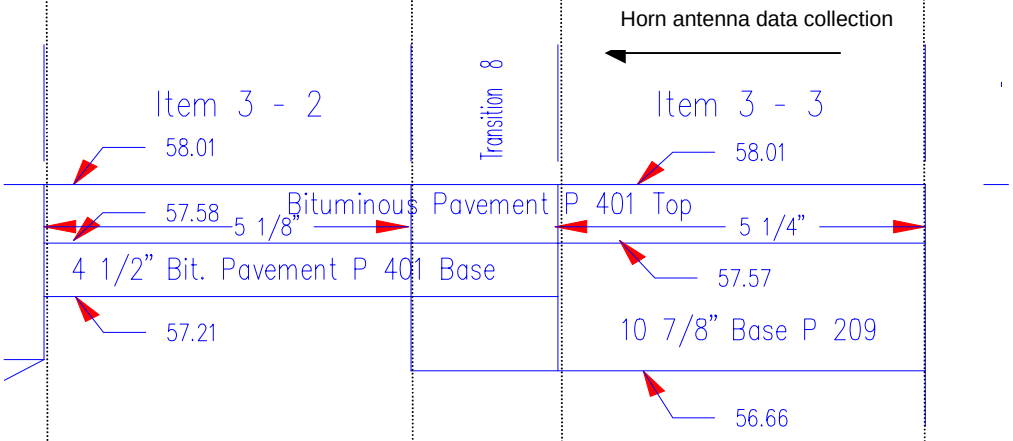

(b) Cross Sectional Layout

marks at 1.52 m (5 ft) intervals

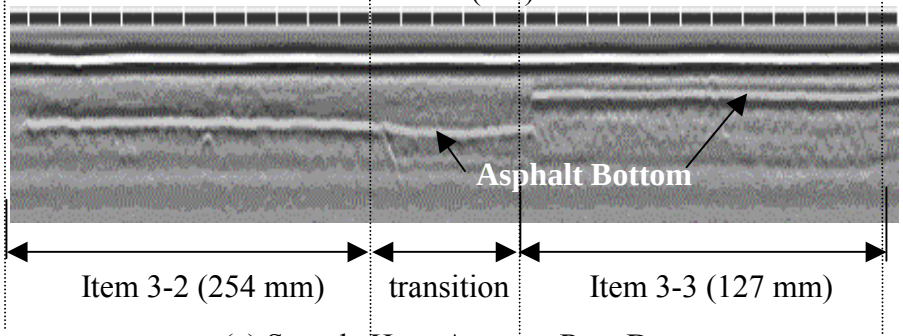

(c) Sample Horn Antenna Raw Data

Figure 34 – FAA Technical Center Pavement Test Sections

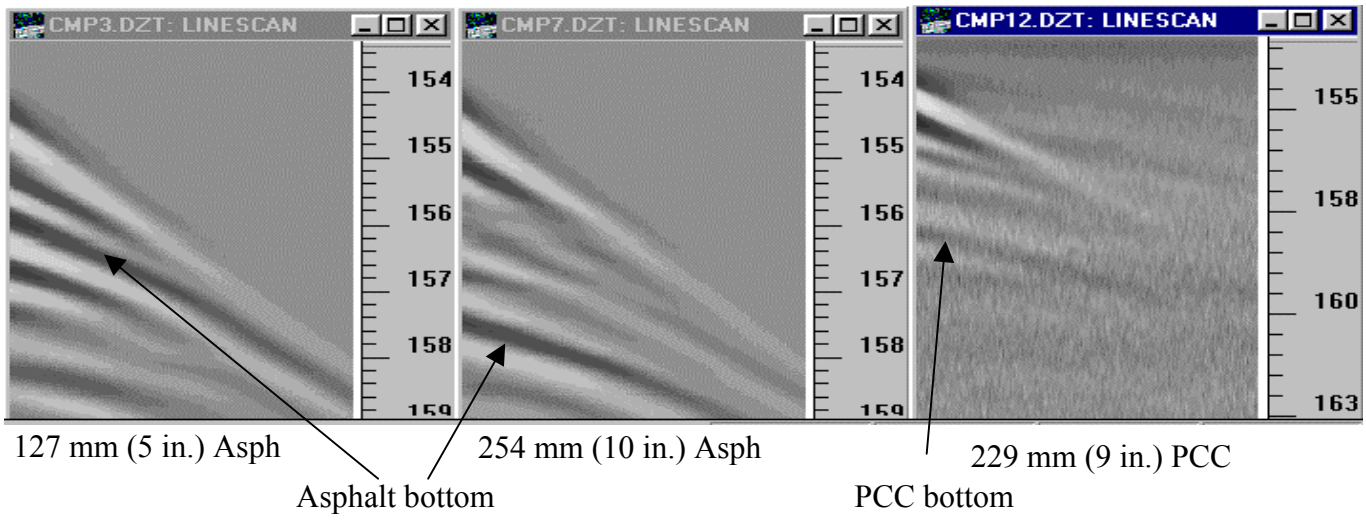

Figure 35 – Sample CMP Data from FAA Facility

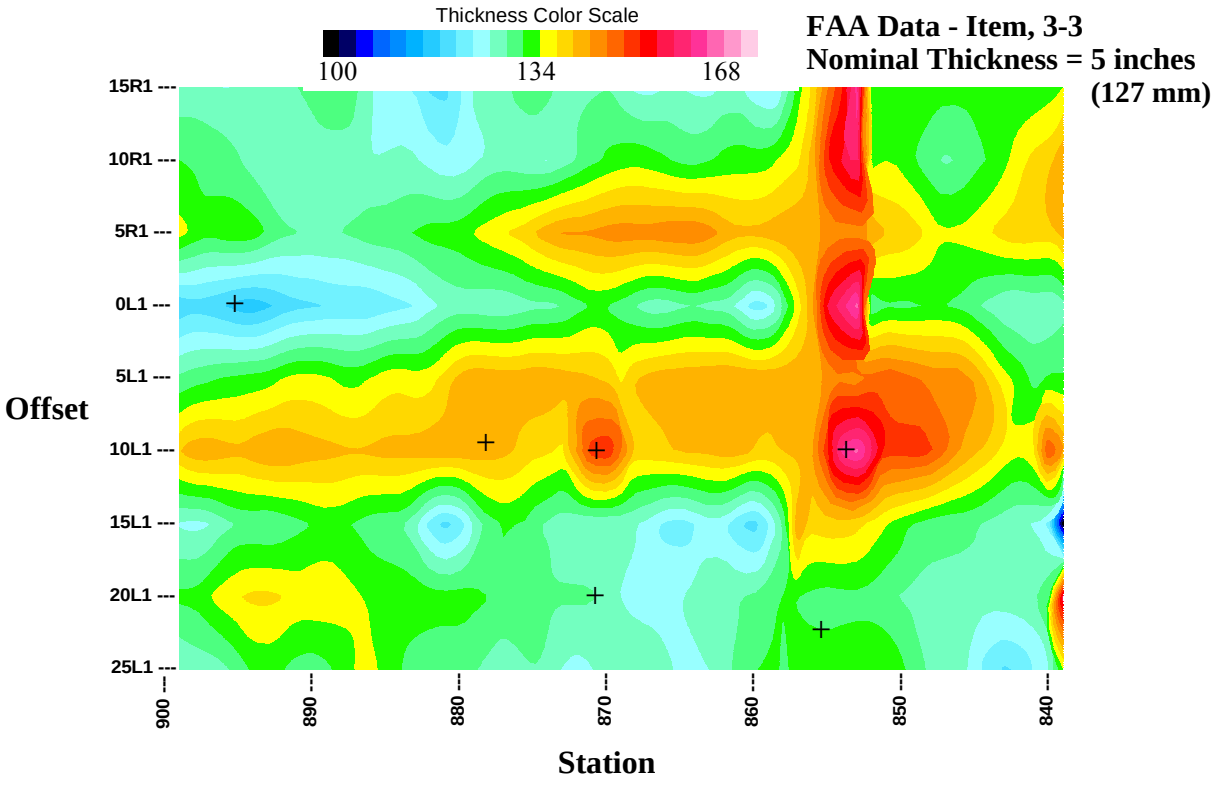

Figure 36 – Contour Plot of Asphalt Thickness from Horn Antenna Data
(with candidate core locations shown as +)

6.2.3 FHWA Accelerated Load Facility (ALF)

The FHWA maintains an accelerated pavement facility at the Turner Fairbanks Research Center in McLean, VA. The facility is used to rapidly collect data on pavement performance under conditions in which axle loading and climatic conditions are controlled. The facility consists of 12 lanes, each 3.7 meters (12 feet) wide and 43 meters (140 feet) long, and each representing different types of pavement construction. Core thickness data was collected by the FHWA on the initial construction prior to application of the loading. The loading was applied in the wheelpaths of each test lane. Figure 37 shows the horn antenna equipment setup and the test area. Note the heavy rutting in the loaded areas of the test lane.

(a) Horn Antenna Setup

(b) Typical Lanes at the FHWA ALF Facility

Figure 37 –Testing at the FHWA ALF Facility in McLean, VA

Data was collected in lanes 1, 2, 3, and 4 of the facility. These lanes were of asphalt construction, and were available for testing. The tests were carried out along the centerline of each lane in the unloaded area. The core locations were marked in the data so that the data at the core location could subsequently be identified.

6.2.4 National Center for Asphalt Technology (NCAT)

The NCAT facility in Auburn, Alabama, is a continuous oval-shaped test track consisting of 52 pavement sections, each with approximately 102 mm (4 inch) of asphalt surface. The asphalt surface material is supported by a low density bituminous base mix. The principal variable amongst the 52 sections is the asphalt mix design. The design and the asphalt density of each section is well documented. Also documented is the average asphalt thickness of each section. The objective of the tests was to evaluate the influence of asphalt mix design on the calculation of asphalt thickness

Figure 38 shows data collection in progress at the test track. The horn and CMP equipment setup was identical to that used in the FHWA and FAA tests. Pavement section transition locations, marked on the side of the track, were marked in the horn antenna data for reference during data analysis. Horn antenna data was collected continuously at 152 mm (6 inch) intervals on both inside and outside wheelpaths of the primary test lane. CMP measurements were made at proposed core locations.

Figure 38 – Horn Antenna Data Collection at the NCAT Facility in Auburn, AL

6.3 Concrete Thickness Testing

6.3.1 FAA Technical Center

A number of sections at the FAA technical center were built of Portland cement concrete. The PCC sections were un-reinforced, and built on a 150 mm (6 inches) thick "econocrete" base. Econocrete was described as a lean Portland cement concrete with lower strength and stiffness than conventional concrete. Two pavement sections (items) with different thickness values were tested under this program – item 1-1 (280 mm (11 inches) and item 3-1 (230 mm (9 inches)). The pavement age was approximately 2 years. The testing was carried out with both the CMP method and the impact echo method. A second mechanical wave method, the MRT method, also underwent some limited testing. Due to the similarity in material properties between the PCC pavement and the Econocrete base, there was some concern that all of the methods would have problems identifying the bottom of the concrete.

Preliminary CMP testing was carried in June of 2001 to evaluate the feasibility of using the CMP method on PCC pavement. Tests were carried out in the vicinity of an existing core. These preliminary tests confirmed that adequate signal strength for CMP processing could be achieved, and that the result of the processing was reasonably close to the core value. A more extensive set of CMP tests was carried out on October 18, 2001. These tests were conducted at 15 locations on the 230 mm (9 inches) pavement and 10 locations on the 280 mm (11 inches) pavement. The measurement locations were at well defined coordinates based on the FAA pavement coordinate layout, and were typically spaced 1.5 to 3 meters apart. Two CMP measurements were made at each location, one in the longitudinal direction and one in the transverse direction. As with the asphalt testing, the intent was to take cores at a number of these locations subsequent to the testing. Figure 39 shows CMP measurements being conducted at the FAA facility.

Impact Echo tests were carried out on the slabs described above using the DOCTer equipment described earlier. As with the CMP tests, preliminary tests were carried out on June 8, 2001 to establish the feasibility of the measurement. The preliminary measurements confirmed that a thickness resonance could be detected. However, the thickness values obtained from these measurements deviated by about 10% from what was believed to be the true pavement thickness. More extensive testing was carried out on October 18, 2001 at 60 locations on the 280 mm (11 inches) slab and 30 locations on the 230 mm (9 inches) slab. Direct p-wave measurements were carried out at 10 of the locations on the 280 mm (11 inches) slab and 5 of the locations on the 230 mm (9 inches) slab. Figure 40 shows the impact-echo equipment used at for the FAA tests.

Subsequent to the CMP and IE measurements, cores were taken at 4 locations in each of the two slabs.

Figure 39 – CMP Concrete Thickness Measurements at the FAA Test Facility

(a) Overall Test Layout

(b) Transducer and Measurement Detail

Figure 40 – Impact-Echo Testing at the FAA Test Center

MRT measurements were made at one location in each of the two slabs during preliminary measurements on June 27, 2001. The limitations on the quantity of testing was due to the prototype nature of the equipment. The equipment used was a laboratory digital oscilloscope, and a home-made "balloon gun" impactor used to project ball bearings onto the pavement surface. The small ball bearings were chosen based on the theoretical requirement for a short (<40 μsec) impact (see Section 4.2). A series of repeat test indicated that a 3 mm (0.1 inches) ball bearing was suitable, and produced an impact duration on the order of 20 μsec. Figure 41 shows the equipment used for this testing.

(a) Digital Oscilloscope and Accelerometers

(b) Balloon Gun Impact Source with Ball Bearings

Figure 41 – Equipment Used for MRT Testing

6.3.2 VA288 Tests

A series of CMP tests were carried out on a newly constructed continuously reinforced concrete pavement (CRCP) on Route 288, Chesterfield County, Virginia, just south of Richmond. The CRCP pavement thickness was 254 mm (10 inches), and was underlain by an open-graded asphalt treated base. The longitudinal rebar were spaced at 178 mm (7 inches), and the transverse rebar were spaced at 1.22 meters (4 feet). The pavement was approximately 1 month old. A series of cores had already been taken by VDOT. The tests indicated some variability in the pavement thickness, ranging from 244 to 307 mm (9.6 to 12.1 inches).

CMP measurements were made on this pavement section on October 23, 2001. Due to the transverse tines in the pavement, the CMP measurements were made in the transverse direction, parallel to the tines. Measurements were made adjacent to 8 previously cored locations. Measurements were also made at additional locations where VDOT was interested in thickness data.

6.4 Asphalt Thickness Results

6.4.1 Horn Antenna Thickness Analysis

The horn antenna data from I-93, FAA, and FHWA facilities was analyzed for pavement thickness and correlated with available core information. The analysis was carried out using the techniques described in Section 3 of this report. For I-93 and FHWA, core data was already available for comparison. For FAA, cores were taken at selected locations. The choice of location was based on the pavement thickness distribution as observed in the data, as discussed earlier. The horn antenna thickness data was correlated with all available core data, and the results of this correlation are shown in Figure 42.

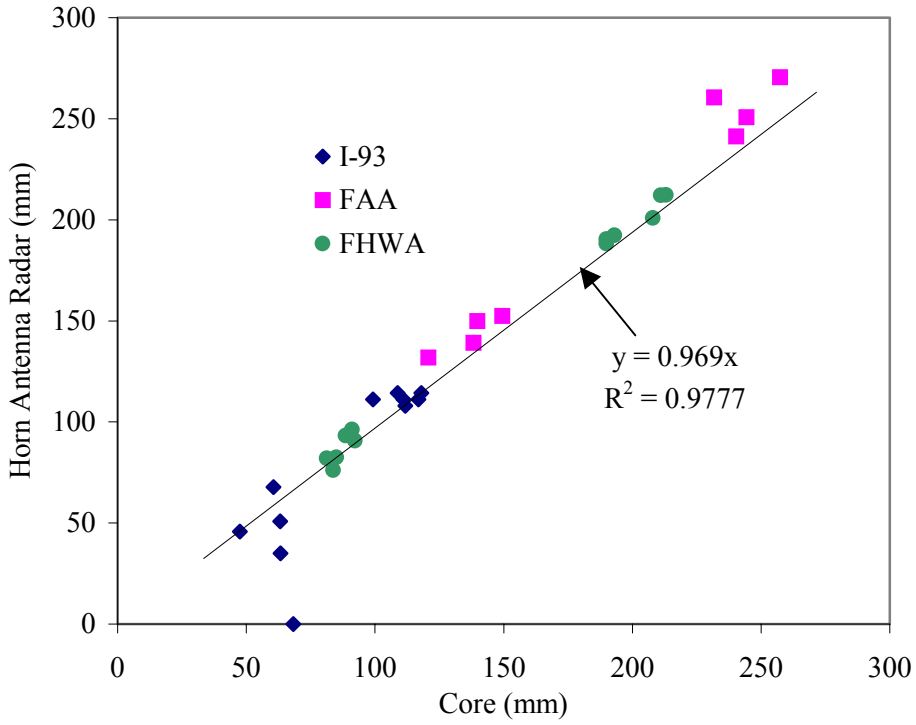

Figure 42 – Comparison of Horn Antenna GPR Thickness Data to Cores

The Figure 42 comparison shows a very good overall agreement between core and horn antenna data, and this type of agreement should be suitable for meeting the requirements of this project.

The NCAT data is not shown on his graph for two reasons: (a) all of the thickness values are in the neighborhood of 100 mm (4 inches); and (b) only average section thickness data was available. In the NCAT case, the average horn antenna thickness data for each of the sections was compared to the average thickness data available from NCAT. The results are presented in Figure 43. Each data point in this figure represents the average thickness for a 61 meter (200 foot) section. The "L" and "R" represent horn antenna data collected the left and right wheelpaths, respectively. The data points are color coded to correspond to the aggregate type used in the mix of that section. The designation "Slag L/S" represents a slag and limestone/sand mix.

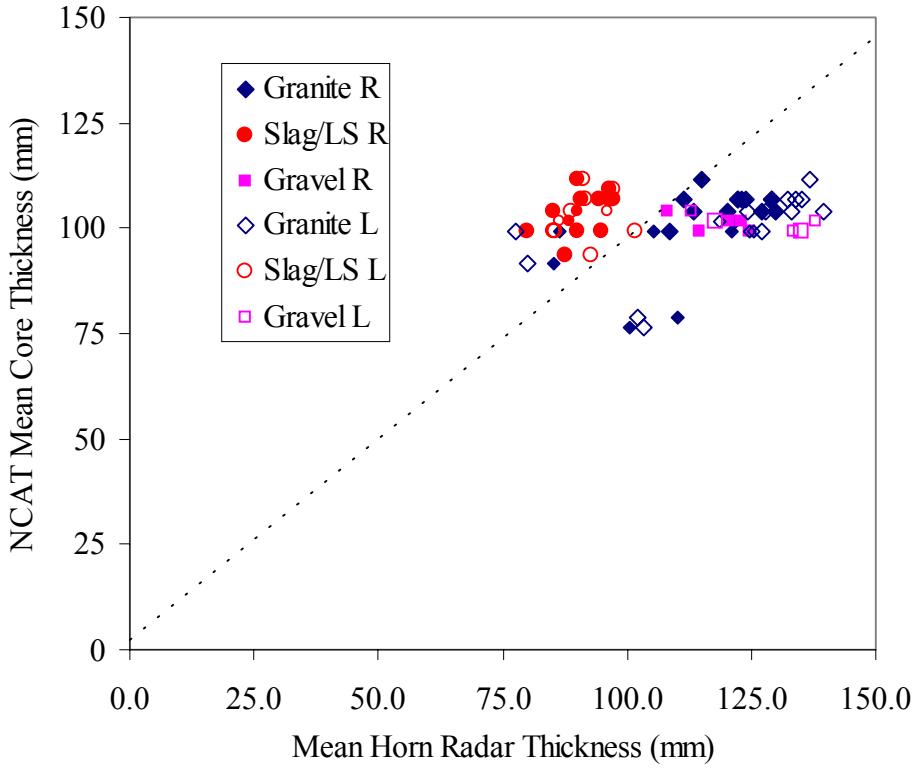

Figure 43 – Comparison of Section Mean Thickness: Horn Antenna vs. Cores

The figure shows that there are systematic errors in the GPR thickness measurement, and that these errors seem to be associated with the aggregate type. The GPR data shows that the aggregate type has a strong influence on the calculated dielectric constant (see Equation (2), Section 3). This observation suggests that some site specific calibration procedure may be necessary in order to adjust for this systematic effect.

It is important to note that the pavement structure, with the AC surface over a low density bituminous base, is not a typical one. The reflection between the AC surface and the bituminous base was often opposite in sign to that which would occur between an AC surface and a granular base, a PCC base, or simply an older binder layer. This sign difference complicated the GPR data interpretation, and could possibly have led to some errors. A second item to note is that the NCAT pavement thickness averages are based on the average of seven cores taken at the end of each

section, while the GPR thickness average is based on data collected throughout the entire section. Therefore we are comparing data collected at different locations.

6.4.2 CMP Thickness Analysis

The horn antenna data from I-93, FAA, and FHWA facilities was analyzed for pavement thickness and correlated with available core information. The analysis was carried out using the techniques described in Section 3 of this report. The core data was the same as that used for the horn antenna evaluation. Figure 44. shows the results of this evaluation. The NCAT data is not included in this figure because cores data at the CMP test locations were not available. Note that the relationship is comparable to that obtained from the horn antenna data (Figure 42). The slope of the regression line (0.93) deviates from unity by a greater amount than for the horn, suggesting that the CMP method tends to over-predict the thickness by a greater degree. Also, note that the CMP method was not able to measure the 51 mm (2 inches) overlay at the I-93 site.

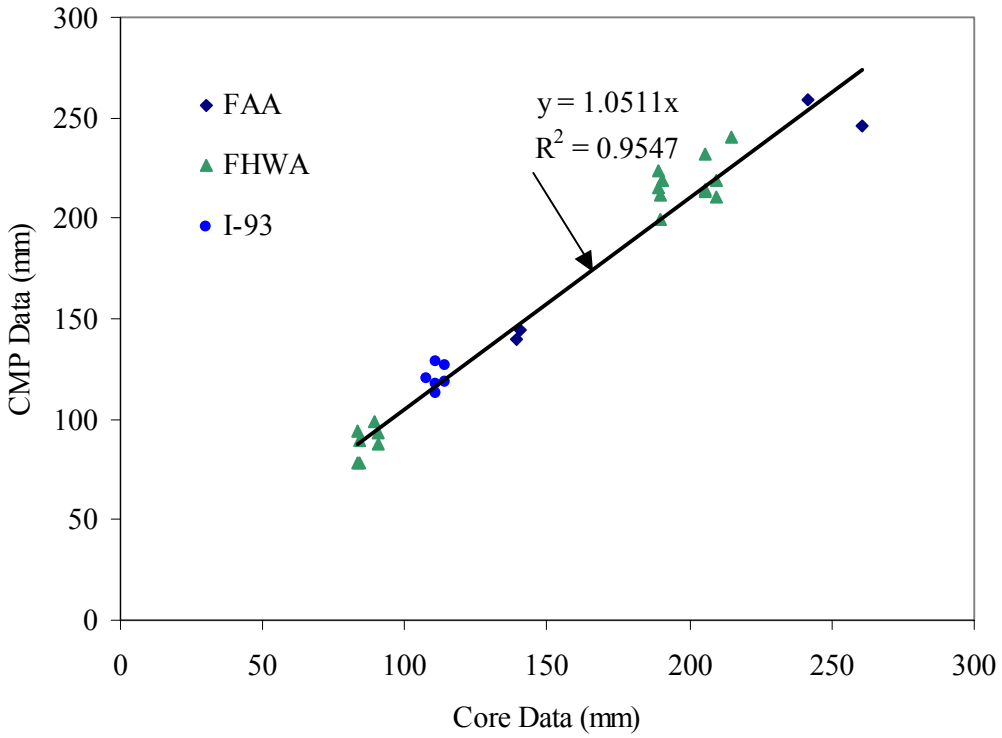

Figure 44 – Comparison of CMP GPR Thickness Data to Cores

6.5 Concrete Thickness Results

6.5.1 CMP Results at the FAATC

Concrete cores were taken at eight locations at the FAATC, four in each of the 229 and 279 mm (9 and 11 inch) thickness sections. CMP measurements were made at each of these locations in both the transverse and longitudinal directions. Table 10 summarizes the results of these measurements. The table shows the station and offset of each test on the FAATC pavement grid, and it indicates the direction of the test. In addition to the thickness, the table also shows the velocity and dielectric constant calculated from the CMP data.

Table 10 – CMP Concrete Pavement Results from the FAATC

			Thickness (mm)			Absolute
Station/Test	**Vel (cm/ns)**	**Dielectric**	**Calculated**	**Core**	**Difference**	**Difference**
005-20R-L	11.08	7.33	275	270	5	5
005-20R-T	10.45	8.24	255	270	-14	14
015-20R-T	10.44	8.26	255	267	-11	11
015-20R-L	*bad data - could not be processed*					
085-20R-L	11.46	6.85	295	259	36	36
085-20R-T	9.75	9.47	244	259	-15	15
095-20R-L	10.75	7.79	271	276	-5	5
095-20R-T	10.99	7.45	279	276	3	3
680-20R-L	10.42	8.29	236	246	-10	10
680-20R-T	10.51	8.15	241	246	-5	5
695-20R-L	11.11	7.29	246	232	14	14
695-20R-T	10.90	7.57	241	232	10	10
720-20L-L	10.60	8.01	227	232	-5	5
720-20L-T	11.19	7.19	243	232	11	11
720-20R-L	9.96	9.07	228	248	-19	19
720-20R-T	10.89	7.59	251	248	4	4
				Average	**0**	**11**

The data shows that, on the average, the CMP thickness values come very close to the core values. Locally, however, there is a good deal of scatter, and the average absolute deviation is close to 127 mm (0.5 inches).

6.5.2 CMP Results From VA288

CMP data were correlated with core data at 10 core locations. Table 11 lists the tests that were conducted, and compares the CMP computed thickness data with the core data. The tests designated "b" represent repeat tests.

Table 11 – CMP Concrete Thickness Results from VA288

CMP File	Vel(cm/ns)	Dielectric	Thickness (mm)		Difference	Absolute Difference
			Caculated	Core		
VAC01	10.67	1.23	298	262	36	36
VAC01b	10.77	1.20	300	262	38	38
VAC02	11.14	1.12	316	257	59	59
VAC02b	9.10	1.68	226	257	-31	31
VAC03	9.50	1.55	261	267	-6	6
VAC04	10.95	1.16	288	251	37	37
VAC04b	9.19	1.65	227	251	-24	24
VAC05	8.79	1.81	235	274	-39	39
VAC07	11.90	0.98	332	244	88	88
VAC08	11.05	1.14	306	249	57	57
VAC08b	12.50	0.89	360	249	111	111
VAC09	9.80	1.45	253	251	2	2
VAC09b	10.10	1.37	268	251	17	17
VAC10	9.43	1.57	251	279	-29	29
VAC13	11.50	1.05	326	272	54	54
				Average	**27**	**41**

The data show a great deal of deviation between the CMP and core thickness. A careful review of the data revealed that the reinforcing steel had a strong influence on the CMP data processing. The presence of the reinforcing steel made it difficult to identify the data from the bottom of the slab. Also, the bottom reflections are distorted to some degree due to the presence of the steel. In retrospect, it would have been preferable to collect the CMP data in the longitudinal direction, parallel the primary reinforcing steel. This orientation would have reduced the influence of the steel on the CMP data. The transverse data collection was chosen to avoid dragging the antennas transverse to the tined surface. Subsequent use of the CMP device on Caltrans pavement utilized a Teflon sheet to minimize the effect of pavement roughness on the CMP measurement.

6.5.3 Impact Echo Results from the FAATC

Impact echo measurements were made at a number of locations on each of the two PCC test areas at the FAA Technical center. Four cores were taken within each of these test sections. The impact-echo data at these core locations, and the comparison of these data to the core thickness values, are shown in Table 12.

Table 12 – Impact-Echo Results on FAATC Concrete Slabs

	IE Thickness (mm)			Core Thickness (mm)	Differences (mm)		
Station	Local V_p Values	Mean of Local V_p	Slab Mean V_p		Local V_p Values	Mean of Local V_p	Slab Mean V_p
005-20R	263	260	250	270	-7	-10	-20
015-20R	241	238	225	267	-26	-29	-42
085-20R	271	260	250	275	-4	-15	-25
095-20R	255	252	250	276	-21	-24	-26
680-20R	234	231	227	246	-12	-15	-19
695-20L	202	214	198	232	-30	-18	-34
720-20L	196	204	194	232	-36	-28	-38
720-20R	220	220	215	248	-28	-28	-33
				Average	-20	-21	-30
				St. Dev	12	7	8

The table shows impact-echo calculations made in 3 ways:

1. Local V_p values: the V_p value determined at the measurement location was used for the thickness calculation
2. Mean of Local V_p values: the mean of the 4 local V_p values obtained for each slab was used in the thickness calculation.
3. Slab Mean V_p: A series of V_p measurements were made throughout the slab, and their mean was used in the thickness calculation. Note that these V_p measurements are not necessarily at the thickness measurement locations.

The data shows that the impact-echo method consistently underestimates the concrete thickness, regardless of the method. It also appears that the use of the local mean V_p reduces the scatter associated with the individual V_p measurements, while the use of the slab mean increases the overall error. Note that all of the calculations in Table 11 are based on Equation (6), incorporating the 0.96 plate correction factor recommended by ASTM C1383-98 (*8*). Omission of this factor improves the results, reducing the average deviation from –20 mm to –12 mm (0.8 to 0.5 inches). Discussion with others who have worked with impact-echo indicates that there is some question regarding the appropriateness of this factor in real applications, and the results here suggest that it may not be appropriate.

Subsequent testing on the individual cores was carried out to directly evaluate the p-wave velocities. The testing was carried out using a commercial device called the "V-Meter" manufactured by James Instruments. The tests were carried out based on procedures outlined in ASTM C597 *Standard Test Method for Pulse Velocity through Concrete.* The average p-wave velocities determined from this method were higher than those obtained from the impact-echo surface velocity measurement. This suggests that the surface measurement is not adequately representing the V_p through the full depth of the concrete slab. In fact, thickness values calculated using the ASTM C597 velocities with impact-echo thickness resonance data come much closer to the core thickness data than those obtained from the surface V_p measurements.

The above findings suggest, as originally suspected, that the surface V_p measurement prescribed by ASTM C1383-98 (*8*) can, under certain circumstances, lead to systematic errors. This finding suggests that some sort of site specific correction or calibration needs to be made to adjust for this error.

6.5.4. Multi-Receiver Technique (MRT) Results from the FAATC

The results of MRT testing at the core locations are shown in Table 13. The test results are mixed. Good results are obtained at some locations, but not at others.

Table 13 – MRT Results on the FAATC Concrete Slabs

Station	MRT Thickness (mm)	Core Thickness (mm)	Difference (mm)
005-20R	212	270	-58
015-20R	230-249	267	-----
085-20R	267	275	-8
095-20R	216-249	276	-----
680-20R	234	246	-12
695-20L	200	232	-32
720-20L	203	232	-29
720-20R	242	248	-6
		Average	**-24**
		St. Dev	**20**

* had difficulty with data interpretation

One of the accuracy issues associated with the MRT method is the accurate determination of the time of impact. For these tests, this "zero" time was estimated by observing the arrival time of the direct surface p-wave at the two accelerometers, and extrapolating back to find the time at the impact location. It appears that this estimation procedure does not provide a sufficiently accurate determination of the impact time. The problem can be solved by designing an impact source with an electronically measurement of the time of impact.

6.6 Summary of Preliminary Testing Results

The results of the preliminary tests on full scale pavement sections are summarized in Table 14. The data presented in the table summarizes the accuracy obtained in the various tests described in this section. For the PCC CMP test, the VDOT tests were not included since they were for CRCP. The technique, as it was applied to CRCP, did not produce valid data. Also, there is not much CRCP used in California. The PCC data in the table therefore applies only to un-reinforced pavement.

Table 14 – Summary of Preliminary Testing

MATERIAL	METHOD	NUMBER OF CORES	ACCURACY (VS. CORES) MM		COMMENT
			MEAN	ST. DEV.	
Asphalt	Horn Antenna	34	3	10	may need on-site calibration
Asphalt	CMP	29	12	12	needs on-site calibration
PCC	CMP	8	-2	14	
PCC	Impact-echo	8	-21	7	needs on-site calibration
PCC	MRT	6	-24	20	not ready for field tests

Asphalt Thickness Measurement—

Based on the data from I-93, the FAATC and the FHWA ALF sites, it appears that both the horn antenna and CMP methods are capable of producing accurate asphalt thickness data on full-scale pavement thickness sections over a thickness range from 50 to 200 mm (2 to 8 inches). Data from the NCAT site suggest that type of surface material might influence the accuracy of the horn antenna thickness calculation. The CMP method appears to have a tendency to over-calculate the asphalt thickness. Both of these factors can be addressed by implementing some type of site-specific calibration.

Concrete Thickness Measurements—

CMP Method: Based on the FAATC tests, the CMP method appears to be able to provide reasonable accuracy for average thickness, although with somewhat more scatter than was obtained for asphalt. Note that the FAATC pavement was two years old, and that the method was less successful in the laboratory when applied to younger concrete.

Impact-Echo Method: The method appears to be capable of providing accurate thickness measurements if some type of bias correction can be applied. Once again, this suggest some site specific calibration to eliminate the bias.

Multi-Receiver Technique: Given the laboratory nature of the current state of the equipment, and the need to implement and test a new type of impact source, further study of this technique was recommended. Since such study was beyond the scope of this project, further evaluation of this technique was discontinued.

7. Field Testing on California Pavements

Tests were carried out with both the GPR and IE methods on pavement sites selected by Caltrans. The asphalt sites were selected to represent three main conditions: (a) thick and thin asphalt on aggregate base; (b) asphalt on concrete; and (c) thick and thin asphalt overlays. The concrete sites were selected to represent variations in concrete thickness and age. Age was selected as a variable because of its influence on GPR penetration and on p-wave velocity. The asphalt pavement results showed that, using one calibration core per site, both the horn antenna and CMP GPR measurements were able to evaluate the section thickness to within 2.5 mm (0.1 inch) of the core values. The CMP method could not measure a surface layer less than 75 mm thick where there were multiple asphalt layers. The PCC pavement results showed that, using one calibration core per site, the impact-echo methods were able to evaluate the section thickness to within 5 mm (0.2 inches) of the core values. The CMP GPR method was not capable of determining the thickness of newly placed concrete.

7.1 Data Collection

Table 15 summarizes the California sites which were tested. Most of the sites were closed to traffic because they were still under construction. The exceptions to this were I-505, I-5, and US-99. These sites had been recently paved but were open to traffic. Temporary lane closures were required at these sites in order to allow for testing.

At each site, a 305 meter (1000 foot) section was identified as the test section. For the asphalt sections, core locations were marked off at 15.25 meter (50 foot) intervals in alternating wheel paths, such that there were 10 core locations in each wheel path and 20 core locations total at each site. The I-505 site, due to its termination at a ramp, was a 152 meter (500 foot) site, and core spacing was at 7.62 meter (25 foot) stations. For the concrete sections, the cores were located based on the IE data. Since all of the concrete sections had a lean concrete base (LCB), it was possible for the IE method to read the combined PCC and LCB thickness rather than the PCC thickness. Therefore, core locations were selected where a clear PCC thickness resonance was obtained. All cores were 100 mm (4 inch) diameter for both asphalt and concrete sites were taken after the NDT thickness data was collected.

For the asphalt sections, the survey lines and core locations were laid out prior to data collection. Continuous data was collected a with the horn antenna at 155 mm (6 inch) longitudinal intervals on survey lines in each wheel path. Manual marks were placed in the data where the antenna passed over the designated core location. CMP measurements were made directly at the core locations, in both the longitudinal and transverse directions for both asphalt and concrete pavements. The horn antenna and CMP equipment configurations were the same as they were for the preliminary tests described in Section 6. The one difference was the addition of a Teflon sheet between the antennas and the pavement (Figure 45). The sheet facilitated the sliding of the antennas over the rough pavement surface, and had no adverse impact on the quality of the data. Also shown in the figure is the overall CMP test arrangement, with the GPR data collection and control unit located in a vehicle. Using the vehicle, the equipment was driven to each core location, the CMP rig was taken out for testing, and then driven to the next core location, and so on.

Impact echo measurements were made on the concrete sections with two different pieces of equipment: (1) the "DOCter" manufactured by Germann Instruments ("DOC"); and (2) the concrete thickness gauge ("CTG"), manufactured by Olson Instruments, Inc. These are the same two pieces of equipment that were used in the laboratory testing described in Section 5. The DOC has the capability of measuring the surface p-wave velocity, while CTG unit computes the thickness using an estimated p-wave velocity. At each test location three measurements were made with each device. If one of the three measurements did not agree with the other two, the measurements were repeated. Following the GPR and IE data collection, cores were taken in the pavement and stored for measurement and photographing.

Table 15 – Caltrans Test Sites

SITE	LOCATION	DESCRIPTION	THICKNESS (MM) (AND AGE)	TEST DATE
US 50	Sacramento	Full depth AC construction	2 lifts 50 over 113	12/3/01
US 50	Sacramento	Full depth AC construction	113	12/3/01
I-505	Vacaville	AC over AC	76	12/4/01
I-5	Tracy	AC over PCC	102	12/5/01
US 180	Mendota	AC over AC	203	12/6/01
US 99	Sacramento	AC over PCC	102	12/7/01
SR14 NB	Palmdale	PCC over LCB	200 (> 2 yrs)	5/13/02
SR14 SB	Palmdale	PCC over LCB	100, 150, & 200 (>2 yrs)	5/13/02
SR14 SB HOV	Palmdale	PCC over LCB	229 (30 day)	5/13/02
SR 30 (PM 5.4-6.6)	San Dimas	PCC over LCB	270 (90 day)	5/14/02
SR 30 (PM 2.9-5.4)	San Dimas	PCC over LCB	270 (14 day & 24 hour)	5/14/02

7.1.1 Description of Asphalt Sections

US 50

Two lanes adjacent to the center median were available for testing at this site. In one lane (the inside lane), the paving was complete. The lane adjacent to the to the inside lane (designated the "outside lane") did not have its final overlay. This arrangement provided the equivalent of two AC/aggregate base sites, each with a different nominal thickness. Figure 45 shows the boundary between the two lanes and the step in elevation. It had rained prior to the testing and the pavement was initially damp. However, the pavement dried out quickly and it did not appear that the moisture had an influence. Figure 46 shows sample cores from each of the two lanes. It appears that the complete pavement (a) was placed in three lifts. For the outside lane, the third lift had yet to be placed.

Figure 45 – CMP Data Collection at US 50 (note Teflon sheet)

(a) Inside Lane, 163 mm (6.5”) (b) Outside Lane, 100 mm (4”)

Figure 46 – US 50 Cores

Interstate 505

This site was a two lane exit ramp off of I-505. The tangent portion of this ramp was approximately 152 meters (500 feet) long. Data collection took place in the left lane behind a temporary lane closure (Figure 47). The site represented a recent overlay. The general pavement

structure as shown from the cores was a 51 mm (2 inches) overlay over a 25 to 37 mm (1.0 to 1.5 inches) leveling course over an original 100-125 mm (4-5 inches) thick pavement. The core recovery varied from core to core. In some cases the full 3 layers were recovered, and in other cases just the first one or two. Figure 47 shows sample cores from this site.

(a) Horn Antenna Data Collection in Right Wheel Path behind Lane Closure

(b) Left Wheel path

(c) Right Wheel path

Figure 47 – I-505 Data Collection and Sample Cores Showing AC Layers

Interstate 5

The test site was the outside lane of Interstate 5. The lane was open to traffic, and so the data collection was carried out behind a temporary lane closure. The pavement structure was nominally a 102 mm (4 inch) AC overlay over PCC. The actual structure as revealed by the cores was a 76 mm (3 inch) overlay over a 25-37 mm (1.0-1.5 inch) leveling course, as shown in Figure 48.

Figure 48 – Sample Core from I-5 Showing AC Layers

SR-180

This site represented a newly constructed outside lane. The construction was still underway, and the site was not open to traffic. The new pavement construction consisted nominally of a 51 mm (2 inch) wearing course, a 64 mm (2.5 inch) binder course, and a leveling course that varied from 38 to 165 mm (1.5 to 6.5 inches). The original pavement was 102 to 127 mm (4 to 5 inches) of AC. Figure 49 shows sample cores. Many of the cores broke between the binder and leveling course, as shown in the left photo.

US-99

This site, opened to traffic, was the outside lane of a heavily traveled road just outside of Sacramento. Due to the heavy traffic volume the work was carried out at night behind a temporary lane closure. The specified pavement structure was a102 mm (4 inch) asphalt overlay on an original concrete pavement, consisting of 25 mm (1 inch) RAC over 46 mm (1.8 inch) AC PRF over 56 mm (2.2 inch) AC. A typical core is shown in Figure 50. The cores revealed a 76 mm (3 inch) pavement structure with a clear boundary between the two AC layers but no evidence of the RAC surfacing.

Figure 49 – Sample Cores from SR-180

Figure 50 – Sample Core from US-99

7.1.2 Description of PCC Sites

The PCC sites were chosen in two locations, one on State Route 14 near Palmdale, and the other on State Route 30 near San Dimas. All of the PCC sites had longitudinally tined surfaces. At each sites, slabs spaced evenly throughout the site were selected as test locations. The specific location within each slab was determined by identifying locations where the impact-echo measurement could distinguish the PCC from the LCB. These locations were marked and numbered with paint. Ten cores in each of the five sections were taken at these locations after the IE and CMP data collection. For the two HVS sites, additional core data was available from UC Berkeley based on previous coring. Additional measurements were made at these locations. The individual sites are described in further detail below.

SR-14

SR-14 was an existing road with two lanes in each direction. The road was being widened to include an HOV lane, and this new construction was available for testing. Close to this new construction were two heavy vehicle simulator (HVS) test sections. These sections were well documented, and provided a good opportunity to cover a range of thickness values. The Northbound HVS Section was of uniform PCC thickness (200 mm (8 inches) over a 100 mm (4 inches) lean concrete base. The section consisted of slabs approximately 4 by 4 meters (13 x 13 feet) square. The length dimension varied slightly from slab to slab. Dowels at the transverse joints existed in some, but not all of the slabs. The dowelled joints were described in the section documentation. Figure 51a shows the test section and the testing in progress. Note that the entire section was behind a concrete barrier, and that HVS testing was in progress at the time of the thickness evaluations.

The Southbound HVS Section was located on a shoulder and not directly exposed to traffic. However, since the traffic was on the adjacent lane, truck-mounted attenuator and arrowboard were provided for protection. The overall section was 210 meters long, and was divided into three sub-sections with concrete thickness of 100, 150, and 200 mm (4, 6, 8 inches) respectively, all over a 150 mm (6 inches) aggregate base. The pavement consisted of 4 x 4 meter mm (13 x 13 foot) slabs, and there were no dowels at the transverse joints. Figure 51b shows the southbound HVS section.

The Southbound HOV section represented new construction approximately 9 miles southeast of the HVS sites. The new construction consisted of the new HOV land and a new PCC shoulder, both constructed of 229 mm (9 inches) PCC pavement over a 121 mm (4.75 inches) lean concrete base. Although the new HOV lane was not open to traffic, there was no fixed barricade. Therefore, for safety purposes, the testing was carried out in the shoulder. Figure 52 shows the site and the testing.

SR-30

The State Route 30 site was an extension of the existing SR-30, and represented approximately five miles of completely new construction. The construction was divided into three projects, representing the west, central, and east sections of the projects. Due to the phasing of the contracts, the concrete age varied with the different projects. At the time of the testing the age of the PCC pavement was 90 days in the Center Section (milepost (PM) 5.4-6.6), and 14 days in the West Section (PM 2.9-5.4). Also, there were parts of the west section that had been paved within the past 2 days. This configuration provided an opportunity to investigate the NDT thickness measurements as a function of pavement age. The 270 mm (10.6 inch) thick PCC pavement throughout this project was placed over a 150 mm (6 inches) thick lean concrete base, and had dowels at the transverse joints. All data was collected in the Westbound direction, close to the project boundary at PM 5.4. Figure 53 shows the test areas.

(a) NB HVS Site

(b) SB HVS Site

Figure 51 – HVS Test Sites on SR-14

Figure 52 – HOV Test Site on SR 14

(a) IE Testing on Center Section

(b) West Section, showing Paving Machine, PCC Pavement over LC Base, and Dowel Bars

Figure 53 – SR-30 Test Areas

7.2 Data Analysis

The data from the various test methods was initially analyzed without the core information. The purpose of this separation was to determine what type of results could be obtained without the benefit of core data. Once the NDE data was analyzed, the core data was made available and comparisons were carried out. The following sections describe the results obtained through this procedure for the asphalt and PCC test sections.

7.2.1 Asphalt Sections

7.2.1.1 Horn Antenna Data

The horn antenna data analyzed continuously from the start to end of each survey run, and the data was presented as thickness vs. distance. The initial analysis was carried out without reference to the core data. Once the data was analyzed, the core data was reviewed, and the horn antenna data at the core locations was compared to the core values. Figure 54 shows a sample output of this analysis. The figure shows the continuous analysis of the asphalt bottom, the core numbers and locations, and the depth (thickness) of each core. Multiple asphalt layers are shown where they appear in the horn antenna data. The prefix "2" for each core indicates that the data is in the right wheelpath.

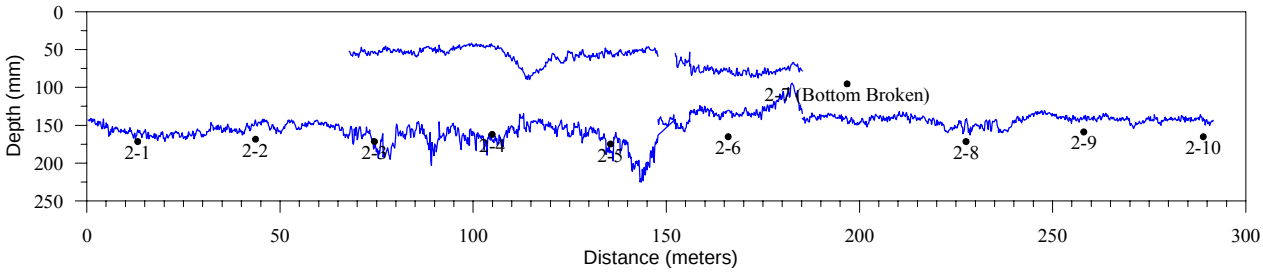

Figure 54 – Sample Horn Antenna Data Analysis
US-50 Inside Lane, Right Wheelpath

For comparison with core data, the average horn antenna data in an interval of ±30 cm (±1 foot) around the core location was used. This averaging takes into account the fact that the core locations were marked in the horn antenna data while the test vehicle was in motion, and that the actual location might vary slightly. These horn antenna data at the core locations were plotted against the core values, as shown in Figure 55. The horn antenna values vs. the core values for each of the six sites tested. Also shown on the plot is an equality line, which represents where the data should ideally be located.

Examination of the data points vs. the equality line reveals that in some sites, the data is shifted, or biased, from where it should be located. This bias is particularly noticeable for the I-5 and US-50 sites. Results of the preliminary testing described in Section 6.5 indicated that some site-specific calibration would be necessary to remove this type of bias from the data.

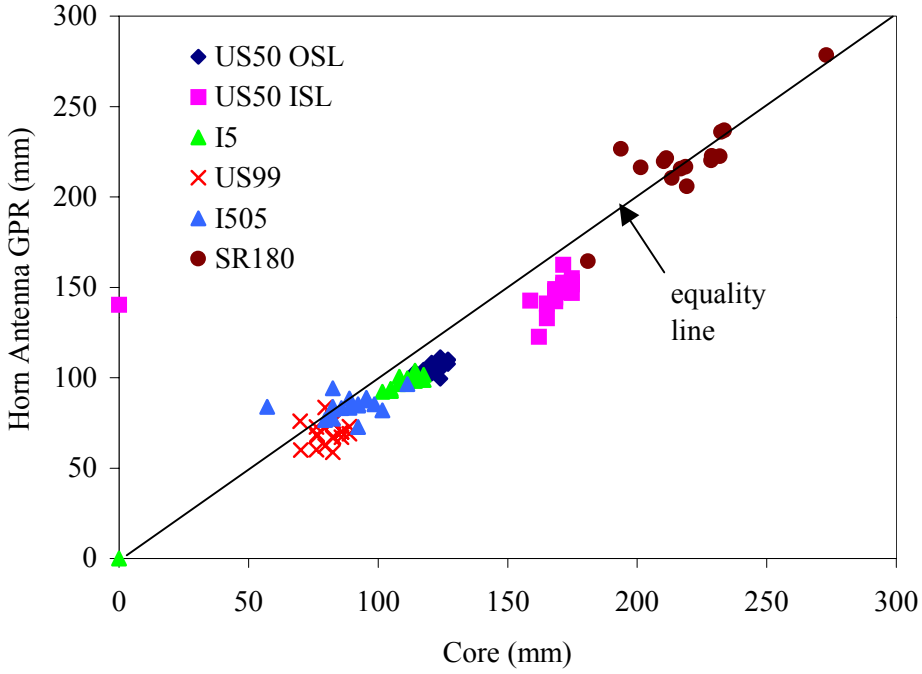

Figure 55 – Horn Antenna vs. Core Data Before Calibration

In order to correct for this bias, a calibration procedure was established. The calibration utilized the data from one core, and scaled all of the horn antenna data based on the ration of that core value to the horn data at that core location. For example, if the core value were 165 mm (6.5 inches) and the horn antenna data were 152 mm (6 inches) at that core location, then all of the horn data would be multiplied by the ratio of 6.5/6.0. The key to this process is the selection of the appropriate core, since different ratios would be obtained using different cores. Also, in future applications, the core could be taken anywhere in the site, so some location selection procedure needs to be established.

A core location selection procedure was developed based on the quality of the horn antenna data. The "data quality indicator" was based on two factors: (a) the strength of the reflection at the asphalt bottom; and (b) the uniformity of the thickness data. Locations with strong asphalt bottom reflection and relatively uniform data would be considered reliable data locations. The core locations were ranked based on these two criteria. The location with the strongest bottom reflection combined with the most uniform thickness data was selected as the calibration location. This criterion is represented mathematically in

$$\text{location} = \max_i (\varepsilon_a/\varepsilon_b)_i \ \cup \ \min_i \text{stdev}(t_i) \qquad (11)$$

where i represents the core number, $(\varepsilon_a/\varepsilon_b)_i$ represents the calculated ratio of the asphalt to base dielectric constants at that location, t_i represents the calculated thickness at core i location, and $\text{stdev}(t_i)$ represents the standard deviation of the calculated thickness values in a range of ± 3 meters around the core location. The formula represents the combination of the two quality indicators described above.

The data quality indicator criterion was applied to the horn antenna data from the six test sites. The horn antenna data at each site was calibrated based on the procedure described above. The calibrated results were correlated with the full set of core data, and the results are shown in Figure 56.

Figure 56 shows a very good correlation between the calibrated horn antenna data and the core data. The regression line shows a slope very close to one, indicating the elimination of the bias. Table 16 summarizes the statistics of this correlation.

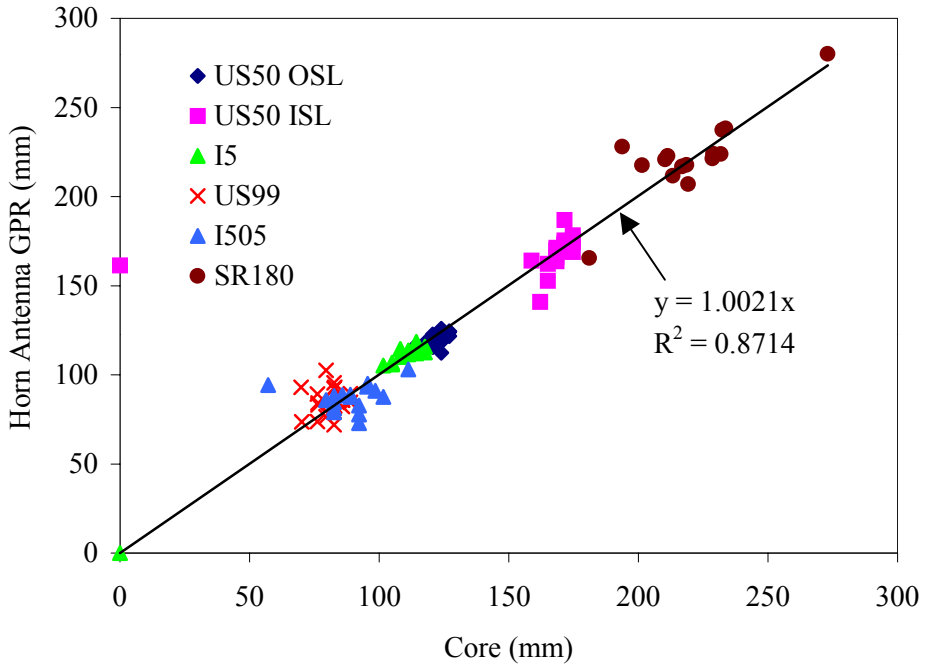

Figure 56 – Horn Antenna vs. Core Data After Calibration

Table 16 – Correlation of Calibrated Horn Antenna Data with Cores

Site	Mean Asphalt Thickness (mm)				Thickness Standard Deviation (mm)			
	Core	Horn at Core Location	All Horn Data	Difference (at core locations)	Core	Horn at Core Location	All Horn data	Difference (at core locations)
US50 OSL	121	119	119	2	4	4	4	0
US50 ISL	169	168	170	1	4	10	13	-5
I505	89	91	89	-2	11	7	8	5
I5	111	112	111	-1	5	4	4	1
US99	81	85	87	-4	5	8	11	-3
SR180	220	219	221	0	21	28	28	-7
			mean	-0.7			mean	-1.5

Table 16 presents the average thickness from the horn antenna data in two ways: (1) as the average of the horn data at the core locations; and (2) as the average of the horn data collected over the entire site (typically 4000 data points). The table shows that the mean horn antenna thickness values agree very closely with the mean value of the core data for each site. For five of the six sites, this difference is less that 2.5 mm (0.10 inches). The average difference for all six sites is -0.7 mm, and (-0.03 inch). The table also shows the standard deviation of the core and horn antenna measurements. This standard deviation is a measure of the variability of the asphalt thickness throughout the site. This variability was shown to play an important role in the assessment of the measurement technology and the implementation of pay factors (See Section 2). The data shows that the standard deviation as determined by the cores relates reasonably, but not precisely, to the standard deviation as measured by the horn antenna data. The correlation between the two standard deviations has an R squared of 0.80. Note that the standard deviation measured at the 20 core locations does not truly represent the entire site, and that the standard deviation measured over the entire site should be more representative.

7.2.1.2 CMP Asphalt Thickness Data

The CMP measurements were taken only at core locations. Two CMP measurements were made at each core location, one in the longitudinal direction and one in the transverse direction. The thickness values obtained from these two measurements were averaged, and the resulting averages were correlated with the core data. Figure 57 presents a plot of the CMP data vs. the core data. The data in the figure show that, with the exception of US 99, the CMP method appears to overestimate the core values. A similar finding was observed in the preliminary testing. Also note that the CMP method was not able to distinguish the asphalt layers from the original asphalt layer at the I-505 site. It was however, able to distinguish the combination of the original asphalt, the leveling course, and the new overlay. Therefore, the full depth CMP data from the I-505 site has been included at those locations where the full asphalt depth was determined from the cores.

Once again, the data suggest that some type of site-specific calibration would be desirable to remove the bias from the data. For the CMP data, a measure of confidence was assigned to each analyzed location. The confidence level was determined by the presence or absence of inter-layers and by the clarity of the CMP reflection polarity. For each site, one location with the highest confidence was selected as the calibration location. The remaining data was calibrated by multiplying the thickness values by the ratio of the calibration location core value divided by the calibration location CMP value. The results of this calibration procedure are shown in Figure 57. Data from the I-505 site is not shown, since the method was not able to determine the desired overlay thickness.

The regression analysis of the calibrated CMP results shows a line of slope very close to one, indicating that the bias has been removed. The data show more scatter than the horn antenna data, particularly at the US-180 site. This site, like the I-505 site, represents an asphalt overlay over an original asphalt pavement. The method apparently has more difficulty dealing with multiple asphalt layers.

Table 17 summarizes the statistics of the correlation between the calibrated CMP data and the cores.

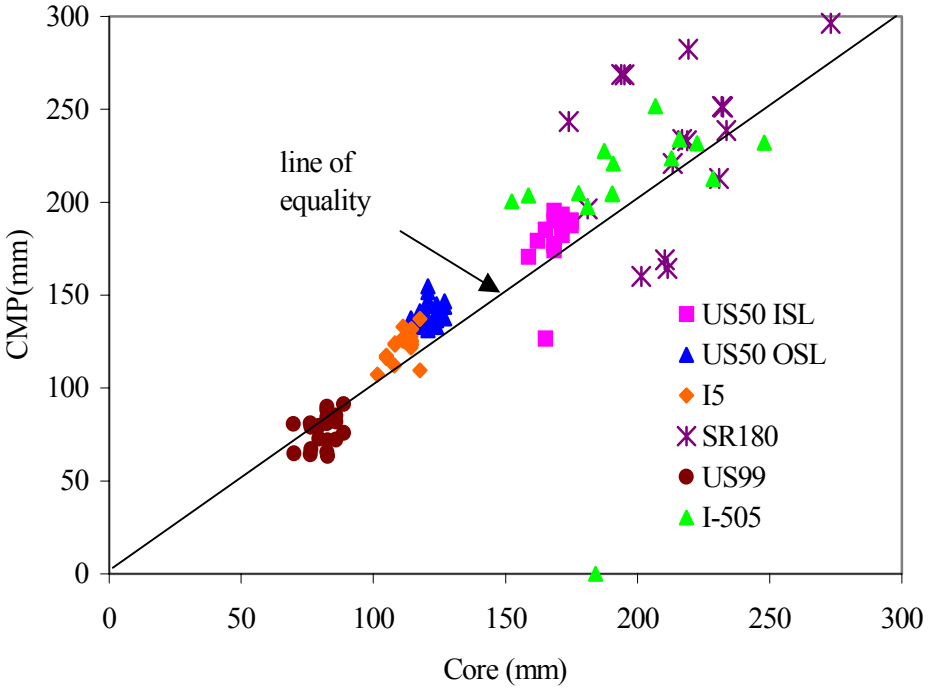

Figure 57 – CMP vs. Core Values at Asphalt Sites Before Calibration

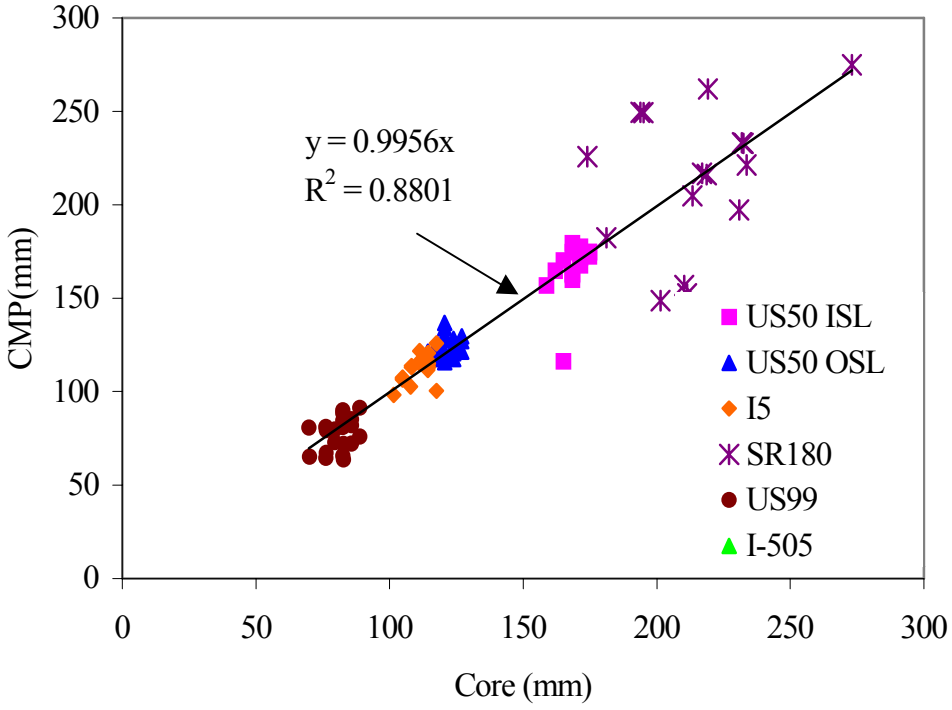

Figure 58– CMP vs. Core Values at Asphalt Sites After Calibration

Table 17 – Correlation of Calibrated CMP Data with Cores

SITE	CORE	CMP	DIFFERENCE	CORE	CMP	DIFFERENCE
	MEAN ASPHALT THICKNESS (MM)			THICKNESS STANDARD DEVIATION (MM)		
US50 OSL	121	125	-3	4	6	-2
US50 ISL	169	167	2	4	14	-10
I5	111	113	-2	5	7	-3
US99	81	77	4	5	9	-4
SR180	215	214	1	24	38	-15

Table 17 shows that the mean CMP thickness values agree fairly closely with the mean value of the core data for each site, with a maximum difference of 3.8 mm (0.15 inches). The average difference for all six sites is -0.5 mm (-0.02 inch) and the standard deviation of the differences is 2.8 mm (0.11 inches). The table also shows the standard deviation of the core and CMP measurements. The data shows that the standard deviation as determined by the CMP method correlates very well with the core standard deviation (R-squared = 0.95) but consistently overestimates the standard deviation by about 50%.

7.2.2 Concrete Sections

7.2.2.1 Impact-Echo Data

Data from the two impact-echo devices were analyzed. For the Doctor device, the p-wave velocities (V_p) values were determined at each location. The data from the Caltrans sites was analyzed using both local and average Vp values. For the CTG device, the data was analyzed using an assumed V_p value. Figure 59 shows the correlation between the impact-echo data and the core data. The data from all of concrete test sites has been combined in this plot. The impact-echo data is the average of the three measurements made at each test location with each device. The V_p value used with the DOC data is the average of the values obtained for each site. The results show that thickness values determined with both methods correlate very well with the core thickness values. As expected, the CTG deviates from the slope of one more than the DOC, due to the use of an assumed concrete velocity. However, even the DOC with its direct V_p measurement shows some bias towards underestimating the actual thickness. Therefore, both methods would benefit from the use of a calibration procedure.

A calibration procedure was established similar to that developed for the horn and CMP GPR methods, as follows. One location was selected as the calibration location, and the IE data and core data at that location provided a calibration factor for the data at the other locations. The calibration location for the DOC device was determined by the repeatability of the measurement. For the CTG device, the calibration core location was based on the reported resonant peak quality factor "Q" obtained provided by the device. The results of the calibration are shown in Table 18.

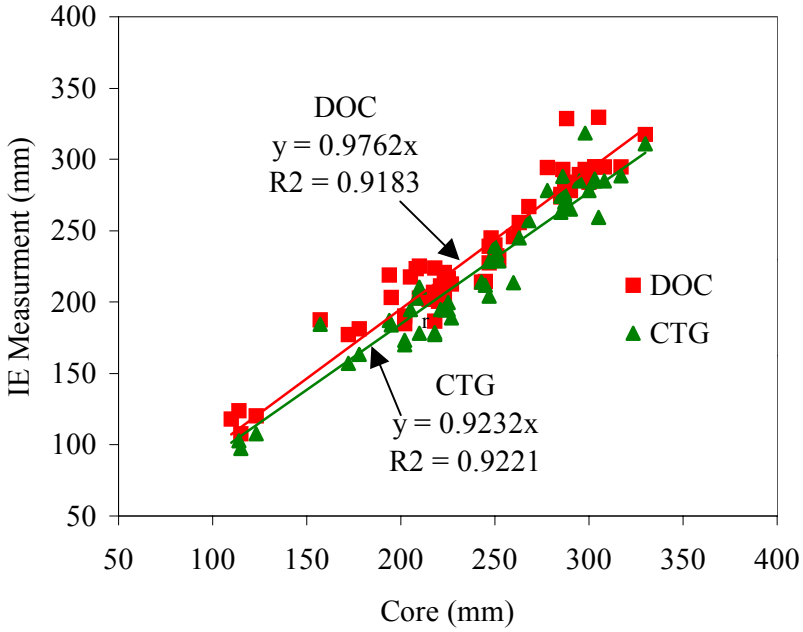

Figure 59 – Impact-Echo vs. Cores Without Calibration

Table 18 – Summary of Impact-Echo PCC Pavement Thickness Data

Site	Mean Pavement Thickness from Cores	Mean Difference (IE - Core Thickness): Without Calibration Core		Mean Difference (IE - Core Thickness): With Calibration Core	
	cm	DOC	CTG	DOC	CTG
1	217	-10	-28	13	0
2	161	10	-03	2	1
3	249	-17	-26	1	-7
4	301	-11	-19	-3	-5
5	281	-01	-06	11	-6
Mean Absolute Difference (cm.)		**10**	**16**	**6**	**4**

The core calibrated IE results show significant improvement, with a mean deviation for all five sites equal to 6.1 and 4.06 mm (0.24 and 0.16 inches), respectively for the two IE methods. While this deviation is somewhat greater than the 2.5 mm (0.10 inch) accuracy objective for QA, it is very accurate by other standards, and it might be workable for QA if the accuracy objectives can be relaxed.

8. Equipment and Method Specifications

The following sections provide a general specification for the methods evaluated during this project. The specification includes both the measurement procedure and the equipment incorporated into the methods.

8.1 Horn Antenna GPR Method for Asphalt Thickness

8.1.1 Equipment Specification

GPR System Consisting of:

- 1 GHz horn antenna (example – GSSI Model 4108) with performance comparable to that specified in the TTI specification
- GPR data acquisition, control, and display system (example - GSSI Model 10B)
- Antenna Cable
- Survey Vehicle with 51 mm (2 inches) square receiver hitch
- Mounting arrangement for Horn Antenna, such that the antenna is suspended from non-metallic rails approx. 451 mm (18 inches) over the pavement, and such that the antenna centerline is greater than 150 cm (5 feet) from the vehicle bumper
- Electronic Survey wheel or DMI with resolution of 20 pulses/foot or more

Data Analysis Software Consisting of:

- Radar waveform processing for asphalt bottom peak detection, including subtraction of direct coupling and surface reflection (eg. GSSI "RADAN")
- Standard spreadsheet software for determination of thickness statistics

8.1.2 Method Specification

Equipment Setup:

- Mount horn antenna onto survey vehicle with mounting equipment
- Connect antenna and electronic survey wheel or DMI to the GPR system
- Conduct metal plate, direct coupling, and height calibration tests
- Setup data collection for two scans per foot of travel
- Identify survey lines for lane under consideration (eg., left wheel path, right wheel path, and centerline)

Data Collection:

- For each survey line, begin data collection at one end of the site and collect data continuously until the far end of the site is reached
- Save the data in a file name that indicates the project ID, section ID, lane#, and pass#
- Repeat data collection for other survey lines and for other lanes

Data Analysis:

- Transfer the data to a computer (if necessary) and analyze data for asphalt thickness at desired distance interval
- Identify the location of calibration core(s) from the procedures implemented in the analysis software
- Collect the calibration core data, and calibrate the initial thickness data using the calibration core
- Import asphalt thickness data into standard spreadsheet software for statistical analysis and graphical presentation

Training and Expertise:

It is estimated data collection training could be completed in 3 days, and that the appropriate background is that of a field technician familiar with the use of electronic equipment. Data analysis training would take 5 days, and the appropriate background is that of a test technician familiar with analyzing test data.

8.2 Common Midpoint (CMP) Method for Asphalt Thickness Evaluation

8.2.1 Equipment Specification

GPR System Consisting of:

- Two 1.5 GHz ground-coupled antennas (example – GSSI Model 5100)
- GPR data acquisition, control, and display system (example - GSSI Model 10B)
- 12 VDC power supply
- Two Antenna cables
- Antenna mounting rig with mechanism to move antennas along the pavement surface in equal and opposite directions from the midpoint
- One linear motion encoder with output of at least 2500 pulses per mm (100 pulses per inch) of antenna movement
- 1 mm (0.04 inch) thick Teflon sheet for sliding interface between the antennas and the pavement

Data Analysis Software Consisting of:

- Radar waveform processing software implementing the CMP algorithm (eg., GSSI "RADAN"
- Standard spreadsheet software for determination of thickness statistics

8.2.2 Method Specification

Equipment Setup:

- Mount ground-coupled antennas into testing rig
- Connect antennas and position encoder to the GPR system
- Conduct metal plate and direct coupling calibration tests
- Setup data collection for one scan every two millimeters of movement
- Identify test locations and ID numbers for lane under consideration
- Allow the GPR equipment to warm up for 20 minutes

Data Collection:

- For test location, conduct two CMP measurements, one in the longitudinal direction and one in the transverse direction
- The data in a files whose name indicates the project ID, section ID, and location number
- Repeat data collection for every test location

Data Analysis:

- Bring data into the office and transfer to office computer
- Apply the CMP software to the test data to determine initial thickness values
- Identify the location of calibration core(s) from the procedures implemented in the analysis software
- Collect the calibration core data, and calibrate the initial thickness data using the calibration core
- Import asphalt thickness data into standard spreadsheet software for statistical analysis and graphical presentation

Training and Expertise:

It is estimated data collection training could be completed in 3 days, and that the appropriate background for data collection personnel is that of a field technician familiar with the use of electronic equipment. Data analysis training would take 5 days, and the appropriate background is that of a test technician familiar with analyzing test data.

8.3 Impact-Echo Method for Concrete Thickness Measurement

8.3.1 Equipment Specification

Impact-Echo System Consisting of:

- A commercially available impact echo device consisting of a short duration impact source, a receiving transducer, and a control and data collection device (examples are the Germann Instruments "DOCTer" and the Olson Instruments "CTG")
- Display unit showing the measured frequency response and the "thickness resonance"
- Processing of the thickness resonance to obtain estimated thickness for assumed p-wave velocity

8.3.2 Method Specification

Equipment Setup:

- Set up impact-echo equipment
- Input estimated p-wave velocity and slab thickness

Data Collection:

- Identify test locations and ID numbers for lane under consideration
- Conduct initial IE measurements at each test location
- Confirm that thickness resonance conforming to the known pavement thickness is observable at the test location. If so, conduct 3 repeat measurements
- If appropriate thickness resonance is not observable, find another location nearby and retest. (note that for PCC over lean concrete base, the required mechanical separation between the two layers is more likely to be found near the edges and corners of the slab).
- Repeat data collection for other test locations

Data Analysis:

- Bring data into the office and transfer to office computer
- Analyze data for concrete thickness using measured resonant frequencies and equation (5). For CTG equipment, use and assumed value for V_p For the DOCTer, use the average of the measured V_p values
- Identify calibration core location, and take calibration core(s)
- Calibrate initial thickness data using calibration core(s)
- Import asphalt thickness data into standard spreadsheet software for statistical analysis and graphical presentation

Training and Expertise:

It is estimated that impact echo data collection and analysis training could be completed in 3 days, and that the appropriate background is that of a field technician familiar with the use of electronic equipment.

9. References

(1) Deacon, J. A., C. L. Monismith, and J. T. Harvey "Pay Factors for Asphalt-Concrete Construction: Effect of Construction Quality on Agency Costs" Technical Memorandum, TM-UCB-CAL/APT-97-1, April 1997.

(2) Maser, K. R., "Pavement Characterization Using Ground Penetrating Radar: State of the Art and Current Practice," *Nondestructive Testing of Pavements and Backcalculation of Moduli: Third Volume, ASTM STP 1375,* American Society for Testing and Materials, West Conshohocken, PA, 1999.

(3) Wenzlick, J. T. Scullion, and K. R. Maser "High Accuracy Pavement Thickness Measurement using Ground Penetrating Radar" Report No. RDT 99-003, Missouri Dept. of Transportation, February, 1999.

(4) Maser, K. R., and T. Scullion "Influence of Asphalt Layering and Surface Treatments on Asphalt and Base Layer Thickness Computations using GPR" TTI Report TX-92-1923-1, September 1992.

(5) Saarenketo, T. and P. Roimela, "Ground Penetrating Radar Technique in Asphalt Pavement Density Quality Control". *Proceedings of the 7th International Conference on Ground Penetrating Radar*, Lawrence, KS, pp. 461-466, May 27-30, 1998.

(6) Ulriksen, C. P. F., "Applications of Impulse Radar to Civil Engineering", published by GSSI, N. Salem, NH, 1993.

(7) Halabe, U., A. Sotoodehnia, K. R. Maser, E. A. Kausel, "Modeling the Electromagnetic Properties of Concrete", *ACI Materials Journal*, Volume 90, No. 6, pp. 552-563, November-December 1993.

(8) Standard Test Method for Measuring the p-wave Speed and Thickness of Concrete Plates Using the Impact-Echo Method (ASTM C1383). Annual Book of ASTM Standards, Volume 4.02, ASTM, West Conshohocken, PA, 2000.

(9) J.S. Popovics, et al. "One-sided stress wave velocity measurements in concrete," *Journal of Engineering Mechanics*, Volume 124, 1998. pp. 1346-1353.

(10) Graveen, C. "Nondestructive Test Methods To Assess Pavement Quality For Use In A Performance-Related Specification" M.S. Thesis, Department of Civil Engineering, Purdue University, W. Lafayette, IN, May, 2001

(11) Clemena, G. "Use of the Impact-Echo Method in Non-Destructive Measurements of the Thickness of New Concrete Pavement" Final Report, Report No. FHWA/VA-95-R10 ,VTRC 95-R10, 38p, Federal Highway Administration (1995)

(12) Sansalone, M., Lin, J., and Streett, W.B., "A Procedure for Determining Concrete Pavement Thickness Using P-Wave Speed Measurements and the Impact- Echo Method", *Innovations in Non-Destructive Testing of Concrete*, Pessiki, S. and Olson, L., Ed., American Concrete Institute, SP-168, Michigan, 1997, pp. 167-184.

(13) Maser, K. R., Holland, T. J., and Roberts, R., "Non-Destructive Measurement of Layer Thickness on Newly Constructed Asphalt Pavement". *Proceedings of the Pavement Evaluation Conference 2002,* Roanoke, VA, October 21-25, 2002.

(14) Maser, K. R. "Ground Penetrating Radar Surveys to Characterize Pavement Layer Thickness Variations at GPS Sites" Final Report, SHRP-P-397, Strategic Highway Research Program, National Research Council, Washington, D.C., 1994

(15) Sansalone, M., Lin, J., and Streett, W. B., "A Procedure for Determining P-Wave Speed in Concrete for Use in Impact-echo Testing Using a P-Wave Speed Measurement Technique*", ACI Materials Journal* 1997, Vol. 94, Iss. 6, pp. 531-539.

APPENDIX A

Model 4108 Horn Antenna Data Processing Methodology

The first step is to extract all of the pertinent information from the data. Typically, a calibration scan is obtained with the horn antenna placed over a metal plate at the same elevation as a scan obtained over pavement. Figures 1 and 2 shown the parameters extracted from the respective scans. At this time we are disregarding an optional scan also collected with the antenna radiating in free space. This is done for 2 reasons: (1) very similar results were obtained between data processed with and without the air-scan subtraction, (2) it is often difficult to obtain a high fidelity air scan in the field.

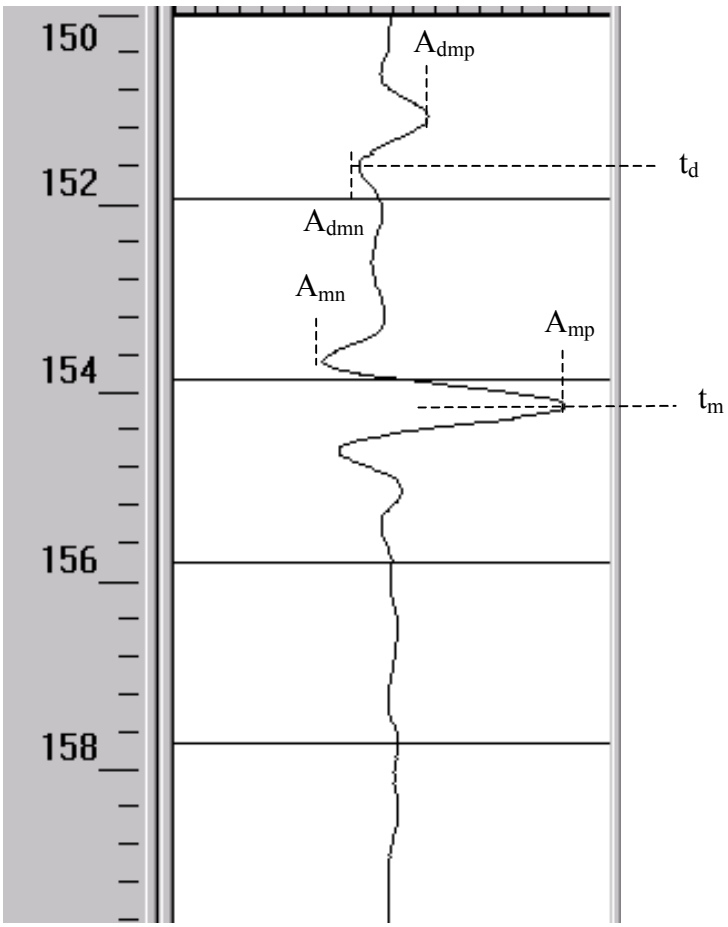

Figure 1 – Information Extracted From Metal Plate Calibration Scan

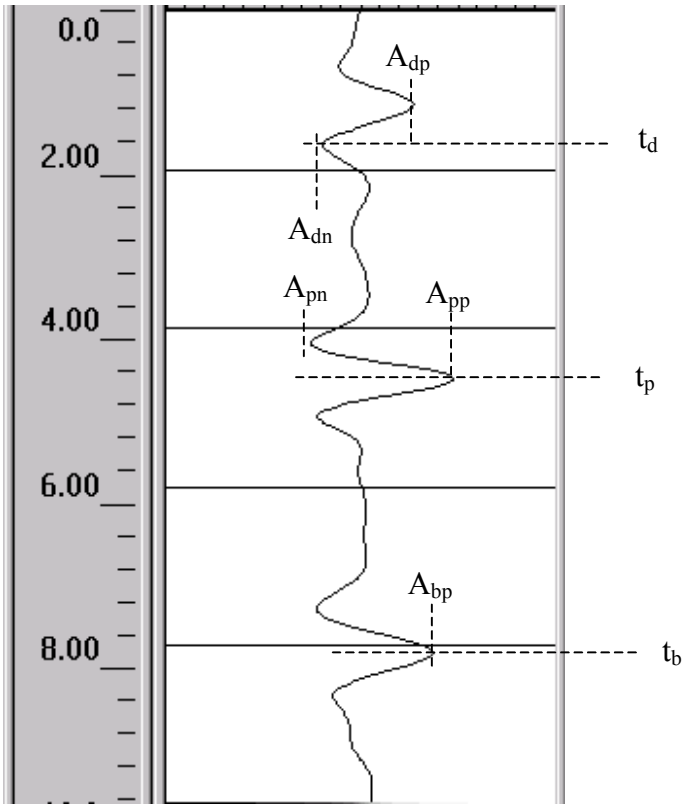

Figure 2 – Sample of Model 4108 Horn Antenna Data

Definitions of parameters shown in Figure 1:

t_d = time corresponding to negative peak of direct-coupling arrival,
A_{dmp} = amplitude of positive peak of direct-coupling arrival in metal plate scan,
A_{dmn} = amplitude of negative peak of direct-coupling arrival in metal plate scan,
t_p = time corresponding to positive peak of metal plate surface reflection arrival,
A_{mp} = amplitude of positive peak of metal plate reflection, and
A_{mn} = amplitude of negative peak preceding positive peak of metal plate reflection.

Definitions of parameters shown in Figure 2:

t_d = time corresponding to negative peak of direct-coupling arrival,
A_{dp} = amplitude of positive peak of direct-coupling arrival in pavement scan,
A_{dn} = amplitude of negative peak of direct-coupling arrival in pavement scan,
t_p = time corresponding to positive peak of pavement surface reflection arrival,
A_{pp} = amplitude of positive peak of pavement surface reflection,
A_{pn} = amplitude of negative peak preceding positive peak of pavement surface reflection,
t_b = time corresponding to positive peak of pavement bottom reflection arrival, and
A_{bp} = amplitude of positive peak of pavement bottom reflection,

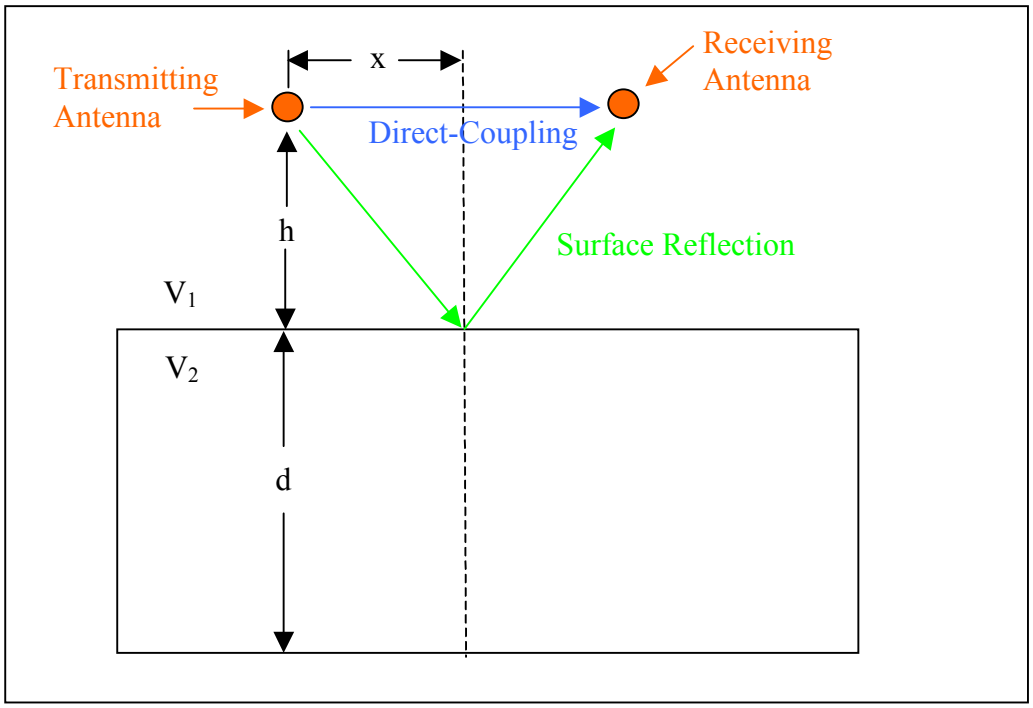

Figure 3 – Shows The Geometry Associated With The Reflection From the Pavement Surface and the Direct-Coupling

The parameters shown in figures 1 and 2 are extracted from data obtained from the horn antenna positioned over a metal plate and the pavement, respectively. The "A" parameters are amplitudes. The "t" parameters are travel times. The amplitudes and travel times of the reflection from the pavement bottom (A_{bp} and t_b) are typically obtained after a template subtraction of a metal plate scan from the data scan (this is not shown in Figure 2).

The antenna height, h, is back-calculated using the Equation 1 and solving for h.

$$(t_p - t_d + t_c)V_1 = 2\sqrt{h^2 + x^2} \qquad \text{Eq. 1}$$

where:

t_c = time constant that corrects for the difference in the arrival time of the negative peak of the direct-coupling and the true time-zero. (This value was back-calculated using the same equation and a series of measurements over a metal plate obtained at known heights. This value is 0.665 ns for Model 4108 antenna S/N 11),

V_1 = propagation velocity of radar waves in free space,

h = antenna height above pavement or metal plate, and

x = ½ bistatic separation between transmitting and receiving antennas (17.75 cm for model 4108 antenna).

The radar wave propagation velocity in pavement is calculated using Equation 2.

$$V_2 = \frac{V_1}{\sqrt{\sin^2\theta_i + \cos^2\theta_i \left(\frac{1-\rho}{1+\rho}\right)^2}} \qquad \text{Eq. 2}$$

where:

V_2 = propagation velocity of radar waves in pavement,
θ_i = angle of incidence, and
ρ = reflection coefficient at pavement surface for angle of incidence θ_i.

Equations 3-4 show how θ_i and ρ are calculated using known parameters.

$$\theta_i = \tan^{-1}\left(\frac{x}{h}\right) \qquad \text{Eq. 3}$$

$$\rho = \frac{-1\left(\frac{A_{pp} - A_{pn}}{A_{dp} - A_{dn}}\right)}{\left(\frac{A_{mp} - A_{mn}}{A_{dmp} - A_{dmn}}\right)} \qquad \text{Eq. 4}$$

The last parameter necessary for calculating the thickness of the pavement is the round-trip travel time of the reflection from the pavement bottom. This value is calculated using the relation shown in Equation 5.

$$t_{tot} = t_b - t_d + t_c \qquad \text{Eq. 5}$$

Figure 4 shows the more complicated ray path geometry of a ray reflecting from the bottom of the pavement.

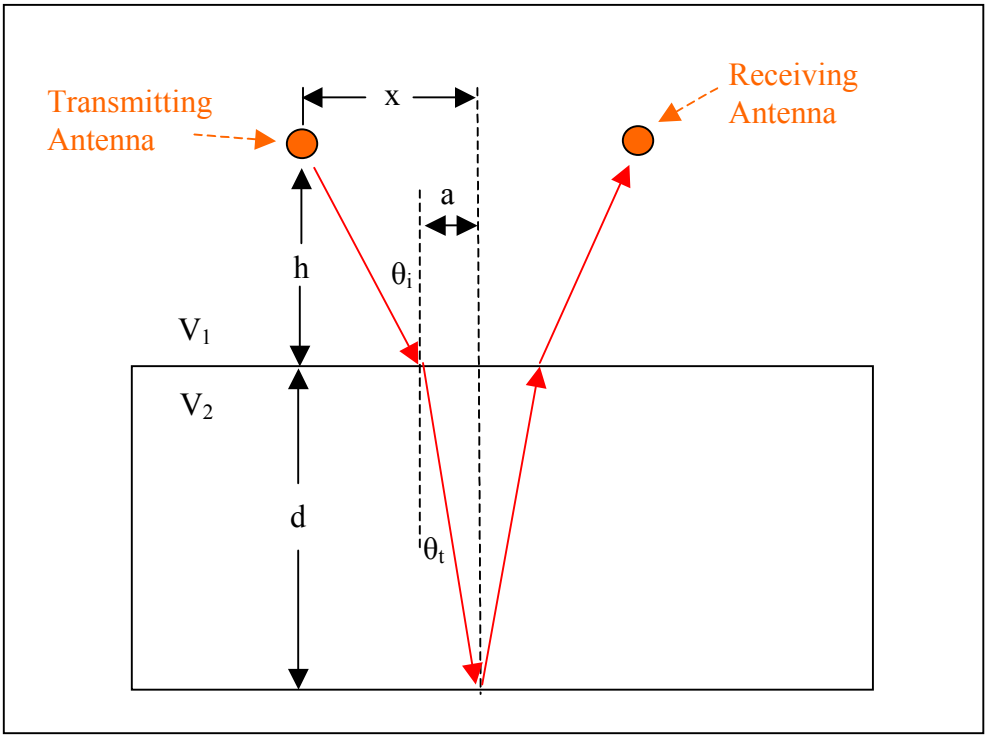

Figure 4 – Geometry of Ray Path Reflecting From Pavement Bottom

The total travel time of this ray is described by Equation 6.

$$t_{tot} = \frac{2}{V_1}\sqrt{(x-a)^2 + h^2} + \frac{2}{V_2}\sqrt{a^2 + d^2} \qquad \text{Eq. 6}$$

where:

x = ½ separation distance between transmitting and receiving antennas,
a = distance between midpoint of antennas and surface location where incident ray refracts through the interface,
d = thickness of layer,
h = height of antenna,
V_1 = propagation velocity in medium 1,
V_2 = propagation velocity in medium 2, and
t_{tot} = total travel time of wavefront reflecting from bottom of layer.

The 2 unknowns in Equation 6 are "a" and "d". The unknown "d" can be removed from the equation using Equations 7 and 8.

$$\tan(\theta_t) = a/d \qquad \text{Eq. 7}$$

$$\sin(\theta_t) = (V_2/V_1)\sin(\theta_i) \qquad \text{Eq. 8}$$

where:

θ_i = incidence angle, and
θ_t = transmission angle.

Incorporating Equations 7 and 8 in Equation 6 results in a messy 4^{th} order polynomial equation in which the only unknown is "a". The 4^{th} order polynomial equation is solved using numerical techniques. Then the value "a" is plugged back into Equation 6 to back-calculate "d".